Key Scientific Challenges in Current Rechargeable Non-aqueous Li-O_2 Batteries: Experiment and Theory

Mahesh Datt Bhatt[1,2†], Hugh Geaney[1,2†], Michael Nolan[2] and Colm O'Dwyer[1,2]*

[1] *Department of Chemistry, University College Cork, Cork, Ireland*

[2] *Tyndall National Institute, Lee Maltings, Cork, Ireland*

Abstract

Rechargeable Li-air (henceforth referred to as Li-O_2) batteries provide theoretical capacities which are ten times higher than that of current Li-ion batteries, which could enable the driving range of an electric vehicle to be comparable to that of gasoline vehicles. These high energy densities in Li-O_2 batteries result from the atypical battery architecture which consists of an air (O_2) cathode and a pure lithium metal anode. However, hurdles to their widespread use abound with issues at the cathode (relating to electrocatalysis and cathode decomposition), lithium metal anode (high reactivity towards moisture) and due to electrolyte decomposition. This review focuses on the key scientific challenges in the development of rechargeable non-aqueous Li-O_2 batteries from both experimental and theoretical findings. This dual approach allows insight into future research directions to be provided and highlights the importance of combining theoretical and experimental approaches in the optimization of Li-O_2 battery systems.

Key Words: Li-O_2 battery, electrolytes, reduction, oxidation, rechargeability, cathodes, catalysts, energy storage, density functional theory, modelling

† Both authors contributed equally to this work. *To whom correspondence should be addressed: c.odwyer@ucc.ie; +353 (0)21 4902732; Fax: +353 (0)21 4274097

Section 1 Introduction

The increasing demand for fossil fuel energy worldwide is straining the resource capacity of conventional fuels and raising their prices. Most importantly, conventional fuels predominantly used in vehicles for transportation are considered a major contributor to global warming due to increased emission of CO_2 into the atmosphere. Ultimately, for these and other reasons, it is necessary to develop electrical energy storage and conversion systems to balance supply with demand as renewable sources are intermittent, and to power upcoming plug-in electric vehicles by the effective utilization of renewable energy sources in future smart grids and power supply systems. Currently, the electrification of transportation and large scale of deployment of renewable energy have been considered an important strategy.[1] However, such a transformation is ultimately limited by the poor performance of current electrical energy storage systems.

Rechargeable battery systems may be a good choice for such energy applications. However, current rechargeable non-aqueous Li-ion batteries have limited energy storage capacities which are far below the requirements for electric vehicles and grid energy storage applications, exacerbating range anxiety (driving distance per charge). For example, the driving distance of electric vehicles with current lithium-ion batteries is limited to less than 100 miles per charge, but a battery system that extends the distance of electric vehicles per charge to 300 miles would be a considerable advance for the electrification of the industry. The ragone plot shown in Figure 1 plots the ranges of Power density (W Kg^{-1}) against Energy density (Wh Kg^{-1}) for various battery systems compared to the internal combustion (IC) engine.[2] A recent material-to-systems analysis of the lithium–oxygen chemistry with comparison to more established Li-ion technologies has shown that the theoretical specific energy of a Li-air battery is not a wholly reliable indicator of the cost, volume, and mass considerations that must be factored into the systems-level manufacture.[3]

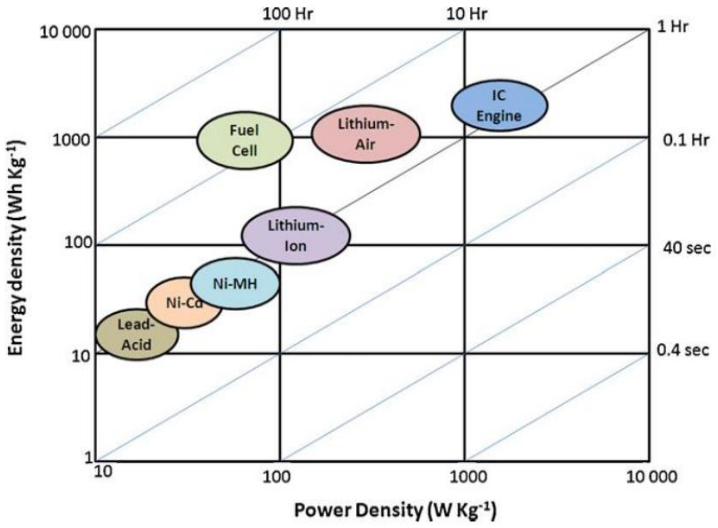

Figure 1: Ragone plot of Energy density vs Power Density for various battery systems compared with internal combustion engines. Reprinted from ref. [2]. Copyright 2011, with permission of Elsevier.

The discovery and initial development of the rechargeable non-aqueous Li-O_2 battery system promised extremely high theoretical energy densities exceeding the maximum energy densities of any Li-ion battery.[4-10] A further expected benefit of the initially proposed Li-O_2 architecture was that the cathode active material (oxygen) could be readily accessed directly from the environment. The Li-O_2 battery has a theoretical energy density approximately equal to 11,680 Wh/kg, nearly equivalent to gasoline.[11] Therefore, significant effort has been devoted to Li-O_2 battery research.[7, 11-13] A wide range of battery technologies available or currently under development, and comparison of their respective energy densities to gasoline are listed in Table I.[11]

Table I. Approximate gravimetric energy densities (Wh/kg) for various types of rechargeable batteries compared to gasoline. Reprinted with permission from ref. [11]. Copyright 2010 American Chemical Society.

Types	Theoretical energy density	Practical energy density
Lead-Acid	less than 2000	40
Ni-Cd	less than 2000	40
Ni-MH	less than 2000	50
Li-ion	less than 2000	160
Zn-air	less than 2000	350
Li-S	less than 2000	370
Li-O_2	≈ 11680	1700

Gasoline	more than 12000	1700

The representative applications of rechargeable batteries are shown in Figure 2.[10]

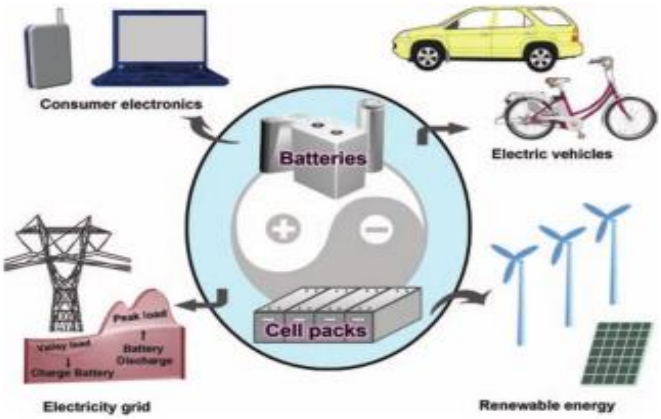

Figure 2 Representative applications of rechargeable batteries. Reprinted with permission from ref. [10]. Copyright 2011 WILEY-VCH Verlag GmbH & Co., KGaA, Weinheim.

Based on the types of electrolytes used, Li-O_2 batteries are divided into four types: aprotic (non-aqueous), aqueous, hybrid (mixture of aprotic and aqueous), and solid state.[6, 14-34] These four chemical architectures are outlined in Figure 3.[35]

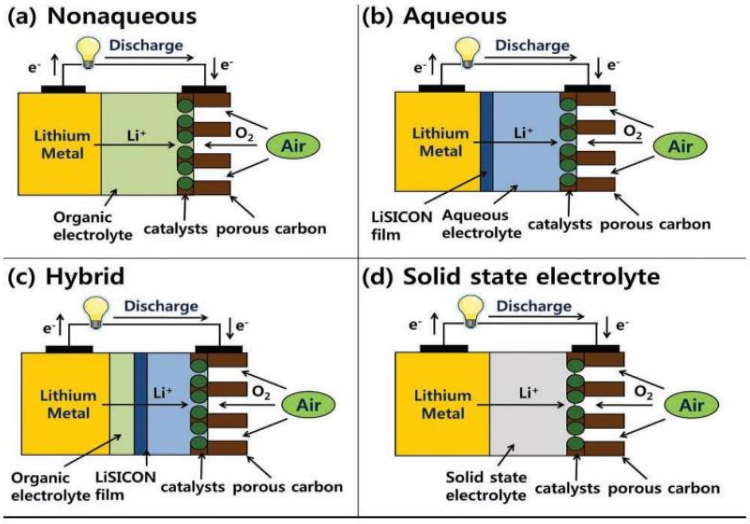

Figure 3 Four chemical architectures of Li-O_2 batteries. Reprinted with permission from ref. [35]. Copyright 2011 WILEY-VCH Verlag GmbH & Co., KGaA, Weinheim.

All four types of Li-O_2 batteries consist of a lithium metal anode and O_2 (air) cathode. Their basic electrochemical reaction mechanisms depend on the types of electrolytes used as given in Table II.[36] As the reduction product of oxygen such as Li_2O_2 can be reversed into the original reagents of the oxygen reduction reaction in non-aqueous Li-O_2 system, it seems to be more advantageous as compared to the other three architectures of Li-O_2 batteries. This non-aqueous Li-O_2 system is the current focus of research worldwide[37] owing to its prospects as a rechargeable high capacity metal-O_2 system and will be the primary focus of this review.

A typical rechargeable non-aqueous Li-O_2 battery consists of a metallic Li anode, porous O_2 cathode with high surface area carbons (with or without catalyst) bound to a metal current collector, and an electrolyte containing lithium salt and aprotic solvent. Despite the high theoretical specific energy of aprotic rechargeable Li-O_2 batteries, their practical specific energy is significantly lower than expected due to several factors. Electrical passivation at the cathode is the dominant capacity-limiting mechanism in Li-O_2 batteries due to pore clogging because of the formation of discharge products while the low conductivity of the same discharge products and their high electronic resistance is also a big challenge for aprotic Li-O_2 batteries.[38-41]

Table II. Types of Li-O_2 batteries with their cell reactions, advantages, and disadvantages. Adapted from ref.[36]. Copyright 2013, with permission of Elsevier.

Types	Cell Reactions	Advantages	Disadvantages
Non-aqueous (Aprotic)	$2Li^+ + 2e^- + O_2 = Li_2O_2$ (2.96 V)	High theoretical energy density, rechargeability	Insoluble discharge products, material challenges
Aqueous	$4Li^+ + 4e^- + O_2 = 2Li_2O$ (2.90 V) $4Li + O_2 + 2H_2O = 4LiOH$ (Alkaline electrolyte) $4Li + O_2 + 4H^+ = 4Li^+ + 2H_2O$ (Acidic electrolyte)	No pore clogging, no moisture effects as discharge products are soluble in aqueous system	Lack of Li-ion conducting membrane, undetermined charging behaviour

Hybrid	$4Li + O_2 + 2H_2O = 4LiOH$ (Alkaline electrolyte) $4Li + O_2 + 4H^+ = 4Li^+ + 2H_2O$ (Acidic electrolyte)	No pore clogging, no moisture effects, natural SEI formation on Li anode in aprotic electrolyte	Lack of solid Li-ion conducting membrane, undetermined charging behaviour
Solid state	$2Li^+ + 2e^- + O_2 = Li_2O_2$ (3.10 V)	Good stability, may use air, rechargeability, avoids dendrite formation	Low conductivity, capacity and energy density

Therefore, the design of functional porous cathode structures with O_2 diffusion channels is paramount in overcoming issues related to pore clogging and its influence on discharge performance. [8, 42-45]Moreover, the mechanisms underlying the basic electrochemical reactions in the Li-O_2 battery system such as oxygen reduction reaction (ORR) and oxygen evolution reaction (OER) occurred during discharge and charge at the oxygen cathode, and the materials and chemistries that influence them, are as yet not fully understood. In order to improve the ORR/OER kinetics in an aprotic Li-O_2 battery system, intensive research efforts have been devoted to various aspects including cathodes,[46-49] anodes,[50] electrolytes,[51] and discharge products[52-55]. A large body of research has reported higher specific capacity for Li-O_2 batteries than other battery systems, but their rate capability, cycle life and power performance are not still satisfactory for practical applications.[56] A porous electrode with high porosity and effective catalytic site distribution is required, which may be a novel porous electrode for Li-O_2 battery system.[57] Williford et al.[58] simulated several air electrodes with a single pore system, double pore system in 2D, and dual pore system with multiple time-release catalysts along with some important parameters such as porosity distribution, pore connectivity, the tortuosity of the pore system and the catalyst spatial distribution.

One of the big challenges for Li-O_2 battery system is the limited electrical efficiency due to the overpotential or polarization losses at the cathode during discharge and charge processes. The large voltage gap between these two processes leads to a low efficiency. Such challenges can be overcome by applying effective catalysts, particularly those with bifunctionality towards improved

ORR and OER kinetics. Many literature reports demonstrate that catalysts can be beneficial for both ORR during discharge and OER during charge, resulting in dramatic increases in overall efficiency of Li-O_2 system.[59]

There are other challenges in practical applications of Li-O_2 batteries such as safety issues, moisture issues and their fast degradation due to decomposition. A pure Li metal anode is the first choice as anode material in Li-O_2 cells because of its extremely high energy density compared to common Li-intercalated carbon anodes. It is well known that Li metal anodes are susceptible to dendrite formation and electrolyte incompatibility, which affect the cycle life and safety of Li-batteries.[60] Major challenges are related to the prevention of water and O_2 access to the Li anode. The issue is exacerbated by the fact that most Li-battery electrolytes easily absorb a substantial amount of water and Li-O_2 batteries using such electrolytes will have a poor cyclability even if pure dry O_2 is used.[4] Electrolyte vapor pressure also plays a crucial role in Li-O_2 battery degradation and is a key consideration in the choice of potential electrolytes.[51]

It is well known that it is quite difficult to perfectly exclude H_2O from the air electrode, particularly if ambient air is used rather than pure O_2. Therefore, the stability of Li metal anodes in electrolytes containing trace water does not facilitate long periods of operation. Density functional Theory (DFT) calculations provide efficient methods to better understand anode properties[61] as well as cathode effects during Li-O_2 battery operation, and as will be reviewed here in details, constitute a critical high-throughput method for the identification of optimum electrode materials for various Li-O_2 chemistries.

The electrolyte formulation has a major influence on ORR kinetic and discharge capacity in Li-O_2 batteries.[62] The cations in the electrolyte solutions of lithium salts strongly affect the reduction mechanism of O_2. Organic carbonate-based solvents (which have dominated Li-ion systems) have been found not to be useful electrolytes in Li-O_2 batteries due to their undesired decomposition during discharge forming unwanted products. Instead of organic carbonates, other organic species (ethers, sulfones etc.), ionic liquids and solid state electrolytes have been proposed as alternative

solvents for electrolytes used in Li-O_2 batteries due to their unique properties such as hydrophobic nature, low flammability, low vapour pressure, wide potential stability window, and high thermal stability. Some additives for electrolytes may be helpful for ORR kinetic in Li-O_2 batteries since these additives may increase the solubility and diffusivity of oxygen in an aprotic electrolyte, which is another limitation for Li-O_2 batteries. The main limiting factors that affect the overall performance of Li-O_2 batteries are summarized in Figure 4.[2]

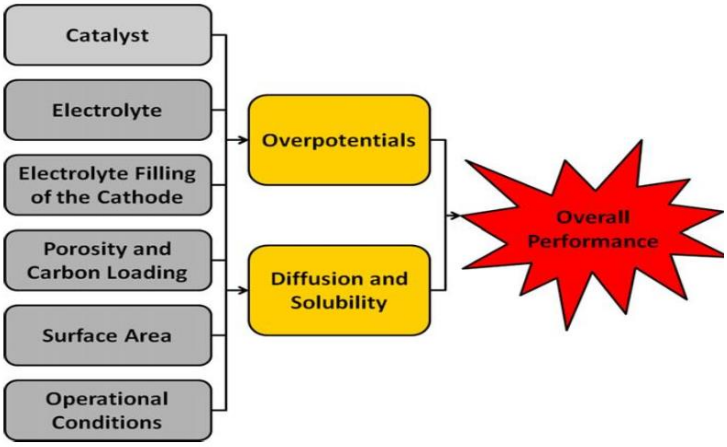

Figure 4: Limiting factors that affect the overall performance of Li-O_2 batteries. Reprinted from ref. [2]. Copyright 2011, with permission of Elsevier.

There are other ways to improve the ORR/OER kinetics. Recently, Mo et al.[63] performed DFT calculations to study the OER of Li_2O_2 in Li-O_2 batteries and found that OER processes are kinetically limited by the high energy barrier for the evolution of O_2 molecules and that the rate of OER processes strongly depends on the surface orientation of Li_2O_2. The kinetics of OER was found slow on the abundant surfaces such as the (11-20) and (0001) surfaces rather than on the high energy surfaces. Therefore, the discharge products of Li_2O_2 with high energy surfaces should be desirable to improve the sluggish kinetics of OER in Li-O_2 batteries.[64] Some of these general challenges are diagrammatically reproduced in Figure 5.[7]

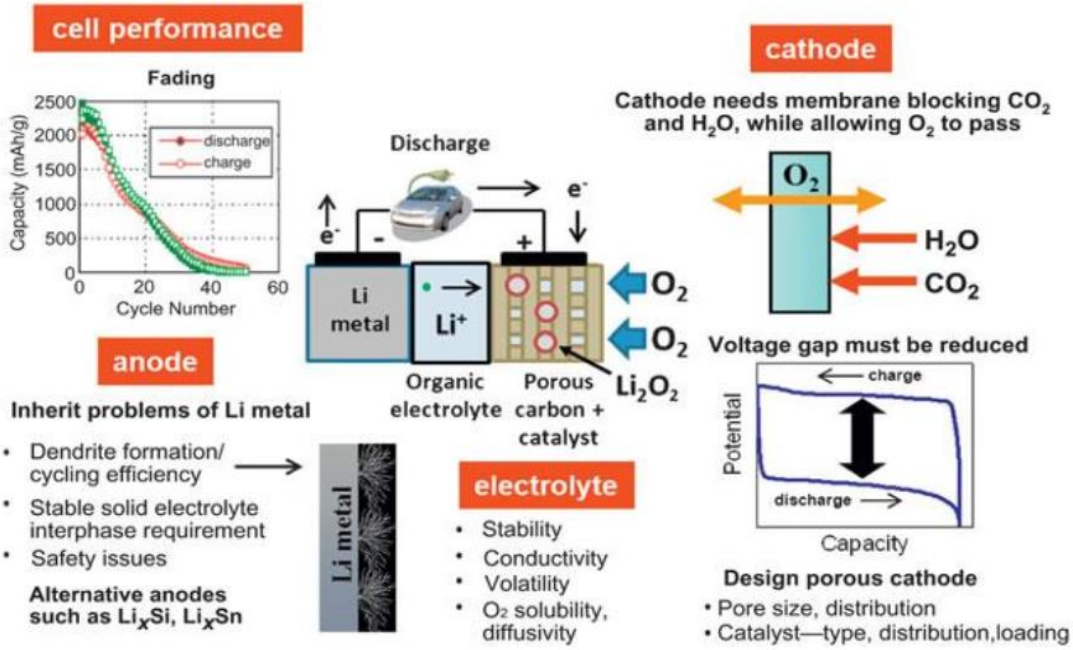

Figure 5 Diagrammatic representation of general challenges in current Li-O_2 batteries. Reprinted with permission from ref. [7]. Copyright 2011 Materials Research Society.

While a number of reviews on the topic of Li-O_2 batteries have been conducted[1, 47, 50, 51, 65, 66] here we present an in-depth critical review based on a combination of experimental and theoretical results. By combining insights from the two approaches, we are able to identify areas for consideration for future research directions. Furthermore, we focus on some recently emerging topics of importance in the experimental section including the formation of Li_2O_2 on Li-O_2 cathodes, crucial operating considerations and the possibility of carbon free cathodes with enhanced stability.

Section 2 Working principles of the aprotic Li-O_2 system

The concept of Li-O_2 chemistry was first introduced by Littauter and Tsai at Lockheed in 1976,[67] but it received little attention until the Li-O_2 battery system with non-aqueous electrolytes

was presented in 1996 by Abraham et al.[68] Such a Li-O_2 battery is comprised of a Li metal anode, a non-aqueous electrolyte and an air (O_2) cathode. The two possible electrochemical reactions are[55, 69]:

$$2Li(s) + O_2(g) \longrightarrow Li_2O_2 \text{ (2.96 V)} \quad (1)$$

$$4Li(s) + O_2(g) \longrightarrow 2Li_2O \text{ (2.91 V)} \quad (2)$$

Equations (1) and (2) are thought to be reversible at extremely applied potentials with discharge products Li_2O_2 and Li_2O. However, Abraham et al.[68] and Bruce et al.[4] proposed that Li_2O_2 is the dominant discharge product with more rechargeability than electrochemically irreversible product Li_2O. Moreover, a recent study remarked that stable Li_2O_2 surfaces are half metallic and those of Li_2O are non-metallic and non-magnetic.[70] In this way, Li_2O_2 can be considered as a more desirable discharge product in Li-O_2 batteries. The discharge/charge reaction in non-aqueous Li-O_2 battery is the oxidation/reduction involving of Li_2O_2 as:

$$2Li^+ + 2e^- + O_2 \longrightarrow Li_2O_2 \text{ (discharge)} \quad (3)$$

$$Li_2O_2 \longrightarrow 2Li^+ + 2e^- + O_2 \text{ (charge)} \quad (4)$$

In a real Li-O_2 battery, the electrochemical reactions break down into anode and cathode as:

$$Li(s) \longleftrightarrow Li^+ + e^- \text{ (anode reaction)} \quad (5)$$

$$2Li^+ + 2e^- + O_2 \longleftrightarrow Li_2O_2 \text{ (cathode reaction)} \quad (6a)$$

$$4Li^+ + 4e^- + O_2 \longleftrightarrow 2Li_2O \text{ (cathode reaction)} \quad (6b)$$

Various mechanisms for O_2 reduction in Li^+ electrolytes have already proposed[62, 71-75] and Bruce[4] suggested a possible mechanism reaction occur at the cathode during discharge as:

$$O_2 + e^- \longrightarrow O_2^- \quad (7a)$$

$$Li^+ + O_2^- \longrightarrow LiO_2 \quad (7b)$$

$$2LiO_2 \longrightarrow Li_2O_2 + O_2 \quad (7c)$$

Here, LiO_2 is an intermediate and unstable, thus decomposes to the more stable Li_2O_2 and releases O_2. Bruce also suggested the charging process mechanism in which oxidation occurs by decomposition as given in equation (4).[76] The schematic operation mechanism of a non-aqueous Li-O_2 battery is shown in Figure 6.[77]

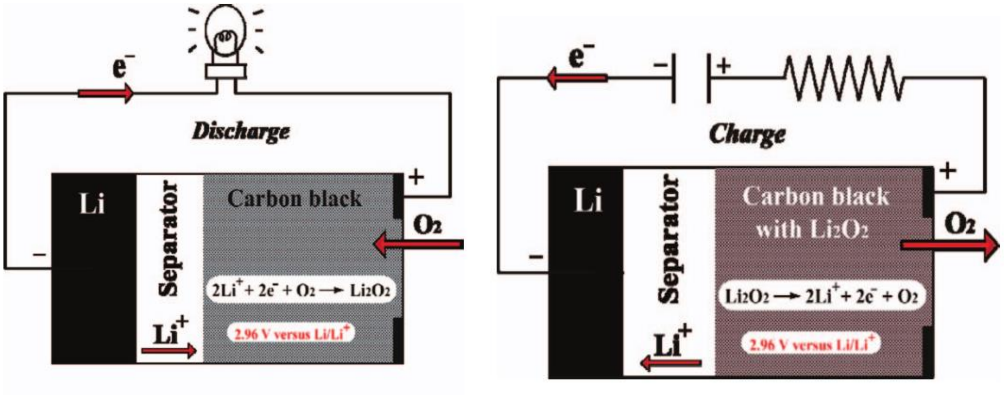

Figure 6 Schematic operation mechanism of a non-aqueous Li-O_2 battery system. Reprinted with permission from ref. [77]. Copyright 2013 The Electrochemical Society.

The precipitation of reactants in the oxygen cathode of the non-aqueous Li-O_2 cell designs is another degradation issue, which limits the capacity of the battery. In such non-aqueous Li-O_2 cell design, the insoluble reaction products formed at the cathode are responsible for passivation of the electrode and cathode pore clogging. Li-O_2 electrochemical reactions get stopped, once the pores are blocked and/or the surface is covered with the reaction products. Thus, the depth of discharge process of non-aqueous Li-O_2 cell is limited by the utilization of cathode. A schematic presentation of the proposed chemistry at the air cathode is shown in Figure 7.[11]

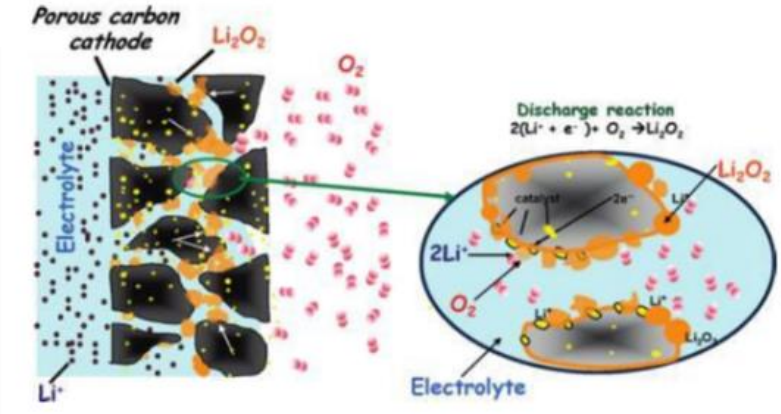

Figure 7 Schematic representation of the air cathode and proposed chemistry at the air cathode. Reprinted with permission from ref. [11]. Copyright 2010 American Chemical Society.

Section 3 - State of the art in experimental Li-O_2 battery research

3.1 Cathode materials

More attention has been devoted to the development of cathodes materials for Li-O_2 batteries than any other component in the system.[2, 13, 35, 36, 46-49, 66, 78-82] From a practical perspective, the ideal material for Li-O_2 cathodes is particulate carbon such as KB, Super P etc. due to its low cost, high surface area, extremely low density and ease of preparation.[5, 83, 84] The light weight of carbon has also afforded some of the highest capacities (per gram) recorded to date. However, the mechanism of Li-O_2 battery operation using pure carbon cathodes has come under intense scrutiny due to poor round trip efficiency and large overpotentials for both discharge and charge (while concerns are also mounting about the stability of carbon)[85], stimulating a wave of research into catalyst materials for carbon based (and also carbon free) systems.[46, 49, 59, 86, 87] Despite this surge of interest, the role of the various catalysts investigated to date (metal oxides, noble metals etc.) remains contentious. The various catalyst materials investigated to date have been the sole focus of a number of reviews.[46-49, 79, 80] The intent of this section is to critically assess the feasibility of each type of cathode material and shed light on the state of the art understanding of the processes occurring at the cathode surfaces. The main focus here will be on insight provided by the various reports in terms of O_2 reduction/evolution catalysis, cycle life improvement and cathode stability. Some issues which are common to every cathode system such as the choice of current collector substrate and the formation of Li_2O_2 on the cathode surface will also be discussed.

a) Li_2O_2 formation on cathodes

While the underpinning operating principle of Li-O_2 batteries has long been established, much recent research has been devoted to developing a greater understanding of the Li-O_2 battery operation in practice through in-depth characterization of batteries under different operating conditions.[41, 52, 54, 88-99] As the formation and decomposition of Li_2O_2 on any cathode surface is

fundamentally important with respect to both the capacity and cycle life of Li-O_2 batteries, this has been a central focus of these investigations. The nature of Li_2O_2 (morphology,[40, 93, 94] crystallinity[100] and location on the cathode[38]) formed during discharge has been probed in several studies with the most commonly noted morphologies for Li_2O_2 as sub-micron spheres/toroids.[41, 56, 101-104] These common morphologies have been noted for a number of different cathode types (pure carbon,[56, 105-109] carbon with catalysts[43, 56, 101, 103],carbon free[110]) and with different electrolytes (ether based,[56, 101, 105, 107, 109] sulfur containing[102, 106] etc.). An example of a typical Li_2O_2 toroid formed on carbon nanofibers is shown in Figure 8 a)[105], while smaller spherical Li_2O_2 particles formed directly on a carbon free, cobalt oxide array can be seen in Figure 8 b).

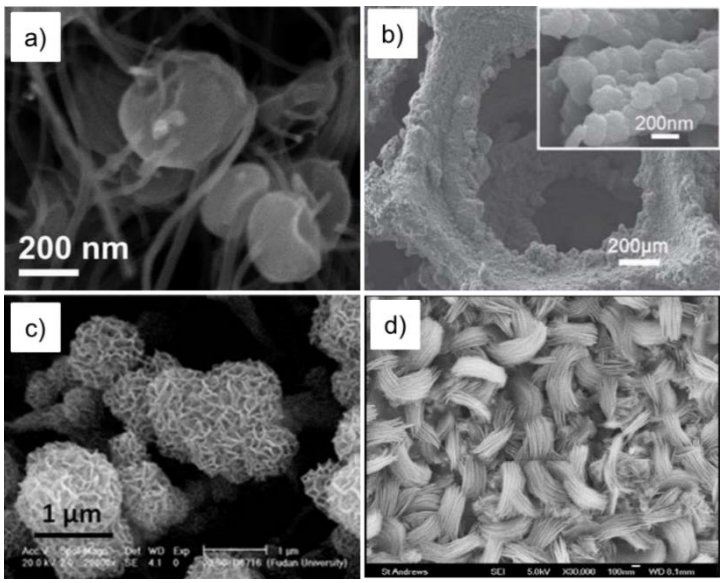

Figure 8 SEM images of the some of the various morphologies of Li_2O_2 formed on different cathode systems. a) Commonly noted Li_2O_2 toroids formed on carbon nanofiber cathode. Reprinted with permission from ref. [105]. Copyright 2011 Royal Society of Chemistry. b) Spherical Li_2O_2 particles formed on Ni foam supported free-standing catalyst cobalt oxide array. Reprinted with permission from ref. [110]. Copyright 2011 Royal Society of Chemistry. c) porous balls of Li_2O_2 deposited on $NiCo_2O_4$ nanowire array. Reprinted with permission from ref. [111]. Copyright 2013 American Chemical Society. d) Layered Li_2O_2 formed on TiC composite electrode. Reprinted with permission from ref. [112]. Copyright 2013 Nature Publishing Group.

It has been found that these at low discharge rates, Li_2O_2 toroids are typically composed of multiple thin layers which splay to form the characteristic 'donut' shape.[96] Given the propensity for

Li_2O_2 formation as a layered material, it is unsurprising that more unusual layered morphologies (Figure 8 c,[111] d[112]) have also been reported for Li_2O_2 formed on Li-O_2 battery cathodes. More unusual porous balls (Figure 8 c) and layered sheets (Figure 8 d) of Li_2O_2 have been reported as the primary discharge products for $NiCo_2O_4$ and TiC composite electrodes respectively. Additional examples of layered discharge products (suggested to be Li_2O_2 but not necessarily confirmed in each case) similar to those presented in Figure 8 c) have also been noted for cathodes based on $MnCo_2O_4$ catalysts[113], Pd/Cu alloy catalyst[114] and MnO_2 nanowires.[115] The role of these catalyst materials in determining the morphology of Li_2O_2 and its implications for decomposition during charge have not been fully investigated and are of interest given the central role played by Li_2O_2 formation in determining Li-O_2 battery capacity and cycle life.

A further investigation into the role of Li_2O_2 in Li-O_2 battery operation was reported recently by Nazar et al. who showed for a given system (Super P carbon on gas diffusion layer cathode and LiTFSI/TEGDME electrolyte) that the morphology and crystallinity of Li_2O_2 formed on the surface of the cathode can be strongly influenced by the applied discharge current. Their results indicated that low applied currents favoured the formation of characteristic, crystalline Li_2O_2 toroids outlined above. Conversely, high applied currents were found to lead to formation of quasi-amorphous thin films of Li_2O_2 on the underlying carbon (depicted schematically in Figure 9). The importance of these observations was further emphasised by the fact that the charge behaviour for the system was found to differ based on the morphology of the Li_2O_2 formed on discharge. It was noted that the large Li_2O_2 toroids, while favouring high capacity compared to the quasi-amorphous films, also led to increased charging overpotentials and inhibited recharge (due to difficulty in decomposition).

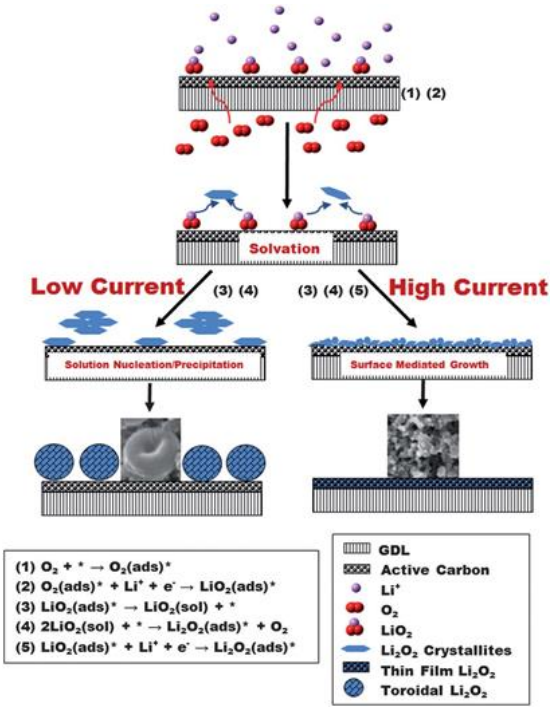

Figure 9 Schematic showing the importance of applied current on the morphology of Li_2O_2 formed on super P carbon cathodes as reported by Nazar et al. Reprinted with permission from ref. [91]. Copyright 2013 Royal Society of Chemistry.

The influence of Li_2O_2 particle size on the recharge behaviour of Li-O_2 batteries was probed by Hu et al. By simply changing the average size of preloaded Li_2O_2 particle on a Super P carbon cathode from 600 nm down to 160 nm, the average charge potential was reduced from 4.45 V to just 4.05 V while the capacity of the cathode was also markedly increased. The impact of catalysts and applied currents on the size, morphology and crystallinity of Li_2O_2 formed upon discharge (and its subsequent decomposition upon charging) is an extremely important research topic given its potential for influencing the capacity and rechargeabililty of Li-O_2 batteries and warrants further study for promising material systems.[91, 112, 116, 117]

b) Porous carbon

Porous carbon (with and without various catalysts) has been ubiquitous in use as the cathode material since the start of the Li-O_2 battery movement.[68, 77, 118, 119] Pure porous carbon cathodes (containing Super P, KB carbon etc. plus binders as shown in Figure 10 a) have typically shown excellent initial discharge capacities but have been hampered by poor cycle life.[87] One such example is shown in Figure 10 c) where the initial discharge capacity of a KB based carbon electrode (almost 3000 $mAhg^{-1}$) rapidly deteriorated upon cycling (down to under 500 $mAhg^{-1}$ at the third discharge cycle). While electrolyte decomposition (which will be discussed in section III) is certainly an issue which hampers Li-O_2 battery cycle life, carbon cathodes have also been found to be extremely unstable over extended discharge/charge cycles.[85, 120] By constructing carbon based cathodes using ^{13}C powder, Thotiyl et al. were able to distinguish between the formation of Li_2CO_3 due to decomposition of the electrolyte (standard ^{12}C TEGDME or DMSO) and the ^{13}C carbon cathodes. As can be seen from Figure 10 b), the amount of $Li_2{}^{13}CO_3$ formed due to the decomposition of the carbon electrode is initially lower than the $Li_2{}^{12}CO_3$ formed due to electrolyte decomposition, however, this trend rapidly reverses with $Li_2{}^{13}CO_3$ present at 10% of the weight of the desired product Li_2O_2 after just 5 discharge/charge cycles. The authors also showed that the main source of carbon electrode decomposition occurs on charging above ≈3.5 V (with smaller amounts of decomposition noted during charge which is consistent with a previous report[121]), meaning that any charging process above 3.5 V is likely to incur the formation of Li_2CO_3 on the cathode surface.

Given the aforementioned issues with carbon cathode stability, several approaches have been explored in an attempt to circumvent (or at least minimize) Li_2CO_3 formation and thus make carbon cathodes more stable. The most simple approach is to operate at a controlled depth of discharge by restricting the discharge to a set capacity figure such as 1000 mAg^{-1} or by reducing the voltage window for discharge and charge (e.g. between 2.4- 4.2V). The benefits of this approach are twofold. Firstly, by avoiding a deep discharge, the cathode is not completely passivated by the insulating Li_2O_2

formed upon discharge. Additionally, due to the fact that the amount of Li_2O_2 formed on the cathode is limited, the cell does not need to be subjected to high voltages during charging and electrolyte decomposition is reduced (Figure 10 b)).[122] However, given the fact that Li_2CO_3 is likely to form at even moderate charging voltages (Figure 10 d),[85] a shift to catalysed carbon cathodes (or the more drastic option of removing carbon from the electrode altogether as will be discussed in section 3i f) must be considered. By product formation that can include Li_2CO_3 is also influenced by the stability of the electrolyte, which stems from the lithium salt's compatibility with it solvent.[123] Specific solvent effects are detailed later in Section 3.2.

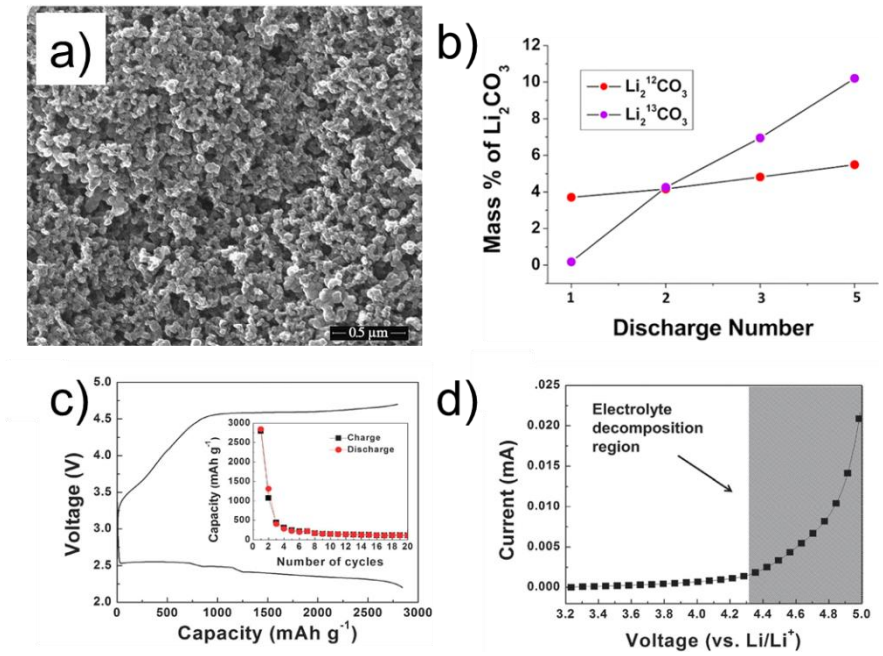

Figure 10 a) SEM image showing the typical Super P/KB composite cathode morphology. Reprinted from ref. [84]. Copyright 2013, with permission of Elsevier. b) Amount of Li_2CO_3 formed as a percentage of Li_2O_2 in the cathode due to the carbon cathode ($Li_2{}^{13}CO_3$) and electrolyte ($Li_2{}^{12}CO_3$). Reprinted with permission from ref. [85]. Copyright 2012 American Chemical Society. c) Example voltage profile of complete discharge/charge cycle conducted between 2.2 and 4.7 V with inset showing the dramatic capacity fading typical for carbon based cathodes under full discharge/charge conditions. Reprinted with permission from ref. [122]. Copyright 2012 Royal Society of Chemistry. d) Cyclic voltammetry of carbon free cathode (i.e. just Li anode, TEGDME based electrolyte and Ni current collector showing the region of electrolyte decomposition. [122]

c) Carbon – Nanotubes and Graphene

Aside from particulate carbons, various other carbon structures (again with and without catalysts) such as carbon nanotubes (CNTs),[92, 94, 124-135] honeycomb-like carbon,[45, 136] mesoporous carbon,[42, 44, 137, 138] microfibers,[139, 140] graphene and its derivatives[8, 26, 108, 141-147] and carbon thin films[148] have been investigated as cathode materials for Li-O_2 batteries. The primary aim of the use of these structures is to increase the surface area of the carbon structure to improve O_2 diffusion while also allowing easier accommodation of Li_2O_2 formed upon discharge.

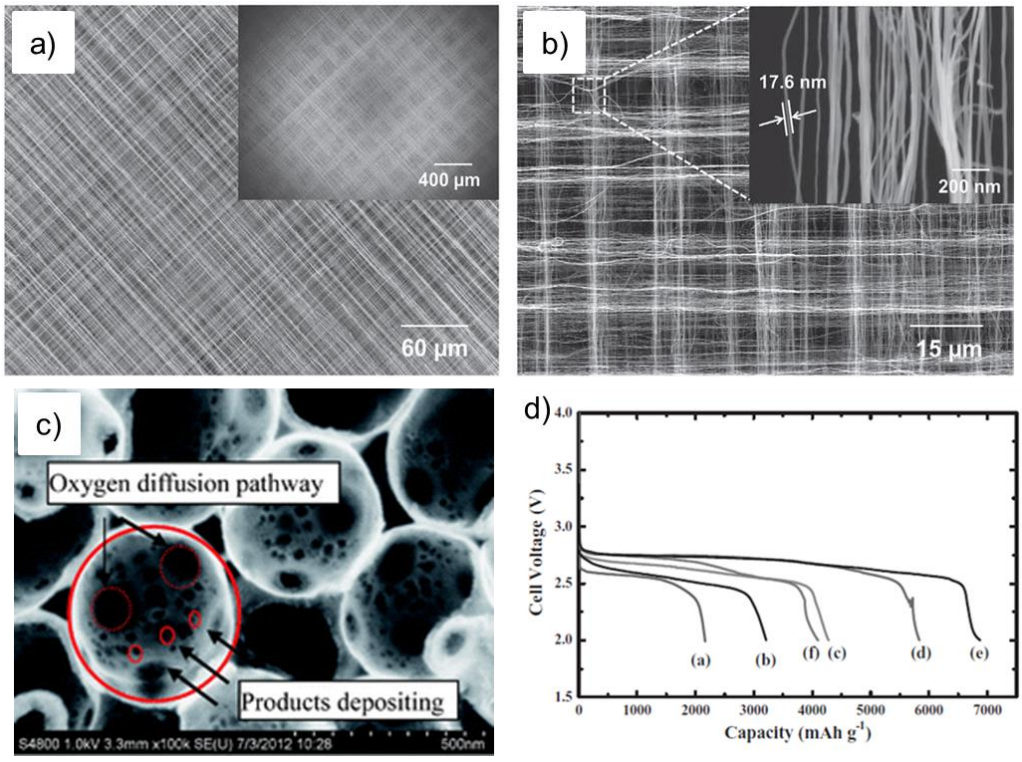

Figure 11 a,b) SEM images of hierarchical-fibril CNT electrode produced by Lim et al. Reprinted with permission from ref. [107]. Copyright 2013 WILEY-VCH Verlag GmbH & Co., KGaA, Weinheim. c) SEM image of honeycomb like carbon. Reprinted with permission from ref. [136]. Copyright 2013 Royal Society of Chemistry. d) Discharge curves of Li-O_2 battery cathodes composed of mesoporous/macroporous carbon sphere arrays (MMCSAs) at varying weight % x (with the remainder composed of Super P 80-x %) and PVDF 20%) a) x=0 b) x=5 c) x=10 d) x=30 e) x=50 f) x=80. Reprinted with permission from ref. [44]. Copyright 2013 WILEY-VCH Verlag GmbH & Co., KGaA, Weinheim.

CNTs are a particularly attractive material for Li-O_2 battery cathodes due to the possibility of making freestanding cathodes composed solely of CNTs, which can eliminate the requirement for weight adding binders.[105, 107, 128, 149] An example of a free standing CNT based fibril electrode produced by Lim et al. is presented in Figure 11 (a,b). The SEM images show an example of the interwoven mesh of CNTs which was formed by alternatively layering sheets of CNTS orthogonal to each other to create a high surface area, free standing structure. The electrochemical behaviour of these woven CNTs was found to be far superior to cathodes formed using standard KB carbon and disordered CNT powder. This superior electrochemical performance manifested as much improved capacity retention when operated in full discharge conditions (cycled between 2.0 V and 4.7 V), while the CNT based electrode could also deliver an impressive capacity of 1000 $mAhg^{-1}$ over 60 discharge/charge cycles when operated at a limited depth of discharge. Similarly impressive capacity retention figures at limited depth of discharge were presented by Chen et al. for multi-walled CNT papers formed using a floating catalyst method employing ferrocene as the Fe catalyst precursor.[128] While the formation of Li_2O_2 on CNT based cathodes has been confirmed through the use of XRD analysis,[128, 149] additional analyses are required to fully gauge the stability of CNT based cathodes in similar manner to that discussed for particulate carbon. Furthermore, the extremely low mass loadings common for CNT based cathodes (e.g. 0.016 mg cm^{-2})[107] may be insufficient to power practical devices. Nevertheless, CNTs represent an exciting class of possible cathode materials which can massively outperform standard particulate carbons. An addition benefit of CNTs is that, due to their high aspect ratios, CNTs represent a far more practical platform than particulate carbon for studying the formation and disappearance of Li_2O_2 on discharge and charge of Li-O_2 batteries using both *ex-situ*[96, 150] and *in-situ*[88, 99] methods as they allow clearer visualization of the discharge product morphology.

Mesoporous carbons have also fostered interest as Li-O_2 battery cathode materials due to their high degree of porosity which can facilitate effective electrolyte immersion and accommodation of Li_2O_2 within the pores (Figure 11 c).[42, 44, 137, 138, 151] Park et al. compared the performance of

mesoporous carbon cathodes with those composed of pure Super P carbon and found that the charge voltage was substantially reduced for the former. While crystalline Li_2O_2 was confirmed post-discharge on the Super P cathode as expected, the mesoporous carbon cathodes showed no evidence for crystalline Li_2O_2 leading the authors to propose that the primary discharge product was in fact amorphous Li_2O_2 (formed within the pores of the mesoporous carbon) which facilitated lower charge voltages.[137] The possible formation of amorphous Li_2O_2 as the primary discharge product has been proposed in the presence of RuO_2 nanoparticle catalysts,[100] however, its formation by simply constraining the Li_2O_2 product within the pores of a carbon host (and the associated reduction in overpotentials for both charge and discharge processes) would be beneficial.

Similarly, Guo et al. showed that a mesoporous/macroporous composite facilitated much higher discharge capacities than standard Super P carbon cathodes.[44] In Figure 11 d) it can be seen that a maximum initial discharge capacity was achieved when the cathode was composed of 50 % mesoporous carbon and 30 % Super P carbon (the remaining 20 % was a fixed percentage of binder) which was over three times higher than the pure Super P cathode. In comparison, the pure mesoporous carbon sample (sample f) showed reduced capacity compared to the optimum composition which was attributed to decreased mechanical strength (and associated delamination) of the pure mesoporous carbon cathode. Unfortunately the crystallinity and morphology of the Li_2O_2 formed in these tests was not probed. Likewise, another report detailing the use of a honeycomb like carbon as the cathode material used a carbonate based electrolyte which (as will be discussed in section 3) led to the formation of Li_2CO_3 as the primary discharge product rather than the desired Li_2O_2. High surface area, mesoporous carbons could prove to be a particularly useful class of cathode material for Li-O_2 batteries given the initial promising results discussed here, however, the stability of the carbon in the electrodes and the nature and reversibility of Li_2O_2 formation needs further investigation.

d) Carbon based Metal Oxides

Various metal oxides materials (MnO_2,[4, 14, 115, 124, 126, 131, 152-169] Co_3O_4,[110, 170-177] CoO,[178, 179] Fe_3O_4,[180] mixed Co/Mn oxides,[113, 181, 182] perovskites,[183-188] $NiCo_2O_4$,[111] $Na_{0.44}MnO_2$[103], $LaFeO_3$[189] etc.) have been investigated for use in Li-O_2 battery cathodes with the vast majority probed as carbon based composites. Despite their widespread usage, the actual mechanism for operation is not fully understood. In fact, it has been suggested that the enhanced capacities noted for the most common metal oxide catalyst MnO_2 may actually be due to enhanced decomposition of the electrolyte/carbon host.[190] Another issue which complicates elucidation of the contribution of the catalyst material to both discharge and charge capacities comes from the fact that the vast majority of reports express capacity in terms of $mAhg^{-1}_{carbon}$ even when a significant portion of the cathode mass is composed of the metal oxide catalyst. Due to the presence of both carbon and metal oxides in these cathodes, these systems are extremely complicated and to date, the enhanced formation and decomposition of Li_2O_2 (compared to pure carbon cathodes) has not been conclusively shown.

Despite these issues, reduced overpotentials (particularly on charging) have been regularly reported for metal oxide/carbon cathodes when compared to their pure carbon analogues. Two examples of reduced overpotentials on charge can be seen for Co_3O_4/reduced graphene oxide[101] (Figure 12 a) and $MnCo_2O_4$[113] microspheres (Figure 12 b). It is worth noting that the discharge potentials in each case are very similar to the pure carbon cathodes, suggesting limited ORR activity by the metal oxides. In future, research should ideally aim to assess the reversible formation of Li_2O_2 and the level of byproduct formation (e.g. Li_2CO_3 and LiOH) for mixed metal oxide/carbon cathode systems. A characteristic fingerprint of the electrochemical performance of the pure metal oxide materials (through either constant current or CV measurements) would also be useful for gauging ORR and OER activity and possible byproduct formation. As non-precious metal catalysts for Li-O_2 batteries have been the sole focus of other review articles, they will not be dwelled on in this section.[46, 49, 80,65] Metal oxide catalysts are well places as lower cost alternatives to precious metals and the well-established synthetic strategies for the formation of metal oxides in high yields[165, 191-194]

suggest that they will continue to be investigated as catalysts for Li-O_2 battery cathodes. Reports into the true stability of electrolytes in the presence of metal oxide catalysts and the role of the catalysts in facilitating Li_2O_2 formation and decomposition are urgently required.

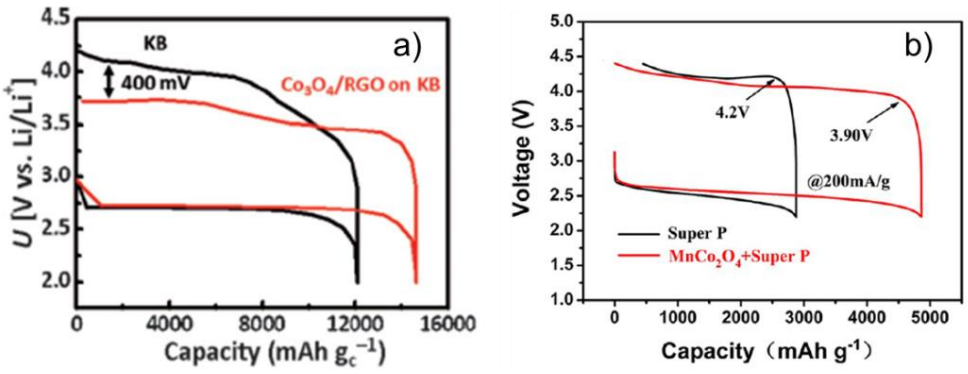

Figure 12 The initial discharge/charge cycle shown for cathodes composed of a) Co_3O_4/RGO cathode compared to KB. Reprinted with permission from ref.[101]. Copyright 2012 WILEY-VCH Verlag GmbH & Co., KGaA, Weinheim. b) Initial discharge/charge for $MnCo_2O_4$/Super P compared with pure Super P. Reprinted with permission from ref.[113] . Copyright 2013 American Chemical Society.

e) Carbon based Noble Metals

Noble metal catalysts (Au,[86, 195-197] Pd,[40, 132, 195, 198-200] Pt[55, 195, 200-204] Ag,[55, 200, 205, 206] and noble metal alloys[59, 207, 208]) have also been the subject of attention as catalysts for Li-O_2 batteries. As was the case for metal oxide catalysts, the majority of reports detailing the catalytic activity of noble metals for Li-O_2 cathodes have been investigated as carbon composite electrodes. Given the propensity for carbon cathode decomposition discussed above and the possibility of misleading electrochemical responses due to catalyst driven electrolyte decomposition, the use of noble metal/carbon cathodes requires careful study.

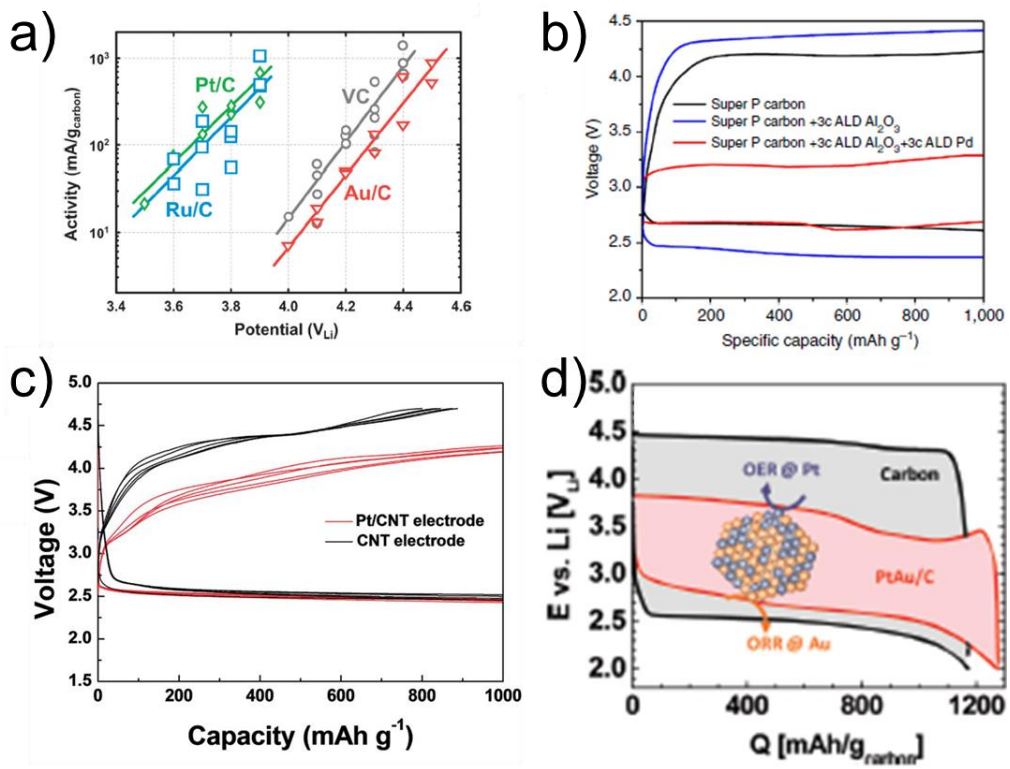

Figure 13 a) OER activity vs. potential for the charging of Pt/C,Ru/C,Au/C and VC cathodes. Reprinted with permission from ref. [86]. Copyright 2012 Royal Society of Chemistry. b) Impact of Al_2O_3 passivation and Pd nanoparticle catalysts on the discharge and charge voltages of Super P carbon cathodes. Reprinted with permission from ref. [199]. Copyright 2013 Nature Publishing Group. c) Discharge and charge curves for CNT electrode and Pt nanoparticle embedded CNT cathode. Reprinted with permission from ref. [202]. Copyright 2013 Royal Society of Chemistry. d) comparison of the discharge/charge processes for pure carbon and Pt/Au nanoparticle catalyst containing carbon cathode. Reprinted with permission from ref. [59]. Copyright 2010 American Chemical Society.

Harding et al. investigated the effect of the addition of noble metal catalysts (40 weight % of 50 nm nanoparticles composed of Au, Pt or Ru) on the charging behaviour of carbon based cathodes preloaded with Li_2O_2 particles.[86] It should be noted that the morphology and surface chemistry of the Li_2O_2 in this study may vary from electrochemically formed Li_2O_2, however, their results indicated that Ru/C and Pt/C cathodes exhibited much higher catalytic activities than Au/C cathodes which were in fact only comparable with pure C cathodes (Figure 13 a)).

The inactivity of Au as an OER catalyst is consistent with the results presented by McCloskey et al. in their study which used DEMS analysis to quantify gas evolution during the charge of

different catalyst materials (MnO_2,Au and Pt).[190] In fact, Au has been found to be a far more effective ORR catalyst which can improve the discharge behaviour of cathodes (rate capability, reducing discharge overpotentials etc.)[56], however, these benefits may be negated in a practical system when considering the cost of Au and the real capacity improvement of the cathode once the mass of Au is taken into account. The impact of ORR catalysts in determining the morphology and crystallinity of Li_2O_2 formed on cathodes during Li-O_2 battery operation has not been widely studied and is critically important given its central role as discussed in this review.

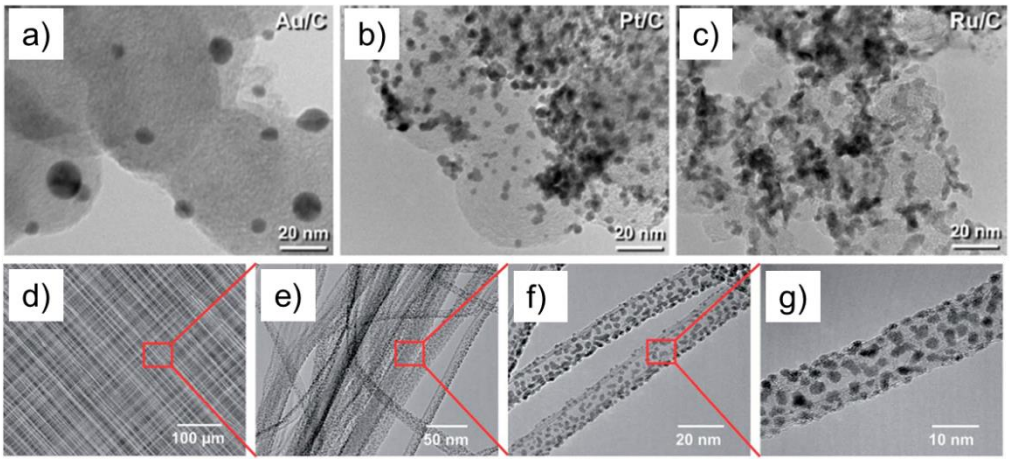

Figure 14 a-c) TEM images of Au,Pt and Ru nanoparticle catalysts supported on Vulcan carbon. Reprinted with permission from ref. [86]. Copyright 2012 Royal Society of Chemistry. d-g) SEM (d) and TEM (e-f) images of Pt nanoparticle catalysts embedded on CNTs. Reprinted with permission from ref. [202]. Copyright 2013 Royal Society of Chemistry.

Pd has been highlighted as a particularly effective ORR catalyst material.[200] In light of this, Lu et al. investigated the impact of atomic layer deposition formed Pd nanoparticles (in conjunction with Al_2O_3 passivation) on the discharge and charge voltages of Super P carbon based cathodes. Their results (Figure 13 b) showed that while Al_2O_3 passivation alone actually increased the overpotential on both discharge and charge, the subsequent addition of Pd nanoparticles resulted in a marked reduction in the charge voltage (to below 3.25 V from above 4 V). Unlike in the case of Au catalyzed cathodes where decreased overpotentials were noted for discharge,[56] the Pd decorated cathodes showed nearly identical discharge voltages to the pristine carbon cathodes. While the

authors confirmed the presence of characteristic crystalline Li_2O_2 toroids on the cathode surface after discharge, the role of Pd in facilitating such dramatic reductions in the charge voltage was not made clear. Additionally, the authors claimed that Al_2O_3 was capable of supressing electrolyte decomposition but characterization techniques to verify this were not included. The charge behaviour of pure Pd nanoparticle catalyzed cathodes in this study showed markedly higher potentials suggesting a strong interplay between the Al_2O_3 and Pd nanoparticles. Additional investigations into this cathode system are required to ensure that the extremely low charge voltage was in fact due to the catalyzed decomposition of Li_2O_2 on the cathode rather than just electrolyte decomposition or byproduct formation. The behaviour of this cathode system (in terms of byproduct minimization) over extended discharge/charge cycles would also be of interest.

The use of Pt as a catalyst material for CNT based cathodes was investigated by Lim et al. (Figure 13 c).[202] Their Pt nanoparticle embedded CNTs showed strongly reduced charging potentials (circa 500 mV reduction) compared to pure CNTs with this reduction consistent with the catalytic activity of Pt suggested in Figure 13 a). Their Pt/CNT cathodes showed a stable capacity of 1000 mAg^{-1} for over 120 discharge/charge cycles. More importantly, when the cathodes were cycled within a wide electrochemical window (i.e. full discharge conditions) between 2.0 V and 4.7 V, good capacity retention was noted with the discharge capacity above 1500 mAg^{-1} after 80 cycles. Caution must be exercised to ensure that the perceived catalytic activity of Pt catalysts presented in Figure 13 c)[202] is solely due to enhanced Li_2O_2 decomposition rather than largely due to electrolyte decomposition as shown in the report by McCloskey et al. where significant CO_2 was evolved for a Pt catalyzed cathode during the charging process.[190] However, the authors did show that the formation and decomposition of Li_2O_2 were the dominant electrochemical processes for at least the early discharge/charge cycles.

The concept of using alloyed nanoparticle catalysts has been more sparingly studied than their single element counterparts.[59, 207, 208] However, this approach has immense potential as it

allows OER properties from one material to be combined with ORR properties of another. This concept was confirmed by Lu et al. who showed that alloyed Pt/Au nanoparticles could act as bifunctional catalysts with ORR activity due to the Au and OER activity coming from the Pt.[59] These effects were manifested in the lowering of overpotentials for both the charge and discharge processes as shown in Figure 13 d) with the marked reduction in charge potential of particular importance. It should be noted that this study of Pt/Au nanoparticle catalysts was conducted using a carbonate based electrolyte system with the apparent catalytic effect likely due to unwanted side reactions. In future, it is crucial that the true catalytic nature of these alloyed nanoparticle catalysts is ascertained (i.e. enhanced Li_2O_2 formation and decomposition on charge and discharge respectively).

Noble metal catalysts within carbon matrices are an ideal platform for investigating the fundamental electrochemical processes involved in Li-O_2 battery operation. Noble metal nanoparticles can easily be formed using solution based growth methods[209-211] and then embedded on particulate (Figure 14 a-c) or CNF (Figure 14 d,e) type supports. While these materials may be prohibitively expensive from a practical viewpoint in terms of scale up (considering that they may account for e.g. 40 % of the cathode mass), much information can still be garnered from future studies using noble metal catalysts and their alloys. These could take the form of investigations on catalyst bifunctionality, the impact of ORR catalysts on Li_2O_2 morphology and catalyst driven electrolyte decomposition.

f) Carbon-free cathodes

Recently, several reports have investigated the use of carbon-free cathodes for Li-O_2 battery applications. While these materials (nanoporous Au,[197] TiC,[112] Ru/ITO[212], Co_3O_4 on Ni[110, 172]) are inescapably more dense than carbon (reducing gravimetric capacity), they have exhibited the most promising stabilities of any systems to date and perhaps represent the most promising material set

for truly rechargeable Li-O_2 battery cathodes. The primary challenge for carbon-free cathodes is to create inexpensive, lightweight electrochemically active materials with a high degree of porosity to accommodate Li_2O_2 formed during operation.

The first carbon-free cathode architecture examined by Cui et al. (depicted schematically in Figure 15 a)) consisted of Co_3O_4 nanorods grown directly on a Ni foam current collector using CVD. Electrochemical analysis of the cathode showed a dramatic reduction in the charge potential, with the majority of charging occurring at circa 3.75 V (at a current density of 0.1 $mAcm^2$). XRD and FTIR analysis suggested that the primary electrochemical process occurring during the single discharge/charge cycles investigated involved the formation/decomposition of Li_2O_2 as desired.

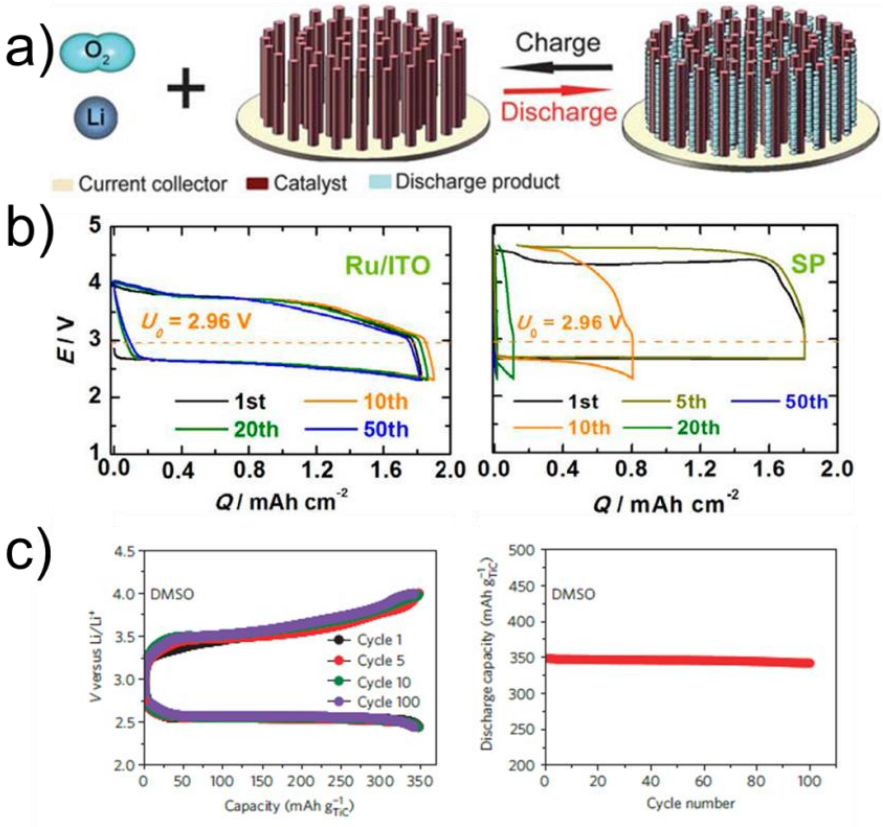

Figure 15 a) Schematic depiction of the carbon free cathode architecture developed by Cui et al. Reprinted with permission from ref. [110]. Copyright 2011 Royal Society of Chemistry. b) Cycling performance of Ru/ITO cathode compared with that of a reference pure Super P cathode. Reprinted with permission from ref. [212]. Copyright 2013 American Chemical Society. c) Cycling behaviour of TiC cathode in DMSO based electrolyte showing capacity retention over 100 cycles. Reprinted with permission from ref. [112]. Copyright 2013 Nature Publishing Group.

The next carbon-free system investigated was a nanoporous Au cathode developed by Peng et al.[197] This report gave clear insight into the benefit of carbon-free cathodes and was in effect the first truly rechargeable Li-O_2 system. As the role of this cathode in circumventing electrolyte decomposition was crucial to its outstanding performance, it will be discussed in more detail in section 3.2 which deals with electrolyte stability. An ITO supported Ru nanoparticle cathode recently developed by Li et al. exhibited excellent capacity retention for up to 50 discharge/charge cycles and charging voltages below 4 V. This capacity retention compared extremely favourably with a common Super P carbon cathode also investigated in the study (Figure 15 b). XPS and IR analysis also confirmed the dominant formation/decomposition of Li_2O_2 and limited formation of Li_2CO_3 which is central to a rechargeable system. While this catalyst system showed excellent stability, its gravimetric capacity was not detailed and the cost of Ru may be a hurdle to widespread use.

In an effort identify a more cost effective alternative cathode material to NPG, Thotiyl et al. examined the use of TiC based cathodes.[112] Along with greatly reduced cost in comparison to Au, TiC is also less dense and was shown to exhibit similarly excellent stability for up to 100 cycles (Figure 15 c). The TiC cathode was able to deliver a reversible capacity of 350 $mAhg^{-1}_{TiC}$ with the reversible formation/decomposition of Li_2O_2 verified when using a DMSO based electrolyte. The authors also stressed that the TiC material investigated was not an optimized morphology (i.e. the cathode did not boast high surface area, high porosity etc.) suggesting that there is room to further enhance the performance of TiC based cathode systems.

As the morphology of carbon-free cathodes is likely to be hugely important in maximizing their gravimetric energy density, SEM and TEM images of the various carbon-free cathodes examined to date are shown in Figure 16. The highly porous Co_3O_4 nanorod/Ni foam cathode architecture developed by Cui et al. (Figure 16 a,b) shows highly dense Co_3O_4 nanorod grown on the supporting Ni current collector and large spaces for O_2 diffusion.[110] The two carbon-free cathode systems developed by researchers in the Bruce group are shown in Figure 16 c,d (NPG[197] and TiC

respectively[112]). While pores are evident in the structure of the NPG cathode, the TiC cathode material appears in large clumps of particles consistent with the non-optimized morphology mentioned in the previous paragraph. Likewise, the Ru/ITO composite shown in Figure 16 e,f) is composed of large particles agglomerated together and may benefit from being formed in a more optimal geometry (for example like that shown in Figure 16 a) in future. The nanoneedles shown in Figure 16 g-i) are actually only one example of the morphologies of the Co_3O_4 catalysts formed on Ni foam by Riaz et al. In this report, nanosheets and nanoflowers were also formed by varying the synthetic process with the enhanced capacities reported for the nanoneedles attributed to more active sites for ORR and better accommodation of Li_2O_2. The promising stability of carbon-free cathodes warrants further investigation.[213] Ideally these cathodes should be investigated as hierarchically porous structures such as those presented by Cui et al. to ensure maximization of the gravimetric energy density.

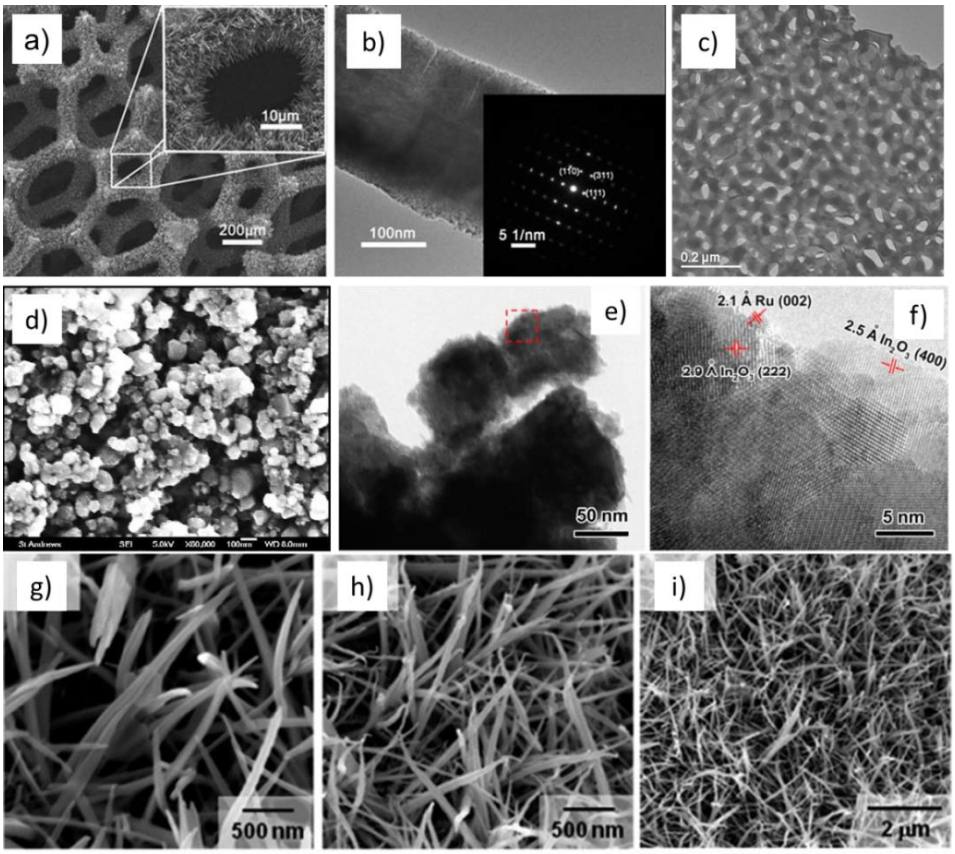

Figure 16 SEM and TEM images of various carbon-free Li-O_2 battery cathode systems. a),b) Co_3O_4 nanorods on Ni mesh. Reprinted with permission from ref. [110]. Copyright 2011 Royal Society of Chemistry. c) NPG cathode. Reprinted with permission from ref. [197]. Copyright 2012 AAAS

publication. d) SEM image of TiC cathode material. Reprinted with permission from ref. [112]. Copyright 2013 Nature Publishing Group. e),f) TEM images of Ru/ITO cathode system. Reprinted with permission from ref. [214]. Copyright 2013 American Chemical Society. g)-i) SEM images of Co_3O_4 nanoneedle arrays. Reprinted with permission from ref. [172]. Copyright 2013 Royal Society of Chemistry.

g) Operational considerations

Outside of the active materials discussed in the previous section, several considerations are required in the design of any practical Li-O_2 battery. These include whether the system is operated in an open (i.e. using air)[198, 215-218] or closed (using pure O_2) geometry, the impact of the operational temperature and the current collector being used. These considerations are likely to play a key role in the future success of the Li-O_2 battery and warrant discussion and further study.

The vast majority of Li-O_2 batteries to date have been operated in a closed geometry to avoid the ingress of moisture and atmospheric contaminants (most notably CO_2).[219, 220] It is widely accepted that a closed geometry is the most promising option for Li-O_2 design in the short-term as no membranes have been shown to prevent H_2O and CO_2 ingress to the desired degree.[66] While the use of a closed geometry for Li-O_2 batteries may necessitate the use of a bulky O_2 tank (which may lead to a decrease in the gravimetric capacity for vehicular applications), it also allows operation at O_2 pressures greater than 1 atm to be probed. In separate reports, Yang[221] and Nemanick[222] showed that initial discharge capacity and rate capability of carbon based cathodes could be dramatically increased by merely increasing the O_2 pressure. In the former report, at a high applied current of 1000 μAcm^2, the discharge capacity could be increased by a factor of 6 (Figure 17 a) by merely increasing the O_2 pressure from 1 atm to 10 atm. The rechargeability of these increased pressure systems was not probed and warrants investigation as the removal of the Li_2O_2 from cathodes discharged at higher pressures may not be a trivial issue. Nevertheless, this approach may be a means of offsetting the capacity losses due to the increased weight of the device due to the likely requirement of operating in a closed system configuration.

The impact of temperature on the operation of Li-O_2 batteries has not received much attention to date which is surprising given that the ultimate goal is to incorporate these devices in automotive applications where temperatures may fluctuate substantially (depending on the geographic location, time of year etc.).[223-225] One report by Park et al. investigated the discharge and charge of carbon based cathodes at a limited depth of discharge/charge (1000 $mAhg^{-1}$) and found substantially different discharge and charge voltages (Figure 17 b) at different temperatures. For the discharge voltages, a 0.4 V difference was noted for a cathode discharged at -10 °C (≈ 2.4 V) compared to that the cathode discharged at 70 °C (≈ 2.8 V). More strikingly, the charge voltages in the same temperature range showed a massive difference of approximately 1.2 V, with lower temperatures leading to increased charge overpotentials. This observation has major implications for the practical adoption of Li-O_2 batteries as such high charging potentials at low temperatures will likely lead to substantial cathode and electrolyte degradation and may greatly impact the cycle life of the battery. The authors used H-NMR to investigate possible side product formation in this system and while their results suggest minimal electrolyte decomposition, only the cathodes discharged at 25 °C and 70 °C were investigated. They also suggest that low discharge temperatures (25 °C) favour the formation of crystalline Li_2O_2 while higher operating temperatures (50 °C and 70°C) resulted in mostly amorphous Li_2O_2 being formed. Such a profound influence on the operation of Li-O_2 warrants significant further investigations. Additionally, because the authors did not investigate the cycle life and operated at a controlled depth of discharge, the influence of temperature on the full discharge capacity of Li-O_2 batteries and capacity retention over extended cycles remain open issues.

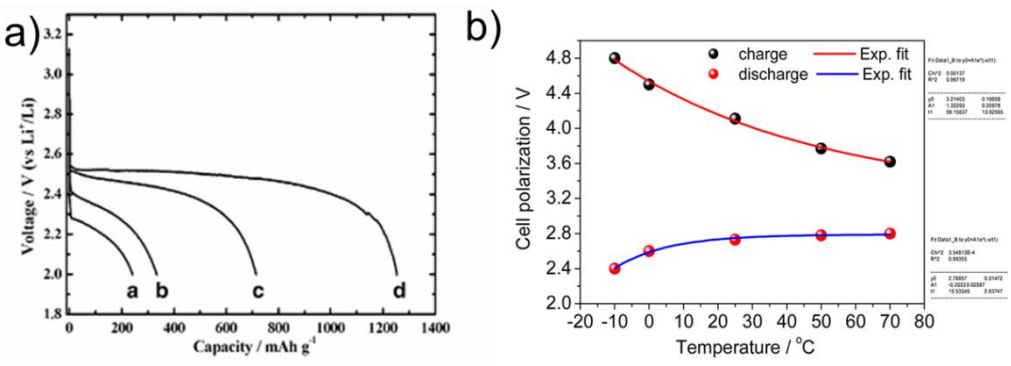

Figure 17 a) Impact of O_2 pressure as reported by Yang et al showing the discharge curves at pressures of a) 1 atm, b) 3 atm, c) 5 atm, and d) 10 atm. Reprinted with permission from ref. [221]. Copyright 2012 Springer Publishing Company. b) Influence of temperature on Li-O_2 battery charge and discharge voltages. Reprinted with permission from ref. [225]. Copyright 2013 American Chemical Society.

A key and only sparingly acknowledging issue is the importance of the cathode current collector substrate.[226] Given the requirement for a high surface area cathode to allow O_2 diffusion and discharge product formation and accommodation, a wide range of current collectors have been examined. These have primarily taken the form of carbon paper/ gas diffusion layers (GDLs)[127, 173, 227-230] and metal meshes and foams (e.g. stainless steel,[85, 112, 129, 197] Ni[5, 106, 116, 172, 231, 232] and Al[87, 233]). The concept of inert versus active current collector substrates has not been widely discussed in the literature to date. From the perspective of a final device, active cathodes (which participate in ORR and OER) such as GDLs and carbon papers are attractive as they minimize dead-weight in the device and are lighter than their metal counterparts, however, the contribution to these cathodes to the discharge time is often ignored, which can lead to overstated capacities. While the capacity of the current collectors may be low (i.e. $mAhg^{-1}_{current\ collector}$) it is the additional time added to the overall discharge time of the cell that should be factored in to the calculation. Furthermore, the instability of nominally inactive current collectors (e.g. Ni[226]) in certain electrolytes must be considered as this factor can hamper cycle life. Other issues do surround reports on Li-O_2 batteries cathodes. Many studies do not take into account the weight of catalyst materials and auxiliary materials such as binders when quoting capacities which again can lead to inflated capacity values. Similarly, the vast majority of studies to date have considered only cathodes with extremely low mass loadings of active material (often of the order of 1 mg cm^2) in an effort to maintain porosity and maximize capacity figures which may not be suitable for real world applications. In considering capacities, total cathode mass (including current collector) or at least total cathode mass (all material on the current collector) should be considered for clarity.

h) Cathodes-conclusions

This section has discussed some of the major considerations for each of the main types of cathode systems currently under investigation in Li-O_2 batteries. Outside of these materials, a wide range of other catalysts have also been investigated to a lesser extent (Ru based,[234-238] nitrides[140, 239-241], selenides[242] cobalt phthalocyanine[243],CuFe catalyzed carbon[244], lead ruthenate pyrochlore,[245] mesoporous $NiCo_2O_4$ nanoflakes[246], metal organic frameworks[247] etc.), yet mechanistic insight for these materials remain elusive. The role of the various catalyst materials in the reversible formation and decomposition of Li_2O_2 and prevention of byproduct formation is a key issue which warrants further study. Another possible concept to improve the charging efficiency of Li-O_2 batteries is to incorporate a redox mediator such as tetrathiafulvalene[9] into the electrolyte to aid in the decomposition of Li_2O_2. Redox mediators function by being oxidized during the charging process and in turn aid oxidation of Li_2O_2.

As it stands, very few cathode systems have been shown to be truly stable over extended discharge/charge cycles and typically used carbon cathodes have been found to be highly reactive in the presence of Li_2O_2 and its intermediates. It is now clear that the stability of any promising cathode/electrolyte system must be verified using a wide range of techniques (Raman,[112, 197, 248, 249] FTIR,[112, 197, 248] NMR,[52, 54] Mass-spectrometry,[98, 112, 197, 249-251] XPS,[90, 157, 248, 252-256] Nonresonant Inelastic X-ray Scattering[53] etc.). Relying on solely XRD to confirm Li_2O_2 formation/decomposition is not sufficient given the wide range of amorphous byproducts which can be formed upon cycling and possibility that Li_2O_2 may be amorphous.[257] The most stable cathode systems are those which do not contain particulate carbon (the stability of CNTs and other carbon related materials remains an open issue), and optimization of the morphology of these materials seems a promising route to improving their limited gravimetric capacities.

In the next section, the role of the electrolyte in Li-O_2 battery operation will be probed. It will be shown that the identification of a stable electrolyte is just as important as the development of novel

cathode systems. It should also be stressed that electrolytes cannot be examined in isolation and that a wide range of electrolyte/salt combinations must be assessed for each promising cathode system.

3.2 Electrolytes

A wide range of electrolytes have been examined for use in Li-O_2 battery applications. Initially, carbonate based electrolytes were investigated, however, these were found not to facilitate rechargeable systems due to their propensity for decomposition and associated Li_2CO_3 formation. The discovery of stable electrolytes for Li-O_2 batteries is absolutely paramount if they are to reach the required cycle life (i.e. hundreds of cycles) required for real world applications. The following section will examine the more prevalent electrolytes used to date in Li-O_2 batteries with particular emphasis on electrolyte stability with respect to decomposition (and associated byproduct formation). The reports highlighted here illustrate the importance of using multiple analytical techniques to examine the true stability of electrolytes. It will also be clear from this section that electrolytes cannot be considered in isolation, i.e. the electrolyte must be considered with the cathode system it is being coupled with as this determines the reactivity of the electrolyte. Readers are directed to the review by Balaish[51] for further insight and discussion into some alternative electrolyte solvents such as nitriles,[62, 258] amides,[233, 259, 260] silanes[261] and esters.

a) Carbonates

Given the position of Li-O_2 batteries as a 'beyond Li-ion' technology, it is unsurprising that initial investigations into Li-O_2 batteries focused primarily on organic carbonate electrolytes given their widespread use in Li-ion batteries.[262-265] In fact, the first report of a Li-O_2 battery reported by Abraham et al. in 1996 used a solid electrolyte composed of ethylene carbonate, propylene

carbonate, polyacrylonitrile and $LiPF_6$ (40:40:12:8 weight respectively).[68] Their initial breakthrough gave insight into the potential high capacities achievable for Li-O_2 batteries while preliminary results suggested the formation of Li_2O_2 rather than Li_2O as the dominant discharge product. Read et al. subsequently examined the performance of liquid electrolytes consisting of various different carbonate mixtures in 2002.[14] This study showed the importance of electrolyte in determining the performance of Li-O_2 batteries while an additional study from the same author in 2003 showed that O_2 transport within electrolytes also played a major role in determining capacity.[266] Carbonate based electrolytes continued to be the widely used[4, 5, 57, 74, 87, 152, 217, 231, 267-270] until their instability was identified by several research groups through the use of various analytical techniques.[248, 271-275] The first report confirming this was by Mizuno et al. who showed using Fourier transform infrared (FTIR) spectroscopy that the primary discharge products formed using carbonate based electrolytes even after a single discharge were actually Li_2CO_3 and Lithium alkylcarbonates rather than the expected product Li_2O_2.[272]

The instability of carbonate electrolytes was unequivocally illustrated by McCloskey et al. by combining a variety of techniques for the characterization of cathodes under discharged and charged states.[249] By combining X-ray diffraction, Raman spectroscopy and differential electrochemical mass spectrometry (DEMS) the authors were able to probe the operation of Li-O_2 batteries in much greater depth than previously achievable. The use of isotope labelled, *in-situ* DEMS analysis (Figure 18) allowed quantification of the O_2 and CO_2 evolved during the first charge for three electrolyte systems (a) DME, b) EC/DMC and c) PC/2DME).

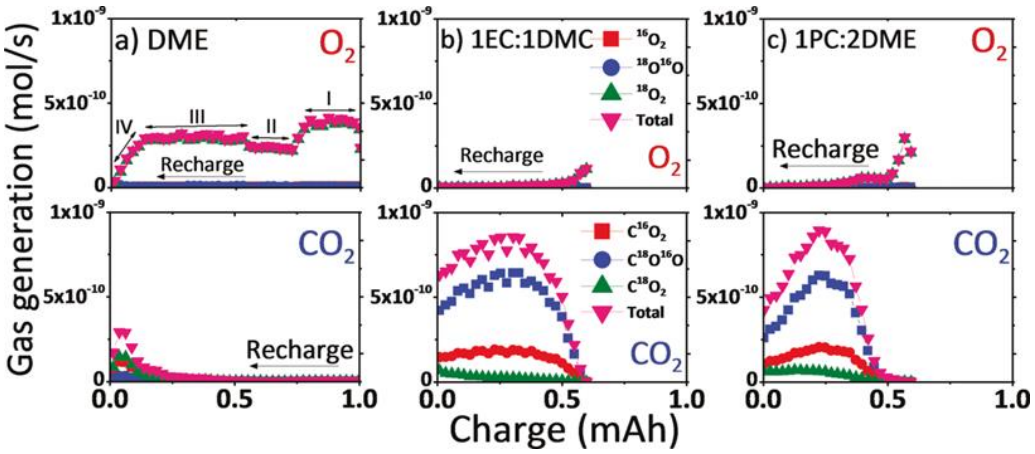

Figure 18 Gas evolution profiles (O_2 and CO_2 upper and lower respectively) for cathodes charged using DME (a), EC/DMC (b), PC/DMC (c). Reprinted with permission from ref. [249]. Copyright 2011 American Chemical Society.

When examining the gas evolution profiles for the three electrolytes, it can be clearly seen that there is major O_2 evolution for the cathode discharged in DME (Figure 18 a) which is consistent with the desired decomposition of Li_2O_2. The gas evolution is also broken in to four distinct sections which relate to different portions of the charge (I: Initial charge, II: Rapid voltage increase from 4-4.5V III: 4.5V plateau and IV: 4.5-4.6). It can also be seen that significant CO_2 is only evolved at stage IV (i.e. above 4.5 V). These results for DME contrast entirely with the carbonate based electrolytes EC/DMC (Figure 18 b) and PC/DME (Figure 18 c) where negligible O_2 was evolved and instead CO_2 was the dominant gas produced upon charge. These results conclusively showed that carbonate based electrolytes are not suitable electrolytes for rechargeable Li-O_2 systems and stimulated interest in the development of more stable electrolyte systems.

b) Ethers

Ethers have been at the forefront of the Li-O_2 research field since the instability of carbonate electrolytes was established.[39, 75, 76, 112, 118, 150, 254, 259, 275-283] In particular, dimethoxyethane (DME) and Tetraethyleneglycoldimethyl ether (tetraglyme/TEGDME) have attracted significant interest owing to their increased stabilities in the Li-O_2 system. The increased stability of ethers compared to

carbonate electrolytes in succinctly illustrated in Figure 18 where the dominant gas evolved after the first charge (using a DME electrolyte) is O_2 liberated by the decomposition of the desired discharge product Li_2O_2. In fact, DME had been incorporated into Li-O_2 electrolytes as early as 2003, however, it was initially combined with carbonates which likely negated its increased stability.[266] In 2006 Read et al. used DME in a 1:1 weight ratio with 1,3-dioxolane as electrolyte.[118] They highlighted the higher dielectric constant and lower viscosities of this mixed electrolyte compared to carbonate based electrolytes while also acknowledging their increased stability.

Despite the enhanced stability of ether based electrolytes in comparison to carbonates (exemplified by the formation of Li_2O_2 as the dominant discharge product for the first cycle), it has been found that TEGDME does not allow the formation of crystalline Li_2O_2 upon repeated cycling.[76] Recently it has been shown through the use of gas chromatography that TEGDME decomposition occurs even from the first discharge cycle as confirmed by the presence of shorter chain ethers (including DME) and alcohols.[284] The fundamental instability of ether electrolytes was further emphasized by the finding that TEGDME can be consumed in the 'charging' process of a Li-O_2 architecture run within an Ar atmosphere (i.e. even without the presence of Li_2O_2).[276] Other reports have highlighted auto-oxidation of ether based electrolytes in the presence of excess oxygen which can lead to further reactions with cathode components such as binders.[253, 259, 279]

While ether based electrolytes are certainly a useful medium for studying the fundamental processes associated with Li-O_2 battery operation, further efforts will likely be required to make them sufficiently stable to allow long term cycling. It has been proposed that functionalization of the β-carbon position may improve stability.[51, 259] Alternatively, the identification of suitable catalysts which allow the charge voltage to be lowered substantially may allow the formation of by-products within ether based electrolytes to be minimized, thus improving cycle life.

c) Sulfur containing electrolytes

An interesting category of electrolytes for Li-O_2 battery are those containing sulphur atoms such as DMSO and sulfolane. These electrolytes have been recently been suggested to exhibit enhanced stability compared to conventional ether based solvents with high capacities and cycle lives of up to 100 (or even 100s) of cycles reported in some cases.[102, 106, 197, 213, 227, 285-287] DMSO was the electrolyte solvent used for the previously mentioned report by Peng et al which showed that the reversible formation/decomposition of Li_2O_2 was achievable over 100 discharge/charge cycles. [197] The study involved the use of the NPG cathode along with a 0.1M $LiClO_4$-DMSO electrolyte. Crucially, the formation and disappearance of Li_2O_2 (during discharge/charge respectively) and almost complete minimization of byproduct formation due to side reactions was confirmed through the use of FTIR (Figure 19 a) and Raman analysis (Figure 19 b). These results were also augmented through the use of DEMS analysis to monitor gas evolution during discharge and charge. The reversible formation and decomposition of Li_2O_2 was further illustrated by the strong O_2 signal during discharge and negligible CO_2 signal present.

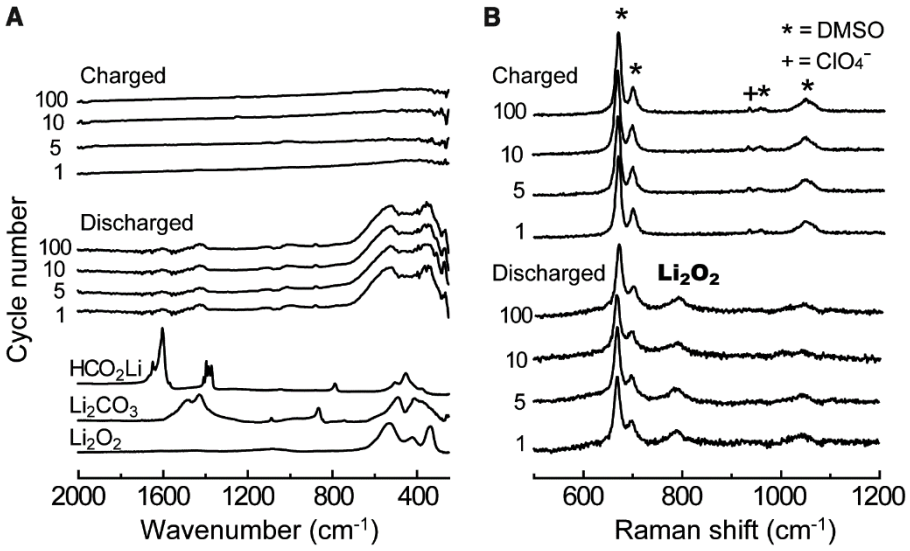

Figure 19 a) FTIR analysis performed on NPG cathode cycled in 0.1 M $LiClO_4$-DMSO electrolyte showing the overwhelming formation of Li_2O_2 upon discharge and its disappearance upon charge. Reprinted with permission from ref. [197]. Copyright 2012 AAAS publication.

These results showed conclusively that DMSO is a stable electrolyte solvent in the presence of a pure Au cathode. However, when the authors repeated the FTIR and Raman analysis for a carbon based cathode discharged in the same electrolyte, significant electrolyte decomposition was identified even from the first discharge which suggests that it is not a suitable electrolyte solvent for carbon based cathodes. Additional studies using DMSO based electrolytes with carbon based cathodes have presented the formation of LiOH as a major crystalline byproduct.[102, 288, 289] While the relative ratios of Li_2O_2: LiOH were not elucidated in these studies, it was shown by Trahan et al. that the LiOH present could not solely be accounted for by water contamination of the electrolyte. Instead they proposed the formation of LiOH was caused by water generated *via* a side reaction between the lithium superoxide and the DMSO electrolyte solvent.[288] Given the detrimental impact of H_2O within the electrolyte on the cycle life of Li-O_2 batteries (and the possibility for over-estimating initial discharge capacities),[290] this issue requires further study. These results suggest that DMSO may not be a practical electrolyte solvent for carbon based solvents,[95] however, more stable cathodes may alleviate these issues.[112, 197] Another study by Black et al. illustrated that reactions between PVDF binders, MnO_2 catalysts and Li_2O_2 discharge products can lead to the formation of LiOH as a byproduct on the cathode surface. Lithium superoxides readily dehydrofluorinate polyvinylidene to give byproducts such as H_2O_2 that react with good peroxide decomposition catalysts to produce LiOH within the electrolyte by reaction of water and Li_2O_2.[109]

More recently Dan et al. investigated the use of sulfolane based electrolytes for carbon based cathodes. They initially showed that sulfolane was quite stable over a wide electrochemical window before reporting high capacities (7735 $mAhg^{-1}$ and 6305 $mAhg^{-1}$ at an applied current of 0.1 $mAcm^2$ for the first discharge and charge respectively). While XRD analysis showed Li_2O_2 as the dominant discharge product (with the formation of LiOH and LiOH.H_2O also noted) it must be acknowledged that this analysis would not account for the formation of any of any amorphous byproducts, suggesting that additional characterization is required in future. Furthermore, the formation of LiOH type species even from the first discharge is not indicative of a stable electrolyte/cathode system.

Two further reports have investigated the long term cycling behaviour of carbon based cathodes using a sulfolane based electrolyte. The first report showed that a Ketjen black carbon cathode could be cycled at limited depth of discharge (1000 $mAhg^{-1}$) for 110 cycles in a 1M $LiPF_6$/ sulfolane electrolyte.[285] In the more recent article, a 1M LiTSFI/sulfolane electrolyte was investigated as the electrolyte solvent. A consistent capacity of 1000 mAg^{-1} was achieved for 800 cycles which suggests a remarkable stability.[227] Unfortunately, in these two reports, the stability of the electrolyte and degree of byproduct formation as cycling proceeded was not discussed. It was also not established what the dominant discharge product was in the system. It should be noted that these tests were both conducted using a carbon paper/gas diffusion layer type current collector which can significantly add to capacity if the mass of the active cathode is omitted when determining the capacity.[227, 285] Sulfolane appears to be a promising electrolyte solvent but additional studies are required to investigate the degree of solvent decomposition during cycling and determine if Li_2O_2 can be reversibly formed and decomposed when carbon cathodes are used.

d) Ionic liquids

The concept of using Ionic liquids was introduced early in the search for suitable electrolyte solvents for Li-O_2 batteries by Kuboki et al. in 2005.[291] The initial report investigated several different ionic liquids as electrolytes, citing the benefits of their hydrophobicity, low volatility and low flammability. The discharge capacities presented were impressive (up to 5360 mAg^{-1}) however, the tests were conducted within air and as a result it is unclear what the discharge products were. More recently, the mechanism of ORR and OER reactions in ionic liquid electrolytes has been probed by Abraham and co-workers.[292, 293] Building on these investigations, Zhang et al. investigated the formation of a cross-linked network gel (CNG) composed of an ionic liquid ($[C_2C_1im][NTf_2]$) and single walled carbon nanotubes (SWCNTs) as a means of improving the properties of pure SWNT cathodes.[127] Their results showed a dramatic increase in discharge capacity compared to pure SWNT

cathodes which was attributed to the improved transport of electrons, Li ions and crucially, diffusion of O_2 through the interlinked CNG. While crystalline Li_2O_2 was noted after discharge through the use of XRD analysis in this study, the long term stability of the ionic liquid was not fully established. To this end, the ionic liquid PP13TFSI was used in conjunction with $LiClO_4$ as electrolyte for CNT based cathodes by Cui et. al. in an attempt to investigate Li_2O_2 and Li_2CO_3 formation during cell cycling.[129]

Through a combination of XPS and XRD analysis, they found that crystalline Li_2O_2 is the dominant discharge product formed in this system during the first discharge. Despite this promising finding, Li_2CO_3 accumulation occurred from the first charge cycle. Unfortunately, the source of the Li_2CO_3 formed in this study was not identified (i.e. whether it was due to decomposition of the electrolyte, the cathode, or a combination of the two) however it does highlight that ionic liquids do not eliminate the issue of Li_2CO_3 formation. A few other reports detailing the use of pure ionic liquids and mixtures of ionic liquids and organic solvents as electrolytes for Li-O_2 batteries have been reported,[97, 159, 293-299] however, the identification of stable ionic liquid/cathode systems remains an open issue and should be prioritized given their attractive properties.

e) Electrolyte salts

In comparison to the many studies examining the stability of various electrolyte solvents for Li-O_2 batteries detailed above, the stabilities of electrolyte salts and their influence on Li-O_2 battery operation (by-product formation, capacities, cycle life etc.) have been more sparingly discussed.[254, 260, 300-303] Because electrolytes are composed of both a salt and a solvent, it is important that both components are stable independently but also when combined. As a result, systematic studies which assess the stability of various possible electrolyte salts within a given electrolyte solvent medium are particularly of interest.

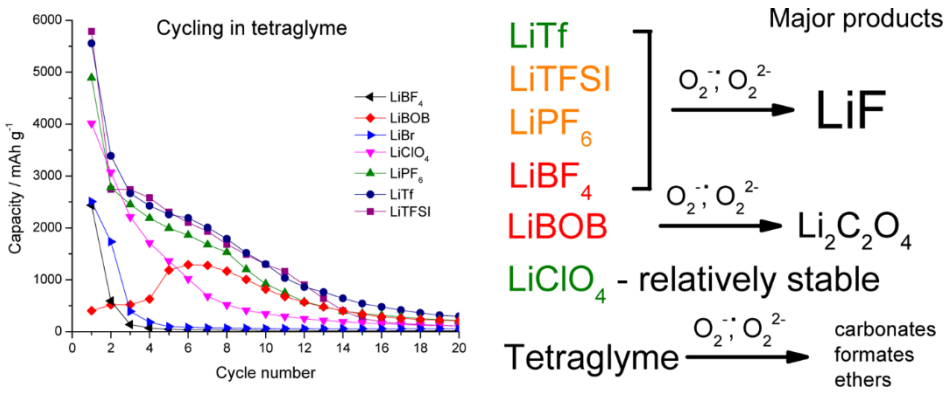

Figure 20 Effect of electrolyte salt on the cycling performance of TEGDME based electrolytes. The main decomposition products for each electrolyte salt are also shown. Reprinted with permission from ref. [300]. Copyright 2013 American Chemical Society.

A systematic study investigating the impact of the electrolyte salt this was presented by Nasybulin et al. who examined the performance and decomposition of various common electrolyte salts (LiTf, LiTFSI, $LiPF_6$, $LiBF_4$, LiBOB, $LiClO_4$) at a fixed 1M concentration in TEGDME (Figure 20).[300] In this study, where all other parameters were kept fixed (cathode composition, test conditions etc.), dramatically different performances were noted even among the most commonly used Li-O_2 battery salts ($LiClO_4$, $LiPF_6$ and LiTFSI). Post-mortem analyses were conducted using XRD and XPS analysis. After a single discharge, the authors noted that $LiPF_6$ and LiTFSI were both partially decomposed to form LiF while $LiClO_4$ was found to be more stable. However, upon extended cycling, $LiClO_4$ based measurements showed quicker capacity fading with the most impressive capacity retention noted by systems based on LiTF, $LiPF_6$ and LiTFSI. In a similar study, Elia et al. compared the performance of electrolytes containing $LiPF_6$, $LiN(SO_2CF_3)_2$, $LiCF_3SO_3$ or $LiClO_4$ salts within a TEGDME solvent.[301] The authors found that the electrolyte salt strongly influenced both the discharge and charge voltage with the smallest voltage gap noted for the $LiCF_3SO_3$ based electrolyte. This preliminary study highlighted a wide range of complex factors including the electrolyte conductivity, interfacial resistance, diffusion rates, electrolyte viscosity, oxygen solubility and lithium solvation/ desolvation as playing important roles in determining the suitability of a given electrolyte. Li et al. also illustrated

that the concentration of the electrolyte salt within the electrolyte is key to ensuring good cycle life.[302]

Additional systematic studies using other promising electrolyte systems (for example more stable ethers, DMSO, sulfones etc.) would be extremely useful given that the stability of the common electrolyte salts may vary in the different electrolyte media. It must also be realized that certain 'catalytic' cathode systems may exacerbate electrolyte salt decomposition in a similar manner to that illustrated for electrolyte solvents.[190] The identification of stable salt/electrolyte solvent pairings will thus likely be highly dependent upon whether a carbon based cathode is under examination.

f) Electrolyte conclusions

The identification of stable electrolyte solvent/salt combinations is an extremely important hurdle if a rechargeable Li-O_2 battery system is to be realized. However, electrolytes cannot be considered in isolation and the stability of electrolytes will likely be strongly dependent upon the cathode with which the electrolyte is combined.[197] The use of carbonate electrolytes can be completely discounted for Li-O_2 batteries with electrolyte solvents composed of ethers and DMSO confirmed as showing acceptable stability in combination with certain cathode systems. The challenge moving forward is to identify more stable electrolyte /cathode pairings which can facilitate the reversible formation of Li_2O_2 at the expense of parasitic by-products.

3.3 Anode

a) Lithium metal anode

The anode is the least widely studied portion of the Li-O_2 battery. Practically all of the research to date has involved the use of metallic lithium foil as the anode material. The high energy density

envisaged for Li-O_2 batteries is strongly dependent on the development of safe, lightweight Li based anodes. Despite the dearth of research on Li anodes for Li-O_2 applications, much is known about the operation of secondary Li-ion batteries with metallic electrodes.[60, 304, 305] This section will discuss the reports which have investigated the operation of pure Li metal anodes for Li-O_2 batteries (focussing on surface reactions like the formation of LiOH and SEI) and possible alternatives to pure Li anodes. The section is focused on systems involving non-aqueous electrolyte media as discussed in section 2. Much research has been devoted to the development of Li-ion conducting ceramics such as LISICON and NASICON aimed at protecting the anode from moisture ingress, however, these are of particular relevance to aqueous and solid state electrolyte systems which are outside of the scope of this report.[19, 20, 24, 50, 306-311] These Li-ion conducting membranes have been discussed in other review articles to which the reader is directed.[312, 313]

The stability of lithium metal anodes during operation in Li-O_2 batteries has been sparingly studied, however, a timely recent report by Shui et al. investigated the reactions occurring at the Li anode during cycling through the use of *in-operando* XRD analysis.[314] This technique provided depth-resolved characterization of the anode at various stages in the discharge/charge process. The voltage profiles for two discharge/charge cycles are shown in Figure 21 a) and are separated into various sections i-ix. In Figure 21 b) the corresponding compositional data from XRD is presented which shows a continual accumulation of LiOH at the surface of the anode and only partial recovery of metallic lithium during the charging process (stages iii-v and vii-ix).

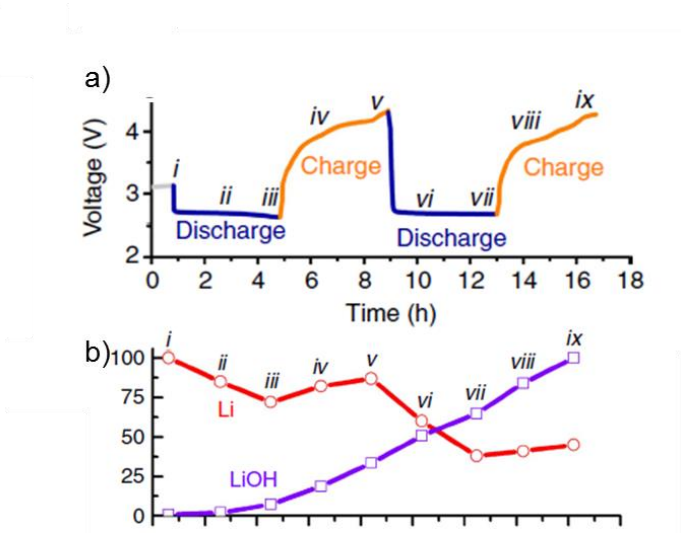

Figure 21 a) Voltage profile showing the discharge/charge cycles analysed with various portions highlighted i-ix. b) Normalized amount of Li and LiOH at the anode interface as a function of cycle time with the points i-ix corresponding to the points highlighted in a). Reprinted with permission from ref. [314]. Copyright 2013 Nature Publishing Group.

The authors were also able to use X-ray tomography of the Li anodes to show the formation of pores within the LiOH coating on the anode surface which facilitated transport of Li ions from the underlying pure Li portion of the anode and facilitated continued operation of the cells until the anode was exhausted. The main source of the LiOH was proposed to be due to the decomposition of the ether based electrolyte along established reaction pathways,[76, 314] due to the low initial water content of the electrolyte investigated (8 ppm). While the formation of LiOH on the anode surface is undesirable as it reduces the total discharge capacity, it was also suggested that this layer acted as a barrier to Li dendrite formation. This commonly encountered issue for batteries utilizing metallic lithium electrodes can lead to thermal runaways and ultimately explosions and would be particularly hazardous given that Li-O_2 batteries will likely be operating with a pure O_2 atmosphere.[50] Thus, there may be a trade-off between LiOH formation on the anode surface and battery safety with the possible reduction in discharge capacity perhaps being offset by increased anode stability. While this study provides crucial insights into the formation of LiOH on the surface of the Li anode during operation, it cannot account for any amorphous product formation due to electrolyte (salt and

solvent) decomposition on the anode surface. It also remains to be seen if the formation of LiOH in the manner reported is consistent for other promising electrolyte systems. Additional efforts are required to further characterize the behaviour of metallic lithium anodes during cycling with particular emphasis on safety.

The formation of a solid electrolyte interphase with the Li anode with specific focus on Li-O_2 applications has been explored in a number of studies.[252, 315, 316] The issue of SEI formation is complicated in the case of the Li-O_2 battery compared to standard Li-ion batteries by the presence of dissolved O_2 in the electrolyte. Younesi et al. examined SEI formation in two separate reports.[252, 316] While carbonate based electrolytes were used in both studies (which have been established to be unsuitable Li-O_2 battery electrolytes as discussed above), detailed information on the complexity of the SEI layers formed was provided. The studies showed the formation of hydrocarbons, ethers, carboxylates and carbonates at the Li surface (presumably due to decomposition of the electrolyte) and also F signal deemed to be due to the transport of kynar binder from the cathode to the anode. The formation of LiOH at the cathode surface was not detailed. The possible interaction of mobile species (particularly binders) from the cathode with the anode is an important observation which warrants further investigation in more stable electrolyte systems.

SEI formation for a Li-O_2 system based on an amide electrolyte system was investigated by Bryantsev et al..[315] This investigation was stimulated by the inability of DMA based electrolytes (which had previously been shown to exhibit superior stability at the cathode compared to carbonate and ether based electrolytes[233, 258]) to form a stable SEI layer at the Li surface. The authors showed that the addition of 2 % DMTFA to LITFSI/DMA electrolyte aided in the formation of a more stable SEI layer due to the formation of LiF. However, they also illustrated instability of this system at the cathode suggesting that further investigations are required to develop an electrolyte system which is stable with respect to both the anode and cathode.

b) Lithium silicon-alloy anode

Given the stability issues associated with lithium anodes under typical Li-O_2 battery conditions, it may be necessary to completely replace the metallic lithium anode with a more stable anode system should a stable electrolyte (i.e. one which leads to the formation of a stable SEI layer and does not cause accumulation of LiOH on the anode) not be identified. Progress in this area is limited, however, Hassoun et al. recently demonstrated that a Li/Si/C composite electrode could be used to successfully replace the typically used Li anode. Their anode was created through mechanical lithiation of a Si/C composite by directly contacting the electrode with metallic lithium in the presence of a $LiPF_6$/carbonate electrolyte under pressure (1 kg cm^{-2}). The composition of the lithium alloy formed within the composite anode was found to be $Li_{2.6}Si$ rather than the fully lithiated phase $Li_{4.4}Si$, yet, the anode was still capable of operating a Li-O_2 cell which exhibited a stable capacity of 1000 $mAhg^{-1}$ over 15 discharge/charge cycles. This preliminary approach showed that the metallic lithium-free Li-O_2 cells could be successfully operated and also hinted at room for further improvement. For example, 70% of the weight of this composite was composed of carbon (presumably as a conductive additive), which added significantly less capacity to the anode than the Si. In future, nanostructured anodes composed of solely lithiated Si (or even just fully lithiated Si as part of a C/Si composite) may allow for increased capacities and minimization of the energy penalty due to the exclusion of metallic Li as the anode. However, further investigation into the reversibility of lithiation and delithiation of the anode upon cycling is required.

c) Anode conclusions

Future investigations into the true stability of Li metal based anodes are key to the development of successful Li-O_2 batteries using organic solvent based electrolytes. Just as the electrolyte and cathode cannot be considered in isolation, the lithium anode and the electrolyte must be considered in conjunction. It seems likely that the central role of the electrolyte in facilitating a reversible

discharge/charge process at the cathode (by minimizing byproduct formation), is likely mirrored in importance at the anode as any suitable electrolyte must be capable of producing a stable SEI layer with metallic Li. Future studies should focus on the reversibility of the Li anode and the formation of LiOH on the anode surface. These studies are particularly relevant given that LiOH may actually act as an Li-ion permeable buffer at the surface which prevents Li dendrite formation.[314] Parallel investigations into the use of Li-X alloy anodes (where X is Si,[262, 317-319] Ge,[320-322] Sn[323-325] etc.) are also of interest. Ideally, the energy penalty associated with the removal of pure metal and replacement with Li alloy composites should be quantified while the repeated cycling behaviour and the influence of O_2 dissolved in the electrolyte should also be assessed.

Section 4 - Theoretical modeling and density functional theory results

In order to address the scientific issues associated with Li-O_2 battery operation, many theoretical studies based on density functional theory methods have been reported. Zheng et al.[31] developed a model for prediction of the gravimetric and volumetric energy densities of non-aqueous Li-O_2 batteries. An issue with previous modeling for computing the capacities of non-aqueous Li-O_2 batteries is the assumption that the active materials and electrolyte are perfectly balanced according to the electrochemical reaction pathways. Ideally, the Li metal efficiently replaces Li ions from electrolyte salts, solid discharge products fill the available pore volume in the air cathode, and the amount of electrolyte permeates this pore volume prior to discharge. Thus, previous models are limited to estimating of the upper limits of the gravimetric and volumetric capacities as well as the mass and volume change ratios of batteries for given amounts of the Li metal, electrolyte and a defined porosity of the cathode electrode. A model is still missing in which we can compute the key quantities of non-aqueous Li-O_2 batteries for the practical applications, in such a way that the Li metal is partially oxidized, the cathode void volume is partially occupied by discharge products, and excess electrolyte is required.

The objective of this section of review, therefore, is summarize the previous theoretical investigations, to address the issues associated with previous modeling, and to suggest possible robust models for predicting the theoretical capacities of non-aqueous Li-O_2 batteries regarding their different components: cathodes, anodes, and electrolytes.

4.1 Cathode materials

The Li-O_2 electrochemical interaction causes, in principle, a dramatic increase in theoretical energy density compared to Li-ion batteries, creating the development of high energy density systems.[8, 69, 265, 268] The theoretical specific energy of Li-O_2 cell was estimated about 3400 Wh/kg. The cathode active material (oxygen) is not stored internally in the battery. Oxygen enters into a porous carbon cathode from the air for the ORR similar to polymer electrolyte membrane fuel cell (PEMFC) cathodes. Li and O_2 react to form metal oxides Li_2O_2 and/or Li_2O during discharge process and the oxides decompose to release Li^+ ions and O_2 again due to charge process.

The basic design of Li-O_2 batteries consists of ion conducting electrolyte sandwiched between a dense Li anode, and a porous carbon based cathode with O_2 from the air entering on one side and interfacing with non-aqueous electrolyte on other side. The performance degradation of Li-O_2 cell over multiple charge/discharge cycles can lead to an important issue, such as safety issue, which arises due to instability of materials, incomplete reversibility of electrochemical reactions, and the loss of electrolyte solvent due to evaporation and reactions with the electrodes.

a) Li_2O_2 and Li_2O surfaces

With regard to the discharge products at the cathode of a rechargeable non-aqueous Li-O_2 battery system due to the oxygen reduction, the formation of both Li_2O_2 and Li_2O were reported in many early studies.[14, 126, 153, 270, 326-328] For example, Read et al.[14] found the proportion of Li_2O_2 and

Li_2O varied with the current density during oxygen volume measurements and Zhang et al.[270] reported that the battery exhibit two discharge voltage plateaus at low discharge currents, and the second one indicates the formation of Li_2O_2 into Li_2O.

In a real rechargeable non-aqueous Li-O_2 battery system, mainly the following electrochemical reactions take place at the cathode:

$$2Li^+ + 2e^- + O_2 \longrightarrow Li_2O_2 \quad (1)$$

$$4Li^+ + 4e^- + O_2 \longrightarrow 2Li_2O \quad (2)$$

It is assumed that equation (2) is not reversible, only equation (1) takes place at the cathode for rechargeability. Radin et al.[70, 329, 330] reported in their DFT calculations that lithium peroxide (Li_2O_2) surfaces are metallic, while lithium oxide (Li_2O) surfaces are not. The authors systematically characterized the stability and electronic structure of 40 distinct surfaces of Li_2O_2 and Li_2O in this article. They found several new oxygen-rich (0001) and (1-100) facets for Li_2O_2 and a single stoichiometric (111) surface for Li_2O most stable, consistent with the previous study.[331] Their surface state analyses revealed that Li_2O_2 surfaces are metallic and magnetic, while Li_2O surfaces are insulating and nonmagnetic. Such distinct surface properties are useful to explain the origin of differing rechargeability of discharge products Li_2O_2 and Li_2O in Li-O_2 batteries. The structures for low energy surfaces for both Li_2O_2 and Li_2O are shown in Fig. 22.[70]

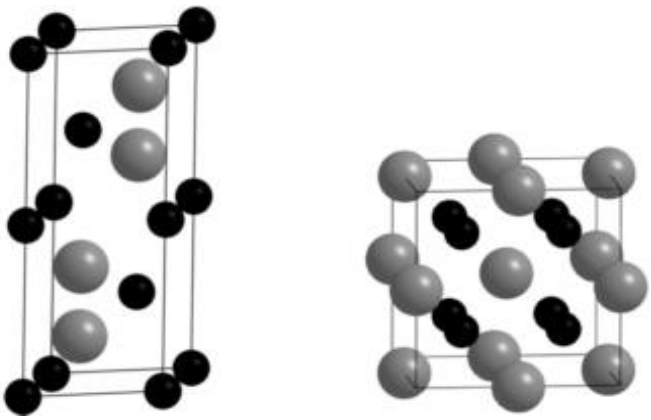

Figure 22 Unit cell for (left) bulk Li_2O_2 and (right) bulk LiO. Gray and black spheres represent O and Li atoms, respectively. Reprinted with permission from ref. [70]. Copyright 2011 American Chemical Society.

Kang et al.[332] investigated a facile mechanism for recharging Li_2O_2 in Li-O_2 batteries using DFT methods. The overall reaction in a Li-O_2 system is the oxidation of lithium to Li_2O_2 upon discharge and its subsequent reduction upon charge[5, 12, 56, 63, 66, 86, 327, 333]

$$2Li^+ + 2e^- + O_2 \underset{\text{charge}}{\overset{\text{discharge}}{\rightleftharpoons}} Li_2O_2 \qquad (3)$$

The authors confirmed a facile path for Li_2O_2 charging that requires overpotential of 370 mV, consistent with experimental results. They found that at the relatively small overpotentials, Li_2O_2 is delithiated topotactically to form off-stoichiometric $Li_{2-x}O_2$ compounds that are energetically stable and exhibit faster kinetics for delithiation processes. The previously reported electronic and ionic conductivity[332, 334-338] in these off-stoichiometric states enhance the delithiation to dissociate into Li^+ and O_2 or O_2^- species with possible dissolution in the electrolyte.[56, 69, 109, 339] Such investigations clearly show that the oxidation reaction with delithiated particles proceeds locally in the electrode, and causes an increase in the measured current. This localization of current is found to be a key factor in the rate capability of Li-O_2 batteries.

Recent theoretical studies investigated that stoichiometric Li_2O_2 is a wide band gap insulator, and that charge transport takes place through polaron hopping.[335, 336, 340] In their density functional theory studies, Kang et al.[332] proposed that an electron injected into Li_2O_2 become trapped by the formation of a small polaron due to the molecular nature of the Li_2O_2 conduction band, whereby an injected electron is localized at an O-O site possessing an elongated oxygen pair. The calculated hopping rate of a small polaron found directly correlated to the extremely low electronic mobility of Li. At the same time, Hummelshoj et al.[335] argued that Li vacancies, which are likely to be created during the discharge process, may induce delocalized hole states in the valence band of Li_2O_2, therefore improving Li charge transport through hole conduction. However, Ong et al.[336] reported that hole states may also become localized through the formation of hole polarons. Although the migration barriers of hole polarons was estimated to be lower than electronic polarons, the resulting

conductivity of Li_2O_2 was still found to be smaller than compared to experimental result. Zhao et al.[338] suggested that growing Li_2O_2 on a graphene layer induces hole-type conducting channels in Li_2O_2. However, this approach is limited by the short penetration depth of surface states into Li_2O_2 layers. Such states penetrate only a few LiO_2 layers inside the Li_2O_2 crystal, thus limiting conduction enhancement to only a thin surface layer. Moreover, Timoshevskii et al.[341] proposed an alternative way of improving the conductivity of Li_2O_2 by means of *ab initio* calculations and showed that the substitution of a small fraction (1.6%) of Li atoms by Si impurities leads to the creation of additional conducting states in Li_2O_2. These states were shown to originate from the partial occupation of oxygen anti-bonding orbitals by electrons, being donated by impurity Si atoms. The elongated oxygen pairs, generating these states, are bound to Si impurities, and are not subject to polaron-induced deformations. The polaron preemption mechanism was supposed to enhance the electron mobility of Li_2O_2. Furthermore, the nature and concentrations of charge carriers and intrinsic point defects in Li_2O_2 have not been reported. Such information is important because the concentrations of these species, when combined with mobilities, relates to the conductivity of bulk Li_2O_2, and thus ties directly to the performance of the battery. In order to elucidate the mechanism of charge transport in Li-O_2 cells, the authors in Radin et al.[342] employed first-principles calculations to predict the conductivity of crystalline Li_2O_2. More specifically, the concentrations of all chemically-relevant intrinsic (point) defects in Li_2O_2 were evaluated as a function of cell voltage; subsequent calculations were used to assess the mobilities of the dominant charge carriers. The crystal structure of Li_2O_2 with alternating layers of trigonal prisms and octahedra/tetrahedral, with oxygen sites lying on the vertices of the polyhedra; the mechanism of oxygen reduction reaction at the cathode; and proposed two-stage recharge mechanism for a Li-O_2 cell are shown in Figs. 23 (i), (ii), and (iii) respectively.[342] The authors calculated point defect formation energies for 23 unique species, including vacancies, divacancies, interestitials, polarons, and bipolarons using first-principles calculations. Under discharge condition, the bulk electronic conductivity was found to be far less than the target value and thus, failed to supply significant charge transport. The fairly high capacities

and discharge products obtained in experiments[13, 81] suggested two possibilities: (i) morphological features may locally enhance the conductivity of the discharge product, and (ii) the oxygen reduction reaction (ORR) does not occurred at the Li_2O_2 surface, but rather at the carbon cathode or catalyst. Figure 23 (ii) summarizes the possible discharge mechanisms graphically. The recharge conditions were found to be more conducive to charge transport compared to discharge. Figure 23 (iii) shows the two-stage recharge process linking charge transport, particles morphology, and overpotentials during recharge. Charging was initiated at low potentials due to the dissolution of thin Li_2O_2 deposits or decomposition at or near the Li_2O_2/electrolyte/carbon three-phase boundary. Charging was then concluded at high potentials where thick deposits decomposed through polaron hopping. However, it should be noted that side reactions involving electrolyte or carbon electrode decomposition might introduce further complications.[56, 79, 343]

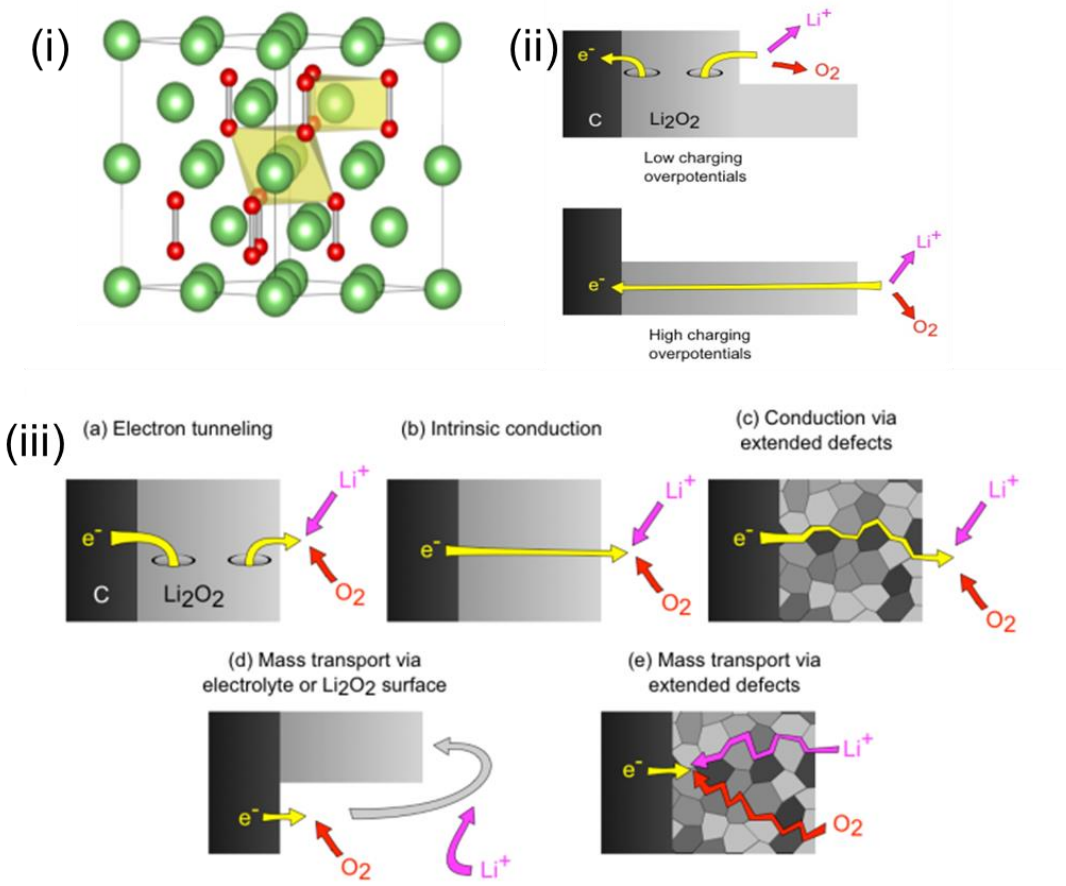

Figure 23 (i) Crystal structure of Li_2O_2 with alternating layers of trigonal prisms and octahedra/tetrahedral, with oxygen sites lying on the vertices of the polyhedral, (ii) Proposed two-stage recharge mechanism, and (iii) Mechanism of oxygen reduction reaction at the cathode for a Li-O_2 cell. Reprinted with permission from ref. [342]. Copyright 2013 Royal Society of Chemistry.

Gaining a better understanding of the fundamental mechanisms of the cathode reactions, such as the oxygen reduction reaction (ORR) during discharge and oxygen evolution reaction (OER) during charge, is essential to guide the experimental efforts in improving the performance of the Li-O_2 battery system. The power density of current Li-O_2 batteries have been found to be very low with current densities of about 0.1-1 mA/cm^2 typically reported[25, 55, 69, 74] which are at least one order of magnitude lower than the requirements for electric vehicle applications.[12] Recent *ab-initio* modeling has provided the energy profile and reaction path for the ORR mechanism of Li_2O_2[335] as well as the ORR on catalytic metal surfaces, such as Au and Pt.[344] Mo et al.[63] performed DFT calculations to study the mechanisms of OER of Li_2O_2 in Li-O_2 battery by calculating the surface energies of infinite slabs of Li_2O_2 with vacuum regions.[345-352] The authors considered the various surfaces of Li_2O_2 such as (0001), (11-20), (11-21), (1-100), (1-101), and Wulff shape to investigate the mechanism of OER process in Li-O_2 system. They calculated reaction paths for oxygen release and concluded that all the surfaces of Li_2O_2 first decompose into a superoxide like LiO_2 structure via the removal of Li atoms. These findings supported experimental findings in which LiO_2 was proposed as an intermediate in the formation of Li_2O_2 in the ORR process.[69, 74, 75] Oxygen evolution typically takes place following the formation of a surface that approximates a superoxide. The most predominant peroxide surface terminations [the (0001) and (11-20) surfaces] have some of the highest energy barrier for oxygen evolution. The surfaces with the most strongly bonded O_2 have been postulated to gain their low surface energy from strong oxygen binding. The energy barriers found for the oxygen evolution steps were significantly higher than those for Li desorption on the most surfaces under consideration, and this reaction barrier of O_2 is a rate-limiting step in the OER. The lowest energy surfaces of Li_2O_2 surfaces are shown in Figure 24.[70]

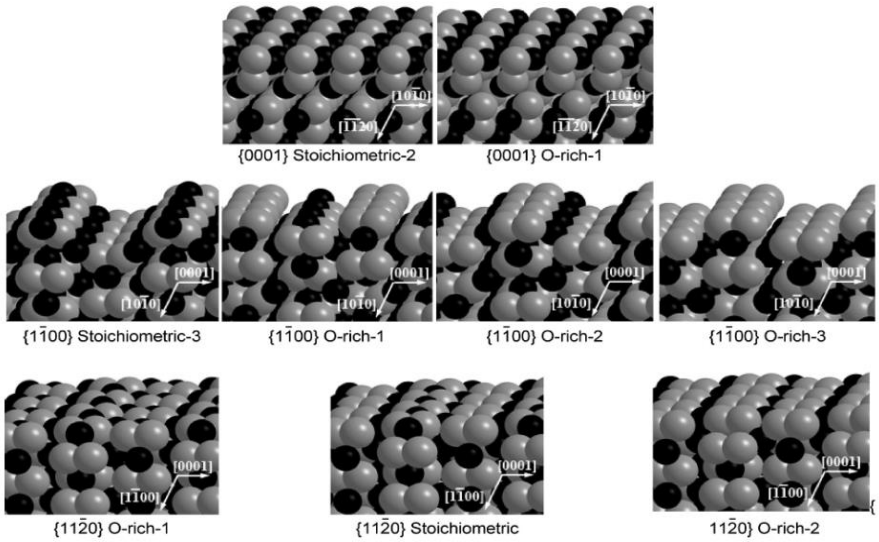

Figure 24 Structures of low-energy Li_2O_2 surfaces. Reprinted with permission from ref. [70]. Copyright 2011 American Chemical Society.

Besides the two-electron transfer process i.e. the formation and decomposition of Li_2O_2 and Li_2O, Hummelshoj et al.[335] have recently suggested that oxygen can be reduced by Li metal through a one-electron transfer process forming an adsorbed Li_2O_2 species on the surface by applying first-principles calculations. Moreover, the metastable product LiO_2 is formed due to the formation of superoxide (O_2^-) [69, 75] with a finite lifetime as a preferred pathway for oxygen reduction in one-electron process during charge/discharge cycles of Li-O_2 cells, before disproportionation into Li_2O_2 and O_2 chemically as LiO_2 is not stable. In general, the electrochemical response of the O_2/ O_2^- redox couple on a particular electrode dependents on the solvent and nature of the counter ion[152, 352] together with the nature of the electrode catalysts.[14, 55, 87, 152, 160] The formation and reduction of both Li_2O_2 and Li_2O is poorly understood yet, thus hindering the progress of this new technology.

Li_2O_2 and Li_2O are both thermodynamically stable within the typical potential range of Li-O_2 batteries due to their similar equilibrium potentials. Thus, it is quite important to develop a correct qualitative understanding of the electrochemical reactions, chemical reversibility and thermodynamic properties for Li-O_2 electrochemical couples to develop the Li-O_2 cells. This may even lead to the study of different bulk stoichimetries of discharge products such as lithium superxide (LiO_2) for example, which remains unexplored by both experimentalists and theorists.[353] In

experimental systems, the discharge products may depend substantially on the oxygen pressure, which is not well understood yet.[221] Theoretically the determination of the Gibbs free energy of formation for the bulk oxides of lithium (Li_xO_y) as a function of oxygen pressure is a useful baseline study for understanding the products of Li-O_2 electrochemical reactions needed for the development of effective catalysts and electrolytes for rechargeable Li-O_2 cells. Lau et al.[354] presented a DFT study of the thermodynamics of bulk crystalline LiO_2, Li_2O, and Li_2O_2 at different oxygen chemical potentials. The authors proposed that LiO_2 and Li_2O_2 are likely to be stable only under O_2-rich conditions with high oxygen partial pressures, whereas Li_2O is the most stable at ambient conditions; the bulk LiO_2 is an ionic molecular solid and it is not an electrochemical reaction product in Li-O_2 cells.

b) Porous carbon

Porous carbon has attracted much interest as a cathode material (as outlined in section 3.1 b) with or without the inclusion of catalysts materials. Porous carbons are generally considered as defective crystallites of graphite.[355] To date, various carbons such as activated carbon, carbon nanotubes, Super P, Ketjen Black, Vulcan XC-72 [4, 5, 59, 124, 216, 244, 356, 357] have been used in Li-O_2 batteries. Yang et al.[358] reported a the comparison of the physical parameters and specific capacities of various carbons as listed in Table III.

Table III. Comparison of surface area, pore diameter, and specific capacity of various carbons. Adapted with permission from ref. [77]. Copyright 2013 The Electrochemical Society.

Carbon material	Surface area (m^2/g)	Pore diameter (nm)	Specific capacity (mAh/g)
Super P	62	50	1736
Vulcan XC-72	250	2	762
Activated Carbon (AC)	2100	2	414
Carbon Nano Tube (CNT)	40	10	583
Graphite	6	-	560
Ball-Milled Graphite	480	-	1136
Messocellular Carbon Foam-C	824	30	2500

Due to small pore size, Active carbon (AC) has the lowest reported specific capacity with the largest surface area. In contrast, Super P has a high specific capacity due to its large pore diameter, with the relatively small surface area. Mirzaeian and Hall [83, 359, 360] first reported the synthesis and use of porous carbon aerogels as cathodes in Li-O_2 batteries with remarks that the discharge capacity increases with increase in pore volume and average pore diameter of carbon aerogels. Li et al.[144] used graphene nanosheets as cathodes in Li-O_2 batteries with the formation a three-phase interface. Park et al.[326] reported the comparison of the performance of some carbon families. From all these review studies, we conclude that both high surface areas and high pore volumes are essential for the high discharge capacity of Li-O_2 batteries. The micro- to nano- structures of carbonaceous materials[356] are important factors related to the performance of Li-O_2 batteries. In practical, Li-O_2 batteries suffer from poor cyclability and reversibility during multiple charge/discharge processes.[5, 87, 105, 126, 152, 327] There is lack of theoretical research on carbonaceous materials used as active cathode materials in Li-O_2 batteries. In order to enhance the performance, safety and lifetime of Li-O_2 batteries, the structure and morphology of carbonaceous materials should be optimized with their utilization in the porous cathodes. Additionally, further insight into the instability of carbon as a cathode material requires urgent theoretical investigation given the observed decomposition in recent experimental studies.[85] As high surface energy lithium peroxides can promote decomposition of carbonate electrolytes, tabulating energies associated with unwanted electrolyte decomposition for non-carbonate-based aprotic solvent/salt systems at various carbon surfaces would be quite useful.

c) Hierarchically porous graphene

The precipitation of reaction products such as Li_2O_2 on the carbonaceous electrode ultimately blocks oxygen pathways and limits the capacity of Li-O_2 batteries. Therefore, it is essential to develop an optimum air electrode with micometer sized pores for rapid oxygen diffusion to catalyze Li-O_2 electrochemical reactions and to prevent the excess growth of discharge products from

blocking their chemical pathways. Xiao et al.[8] suggested the design of hierarchically porous air electrodes with functionalized graphene sheets with lattice defects and hydroxyl, epoxy, and carboxyl groups.[361] The authors performed DFT calculations to investigate the fact that only weak interaction exists between Li_2O_2 monomer and graphene substrate similar to a physical adsorption mechanism, stressing the importance of functional group rather than lattice effects. The top and side views of optimized structures of Li_2O_2 and $(Li_2O_2)_6$ clusters on perfect graphene, the 5-8-5 defect graphene, and 5-8-5 graphene with COOH group is shown in Figure 25.[8]

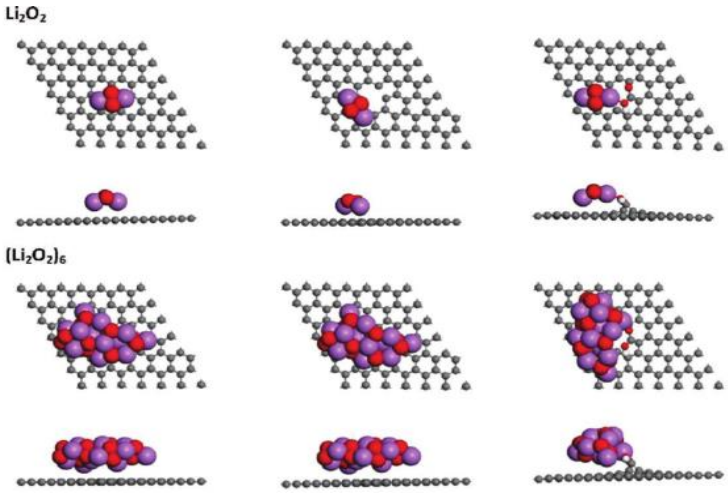

Figure 25 Top and side views of optimized structures of Li_2O_2 and $(Li_2O_2)_6$ clusters on perfect graphene, the 5-8-5 defect graphene, and 5-8-5 graphene with COOH group. Reprinted with permission from ref. [8]. Copyright 2011 American Chemical Society.

The calculated free-energy change as a function of $(Li_2O_2)_n$ cluster size is shown in Figure 26.[8] For a pristine graphene surface, the aggregation of adsorbed Li_2O_2 monomers was shown to be energetically favorable until it reaches a cluster size of n = 5. Monomers are easily mobile and can aggregate on pristine graphene, but this process becomes self-limiting. Clusters greater than n =5 are not energetically favourable. These investigations show how important the carbon structure is for the deposition of the reaction products. The calculated changes in free energy as a function of the size of peroxide clusters at large sizes on graphene demonstrate that such clusters remain as isolated islands that are immobile, preventing clogging of the oxygen diffusion pathways during the discharge process at least. This graphene structure mediated limitation reported by the authors does

have a trade-off: while preventing continuous peroxide formation and ensuring better gas flow and allow controlled discharge product formation and a limitation in unwanted internal resistance, it formally limits the density of discharge product formation per unit volume. The calculations are important since they demonstrate the sensitivity of peroxide nucleation mechanisms to the structure and defect density in ordered carbon surfaces.

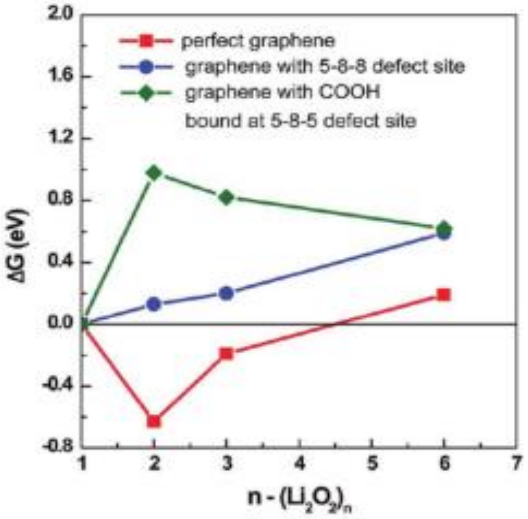

Figure 26 Calculated free-energy change as a function of $(Li_2O_2)_n$ cluster size. The negative value of ΔG indicates an energetically more favorable aggregating process. On the perfect graphene surface, the aggregation of adsorbed Li_2O_2 monomer is energetically favorable up to $(Li_2O_2)_5$, while it is energetically unfavorable from the beginning on the5-8-5 defect graphene surface with or without a functional group (COOH). Reprinted with permission from ref. [8]. Copyright 2011 American Chemical Society.

Graphene and graphene composites have been studied as electrode materials in supercapacitors,[362] Li-ion batteries,[363] and proton exchange membrane fuel cells (PEMFC).[364] In all studies, the graphene sheets readily restacked due to either Van der Waals or capillary forces and caused the formation of two dimensional structures that hinder rapid gas diffusion, which is essential for the effective operation of Li-O_2 batteries.[26] As there is lack of theoretical research works on graphene and grapheme-based materials as active cathodes in Li-O_2 batteries, more DFT calculations should be devoted to investigate the mechanisms of ORR and OER.

d) Au/Li_2O_2 and Pt/Li_2O_2 model cathode surfaces

Catalysts such as MnO_2,[4] Au,[365] and Pt,[59] have been ubiquitous in Li-O_2 batteries since their inception as previously discussed in this review ,however, more efficient catalytic systems and understanding of the role of catalysts is required. [33, 59, 87, 118, 266, 327, 365-367] The Li-O_2 cell has limited electrical efficiency due to overpotential/polarization loss at the cathode during charge and discharge,[4] and limited power and current densities.[221] The overpotential is the energy loss in the process as ($U_{charge} - U_0$) and ($U_0 - U_{discharge}$) respectively, where U_0 = 2.96 V for Li/ Li_2O_2, is equilibrium potential, U_{charge} and $U_{discharge}$ represent the equilibrium potentials under charge and discharge conditions respectively. In case of porous carbon cathode in Li-O_2 cell, a large asymmetry is observed in the overpotentials for charge and discharge, for example, U_{charge} = 4.5 V (approx.) and $U_{discharge}$ = 2.5 V (approx.),[55] indicating the charging overpotential as the most important issue to be solved. Renner et al.[365] reported low overpotential for discharge with Au catalyst and Lu et al.[55] reported low overpotential for charging with a Pt catalyst at the cost of reduction in capacity of the battery system. At the same time, Lu et al.[59] demonstrated a bifunctional PtAu/C catalyst to retain the properties of the two catalysts Pt and Au on charge and discharge respectively. The authors obtained these results by optimizing O_2-conditions at low current densities, which showed that overpotential grows significantly with increase in currents. Such observations are important to understand the electronic conduction mechanisms at insulator-catalyst surface. The authors in Chen et al.[334] applied non-equilibrium Green's function calculations[368] along with DFT methods to investigate the electronic transport through Li_2O_2 as well as Li_2O_2 deposited on the two catalysts Pt and Au. They investigated transport through Li_2O_2 grown on the close packed metal (111) surface for the defect free interfaces and for lithium vacancies and showed that the transport depends on the alignment of O_2^{2-} peroxide ions in Li_2O_2 to the metal surface; bulk Li vacancies were found to pin the Fermi level at the top of antibonding peroxide $\pi^*(2p_x)$ and $\pi^*(2p_y)$ levels in the valence band during the charging process; and the electronic transport is reduced during charging under an applied bias condition. Such findings are important to explain the asymmetry observed in the overpotentials for battery charge and discharge.

Moreover, Lu et al.[199] performed DFT calculations on amorphous Li_2O_2 that is likely present in the grain boundaries and showed that amorphous Li_2O_2 may have a metal-like density of states. The authors investigated all cathodes with the same TEGDME:$LiCF_3SO_3$ electrolyte. The two cathodes C and Al_2O_3/C have much higher charge potentials (4.2-4.4 V). The coating in the cathode Pd/Al_2O_3/C has a key role in lowering the charge potential in Li-O_2 batteries. This coating may also prevent decomposition of the TEGDME electrolyte by blocking reaction of the TEGDME solvent molecule with the defect sides on the carbon surface. Electrolyte decomposition on carbon defect sites may result in the deposition of contaminants such as carbonates on Li_2O_2 or on the carbon surface and likely increase the charge potential.[255] Moreover, a low charge potential less than 3.5 V found for Pd/Al_2O_3/C may prevent side reactions including the carbon surface and Li_2O_2 may occur on charge[85, 255] however, decomposition reactions on Li_2O_2 surface may still occur.[255, 280]

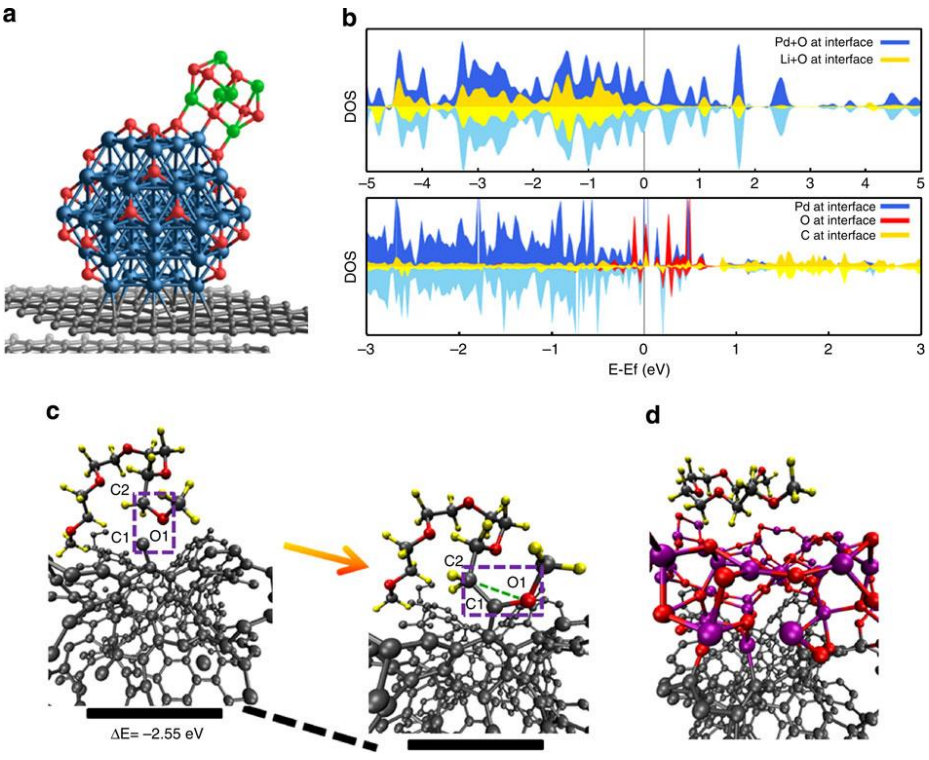

Figure 27 (a) Density functional theory (DFT)-calculated structure of the Li_2O_2/$Pd_{55}O_{21}$/C interface, where $Pd_{55}O_{21}$ represents a partially oxidized palladium nanoparticle. Colour code: palladium (blue), aluminium (purple), oxygen (red), lithium (green), hydrogen (yellow) and carbon (grey). Lithium peroxide (Li_2O_2) is represented by a cluster containing three Li_2O_2 monomers. The carbon electrode (C) is represented by two stacked graphene layers. The average Pd-C bond length is 2.4 Å and the average Pd-O bond length with lithium peroxide is 2.0 Å. (b) Projected density of states at the Li_2O_2/$Pd_{55}O_{21}$ interface (top) and $Pd_{55}O_{21}$/C interface (bottom). In both cases, only the interface atoms that are in direct contact with each other have been considered. The up and down spin

electron densities are represented by dark and light colours, respectively. (c) DFT calculations of a TEGDME solvent molecule binding on a carbon defect site on a bare graphitized carbon surface. The TEGDME molecule decomposes and forms new C-O and C-H bonds on these sites. (d) Weakly bound TEDGME molecule (0.1 eV) on an Al_2O_3-coated carbon surface. Reprinted with permission from ref. [199]. Copyright 2013 Nature Publishing Group.

The DFT-calculated structure of the $Li_2O_2/Pd_{55}O_{21}$/C interface, projected density of states at the $Li_2O_2/Pd_{55}O_{21}$ interface and $Pd_{55}O_{21}$/C interface, DFT calculations of a TGDME solvent molecule binding on a carbon defect site on a bare graphitized carbon surface, and weakly bound TEGDME molecule on an Al_2O_3-coated carbon surface are shown in Figure 27.[199]

e) Li and O_2 reactions with transition metal oxide catalysts

Although organic solvents have been shown to be unstable on discharge in Li-O_2 batteries, it is still interesting to investigate the mechanisms of electrochemical reactions with various catalysts that can enhance the 2-electron and 4-electron reduction of oxygen to Li_2O_2 and Li_2O respectively. Therefore, our focus in this topic is to explore the design of new electrode/electrocatalytic materials with more promising electrolytes[249, 261, 282] for the oxygen electrode to overcome the key challenges in current Li-O_2 batteries. As alternatives to noble metals, transition metal oxides represent a widely explored group electrocatalysts with many advantages such as low cost, high abundance, ease of fabrication and being environmentally benign etc.

Trahey et al.[158] demonstrated the role of α-MnO_2/ramsedellite (R)-MnO_2 catalyst in the formation of discharge products Li_2O_2 and Li_2O in Li-O_2 batteries using DFT methods. The authors performed DFT calculations to investigate the structure and energetics of Li-O_2 discharge products in α- and R-MnO_2 tunnels. The Li_2O units were accommodated into the 2 x 2 tunnels of α-MnO_2[369] and both α- and R-MnO_2 can intercalate Li^+ ions with continuous reduction of MnO_2.[369-371] The α-MnO_2 framework provided a sufficient space for readily reversible Li_xO_y storage within the 2 x 2 tunnels, with Li_xO_y- MnO_2 intermediate structure during discharge and charge reactions. The manganese ions in both α- and R-MnO_2 were found in a mixed valence $Mn^{4+/3+}$ state during Li-O_2 reactions. Such

mixed valence states of manganese ions were found to assist in O_2 redox reaction kinetics.[372] Moreover, the intercalation of Li^+ ions into tunnels could enhance the formation of oxygen-rich surfaces with Li-O_2 products having lower oxygen evolution reaction overpotentials.[63] Such findings are important in the sense that α- and R-MnO_2 structure can act as a dual functioning electrode/electrocatalyst in Li-O_2 batteries.

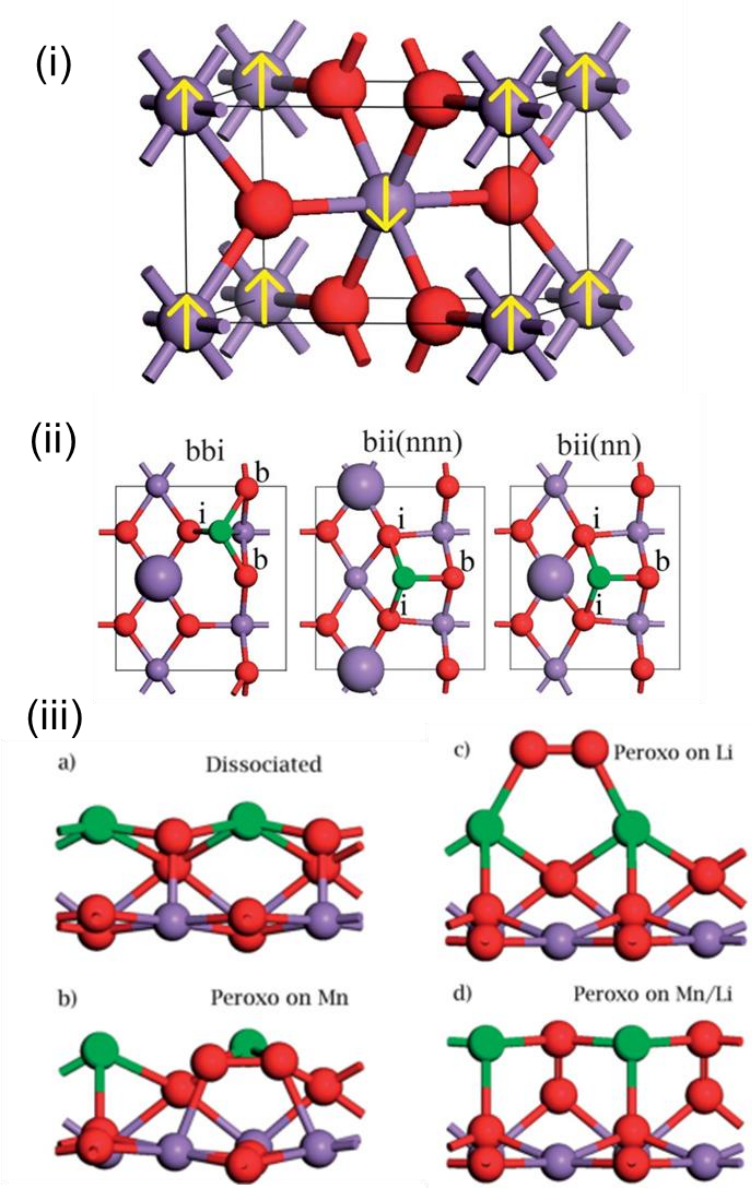

Figure 28 (i) The rutile unit cell of MnO_2, (ii) Li adsorption on MnO_2 (110) surface, and (iii) adsorption of two oxygen atoms at the Li/MnO_2 (110) surface. Reprinted with permission from ref. [373]. Copyright 2013 Royal Society of Chemistry.

Mellan et al. [373] performed DFT calculations for the adsorption and co-adsorption of lithium

and oxygen at the surface of rutile-like manganese dioxide (β-MnO_2) and found that the (110) surface is the most stable surface in the absence of lithium and it absorbs oxygen in the form of peroxo groups bridging between two manganese cations; however, lithium atoms adsorb in two different sites on the (110) surface with tri-coordination to surface oxygen anions in the absence of excess oxygen probably due to transfer of one electron from the adatom to one of the five-coordinated manganese cations at the surface with generation of Li^+ and Mn^{3+} species. The co-adsorption of Li and O_2 leads to the formation of a surface oxide with dissociation of O_2 molecule due to binding of O adatoms to Li adatoms as well as O adatoms saturate the coordination of surface Mn cations. Such type of process was found by the authors to be energetically more favorable than the formation of gas-phase Li_2O_2 monomers, but less favorable than the formation of Li_2O_2 bulk. It clearly suggests that MnO_2 is capable of lowering the energy during initial reduction of oxygen in the discharge process. The rutile unit cell of MnO_2, adsorption of Li on MnO_2 (110) surface and adsorption of two oxygen atoms at the Li/ MnO_2 (110) surface are shown in Figs. 28 (i), (ii), and (iii) respectively.[373]

4.2 Anode materials

The anode is an important part of all Li-batteries. As Li metal has a high energy density, it is the primary choice as the anode material in Li-O_2 batteries; however, it has also disadvantages such as safety issues and degradation during operation (as highlighted in section 3.3 b). Therefore, research needs to be devoted to the development of possible new anode materials in Li-O_2 batteries aided by theoretical investigations and predictions.

a) Lithium metal anode

Electrolyte decomposition results in anode degradation due to oxygen crossover (diffusion of oxygen) to the anode and safety issues due to the presence of traces of water in the electrolyte solvent. These are critical problems for a long period of operation of the cell. Therefore, many efforts have been made to prevent Li metal anode from moisture corrosion by separating a lithium anode

from the liquid electrolyte with the protective layers comprised of Li-ion conducting polymers or ceramics or glasses coated on the metallic lithium. Assary et al.[374] performed both experimental and DFT investigations for possible reactions occurred at the Li anode with electrolyte based on TEGDME. The authors found in their DFT calculations that the binding energy between O_2 and TEGDME anion is 3.3 eV (exothermic) due to larger electron affinity of TEGDME resulting the electron transfer to O_2. Such types of investigation support the need to control reactions of electrolytes at the Li anode through suitable membranes or passivation films to achieve optimal performance of Li-O_2 batteries. The electrolyte vapor pressure also plays a crucial role in Li-O_2 battery degradation. The development of hydrophobic electrolytes with low volatility is essential to address the above issue. As alternatives, various water-stable solid state electrolytes such as LISICON type Li metals and their composites with PEO-based polymers and lithium phosphorous oxynitride (LIPON) have been used to improve stability in electrolytes containing water[20, 374, 375]; however, the lithium conductivity in solid state electrolyte is very low. Hydrophobic ionic liquid electrolytes such as 1-ethyl-3-methyl imidazolium bisfluoromethyl sulfonylamide can prevent electrolyte vaporization and anode hydrolysis.[291] Truong et al.[376] reported the development of single crystal silicon membranes with high Li conductivity and found that Li^+ ion conductivity supported a high current density of 1 mA/cm^2; however, the conductivity of the Si membrane was found too small compared to the LISICON-type Li conducting membranes.

Theoretical studies of Li anodes (and indeed other anodes systems) for Li-O_2 batteries are at an infancy stage and require further investigation given the important role played by the anode in determining the cycle life of the battery.

4.3 Electrolyte (solvent and salt) materials

There is increasing evidence that electrolytes such as organic carbonates and ethers are not found stable in case of Li-O_2 batteries (as outlined in section 3.2). The reason is the formation of Li_2CO_3 and other alkyl species along with Li_2O_2 during discharge of the cell because of the

decomposition of electrolyte, which is a major challenge in Li-O_2 batteries. Therefore, a detailed understanding of related decomposition mechanisms may provide an important basis for the selection and design of stable electrolytes for Li-O_2 batteries. As a result, alternative electrolytes for Li-O_2 batteries such as ionic liquids, solid-state electrolytes, oligoether-functionalized silane electrolytes, polysiloxanes, etc. have been examined.

a) Organic carbonates

Theoretical investigations have confirmed the instability of organic carbonates e.g. ethylene carbonate (EC), propylene carbonate (PC), and dimethyl carbonate (DMC) commonly used in Li-ion batteries in Li-O_2 batteries (as illustrated in experimental reports) due to the formation of Li_2CO_3 and other organic species due to decomposition during the discharge process.[255, 271] In this way, the electrolyte decomposition in the discharge process is one of the major challenges in Li-O_2 batteries. Many of the theoretical works to date have focussed on investigating the reaction mechanisms through which the reactive oxygen species attack various electrolytes. Zhang et al.[261] Bryantsev et al.[377] and other groups[249, 278] have used density functional theory (DFT) calculations with an implicit solvent model to compute the reactivity of a series of electrolytes towards nucleophilic substitutions by superoxide and showed that the decomposition of PC occurs during the discharge process due to breaking of C-O bond, yielding Li_2CO_3 and other lithium alkyl carbonates with the authors concluding that PC is unstable to oxygen reduction species in Li-O_2 batteries.

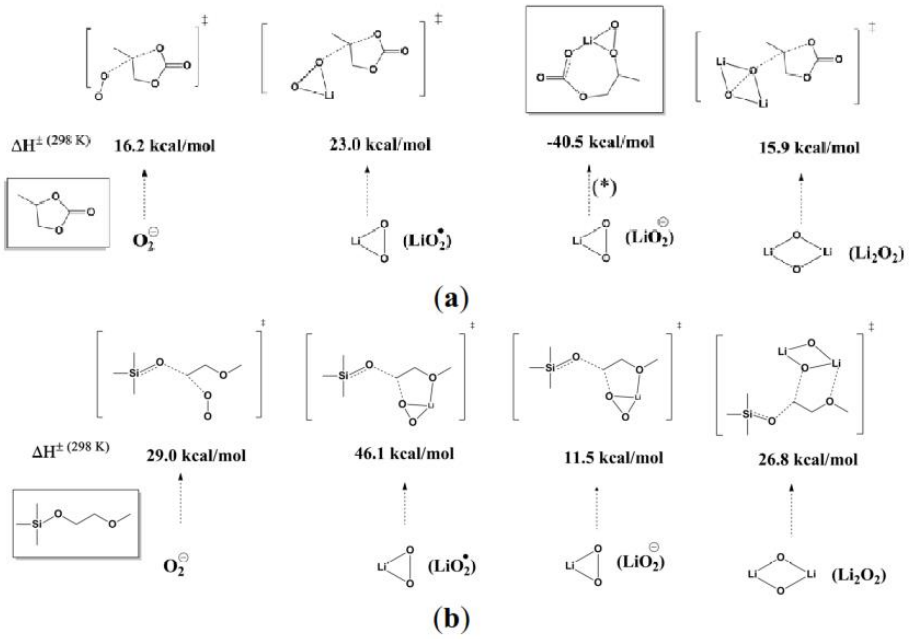

Figure 29 Comparison of the computed barriers (enthalpies) for activation of (a) PC decomposition and (b) 1NM3 decopmposition by O_2 anion radical (O_2^-), Li_2O radical, Li_2O anion radical (Li_2O^-), and Li_2O_2. Reprinted with permission from ref. [261]. Copyright 2011 American Chemical Society.

Moreover, Zhang et al.[261] illustrated that a new silicon-containing oligo (ethylene oxide) solvent namely tri (ethylene glycol)-substituted methyltrimethyl silane (1NM3) is more stable to the highly active oxygen reduction species compared to PC by performing DFT calculations. The comparison of the computed barriers (enthalpies) for activation of PC decomposition and 1NM3 decopmposition by O_2 anion radical (O_2^-), Li_2O radical, Li_2O anion radical (Li_2O^-), and Li_2O_2 are shown in Figs. 29 (a) and (b) respectively.[261]

b) Ethers

Recent experimental findings on electrolytes showing that a tetra (ethylene) glycol dimethyl ether-lithium triflate (TEGDME-$LiCF_3SO_3$) electrolyte[377] and $LiClO_4$ in dimethyl sulfoxide (DMSO)[278] can support highly reversible formation-decomposition of Li_2O_2 at the cathode on cycling, represent a useful platform for further investigation on non-aqueous Li-O_2 battery electrolytes by theoretical methods. Assary et al.[280] performed DFT calculations to investigate the interactions of

dimethoxyethane (DME) with Li_2O_2 clusters as shown in Figure 30[280] and found the energetically favourable chemical mechanisms for DME decomposition at the Li_2O_2-electrolyte during discharge or charge in Li-O_2 cells due to a hydrogen abstraction mechanism.

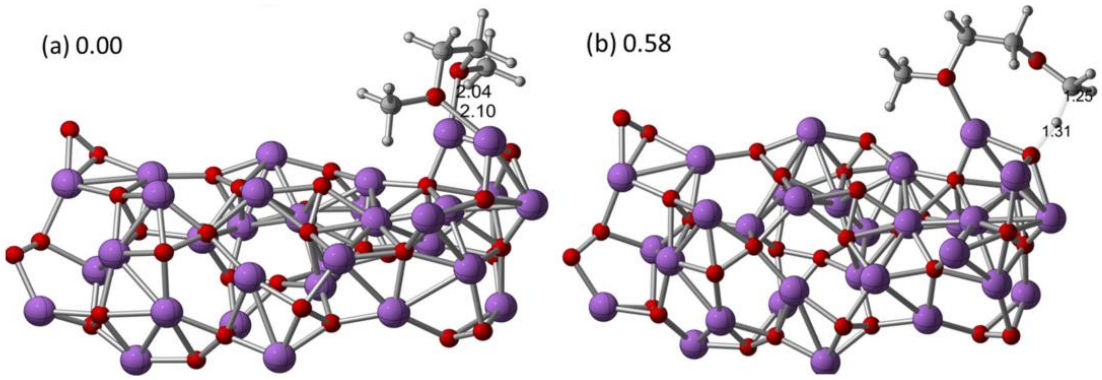

Figure 30 Optimized structures of (a) $(Li_2O_2)_{16}$-DME cluster and (b) transition state structure for the abstraction of a primary hydrogen from the DME at the B3LYP/6-31G(d) level of theory. Reprinted with permission from ref. [280]. Copyright 2013 American Chemical Society.

Therefore, as highlighted above, neither carbonate nor ether electrolyte represent long term solutions as the electrolyte solvent for Li-O_2 batteries and identification of solvents resistant to attack by reduced O_2 species remains an issue.

c) Ionic liquids

Hydrophobic room temperature ionic liquids are attractive electrolyte solvents for Li-O_2 batteries mainly due to their unique properties such as hydrophobic nature, low flammability, low vapor pressure, wide potential window, and high thermal stability. Due to their hydrophobic properties, these can better protect the Li metal anode from moisture compared to other aprotic solvents. The hydrophobicity and negligible vapor pressure make the ionic liquid as a promising electrolyte for Li-O_2 battery system.[378-380] Some researchers have already considered ionic liquids as electrolyte systems in Li-O_2 batteries[291, 381] for example, Kuboki et al.[291] utilized 1-alkyl-3-methylimidazolium bis (trifluoromethylsulfonyl) imide (EMITFSI) in Li-O_2 batteries. Allen et al.[292] also investigated the oxygen electrode rechargeability in a room temperature ionic liquid EMITFSI and

found that the nature of the electrode affects the reaction mechanism, for example, gold showed the ability for high efficiency recharging of the oxygen without electrode passivation. Therefore, ionic liquids can be considered as promising electrolytes for Li-O_2 batteries with Li metal and oxygen electrodes for future research.[292]

In fact, current Li-O_2 batteries utilizing ionic liquid electrolytes have lower discharge capacity compared to carbonate-based electrolytes due to their high viscosity and hence inferior wetting of the oxygen electrode. Ionic liquids with high electrochemical stability and low viscosity are currently the electrolyte component of choice. Moreover, more research work should be devoted to investigate the side-reactions due to electrolyte decomposition for ionic liquid electrolytes in Li-O_2 batteries.

d) Oligoether-functionalized silane electrolytes

Zhang et al.[261] performed combined experimental and DFT investigations on electrolyte based on 1NM3 and oligoether-functionalized silane and reported that ethers are more stable towards oxygen reduction discharge species than PC. Such type of investigations provides a new research direction to improve the stability of new alternative electrolytes by functionalization and modifications.

e) Polysiloxanes

Assary et al. [382] performed quantum chemical calculations to investigate the polysiloxanes oxidation potential and decomposition reactions and suggested that Si-O group gives enhanced stability than their carbon analogs and they were found to be more resistant to thermal decomposition than carbonates. In this way, polysiloxanes may be more suitable as electrolytes for Li-O_2 batteries compared to organic carbonates and ethers, however, this requires further study.

5. Future Research Directions

There are many scientific challenges to be addressed with regard to Li-O_2 battery operation if stable systems with energy densities which are close to their immense theoretical capacities are to be realized. As highlighted in this review article, such challenges are frequently rooted in materials discovery and optimization. Future research should emphasize the development of i) high efficiency Li metal anodes to overcome the degradation and safety issues, ii) new air cathode support materials (be they based on carbon or carbon-free) with increased stability which allow optimization of the transport of reactants such as O_2, Li^+, and electrons to the active catalyst surface, iii) cost-effective catalysts to reduce the overpotentials for the discharge and charge processes, and iv) oxidation-resistant electrolytes and cathodes that can withstand high oxidation potentials in the presence of oxygen.

Unfortunately, the development of the various portions of the Li-O_2 battery cannot be considered in isolation and it is clear that optimal systems will require the marrying of compatible anode/electrolyte/cathode choices. Recent studies have shown that carbon free cathode materials (in combination with DMSO based electrolytes) are the most stable cathode/electrolyte systems and the challenge becomes the optimization of electrolyte/cathode systems such that the modest (but crucially reversible) capacities exhibited by these materials can be improved.[112, 197] Ideally, this goal would be achieved using cheap, lightweight carbon based materials with increased stability and compatibility with simple electrolytes. Future research must confirm that all of observed electrochemical response in a given Li-O_2 cell is due to the formation and decomposition of Li_2O_2 rather than unwanted side reactions. Furthermore, scalable systems with higher mass loadings must be investigated. While mass loadings of circa 1 mg cm^2 may deliver high gravimetric capacities, they are likely to be insufficient to power real world devices.

Additional modelling efforts are required to both supplement and guide experimental studies. In addition, accurate modelling of the interfacial reactions that combine the chemistry with diffusion of radicals and formation of lithium carbonates and the discharge products that clog the cathode pores

as well as the lithium metal anode degradation, which is largely unaddressed. Computational approaches that involve large-scale screening of various materials in the spirit of the Materials Genome Project, would also be extremely beneficial. DFT-based approaches can successfully describe the potentials, energetics and facet-dependent reactivities and pathways for lithium oxides and metal-oxides. Developing a 'genome' for the energetics of peroxide formation on various surfaces could provide a route to materials design and choice for a given electrolyte. Knowing which carbons, which catalytic surfaces and their effect on ORR and OER, together with details on the mechanism of peroxide formation (nucleation, deposition and density; delithiation and decomposition processes) might help optimize cathode, catalyst and electrolyte components in conjunction with experimental evidence of high performance cells under real-world loading in applications such as EV batteries.

6. Conclusions

In this review, the major progress to date in the field of Li-O_2 batteries has been presented from both an experimental and DFT background. The various components (cathode, anode, and electrolyte materials) of rechargeable non-aqueous Li-O_2 batteries have been examined and we have tried to provide a combined perspective to better understand the operation of the various materials in Li-O_2 batteries. The experimental results highlight the immense potential for Li-O_2 systems but also the many hurdles which must be overcome if this is to become a viable next-generation energy storage system.

With the help of advanced theory and computational techniques, effective design and in-depth exploration of promising Li-O_2 battery materials can be accelerated. Starting from fundamental DFT methods and input configuration, DFT calculations can provide the detailed electronic structures of the specific applied component materials in Li-O_2 batteries. Such theoretical investigations could facilitate the understanding of the elementary kinetics in ORR and OER during discharge and charge

processes respectively as well as the electronic conductivity properties of the formation/decomposition of the lithium oxide layers. Physical modelling also has a major role to play in the clarification of the impact of the electrolyte composition on the performance and durability of Li-O_2 batteries. Another level of modelling concerns the end user application for an optimized Li-air system, whatever chemistry and design is eventually chosen. This involves the full loading requirements for various applications, and the associated drive-train for power delivery under different conditions. Even the most promising Li-O_2 battery has not been fully tested at EV scale, under real-world driving conditions. Important parameters such as energy density, price per capacity, C-rate, and cycle life are paramount. The latter has been the primary focus, and the materials and chemistry are still under development. However, it is advisable for systems that do offer cycle life approaching several hundred cycles (irrespective of true specific capacity) that various C-rate testing be benchmarked. Such information is lacking in the literature and critical for various loading conditions demanded by real world applications.

The future development of functional electrode and electrolyte materials for Li-O_2 batteries are best investigated through a combination of experimental and advanced computational approaches. If the hurdles to Li-O_2 batteries outlined in this review can be overcome, then the benefits for electrification of transport, static energy storage, and hence reduction in CO_2 emissions would be transformational.

Acknowledgement

This research has received funding from the Seventh Framework Programme FP7/2007-2013 (Project STABLE) under grant agreement n°314508.

References

1. Z. Yang, J. Zhang, M. C. Kintner-Meyer, X. Lu, D. Choi, J. P. Lemmon and J. Liu, *Chemical Reviews*, 2011, **111**, 3577-3613.
2. R. Padbury and X. Zhang, *Journal of Power Sources*, 2011, **196**, 4436-4444.
3. K. G. Gallagher, S. Goebel, T. Greszler, M. Mathias, W. Oelerich, D. Erogluab and V. Srinivasan, *Energy Environ. Sci*, 2014, **7**, 1555-1563.
4. T. Ogasawara, A. Débart, M. Holzapfel, P. Novák and P. G. Bruce, *Journal of the American Chemical Society*, 2006, **128**, 1390-1393.
5. S. Beattie, D. Manolescu and S. Blair, *Journal of The Electrochemical Society*, 2009, **156**, A44-A47.
6. Y. Wang and H. Zhou, *Chemical Communications*, 2010, **46**, 6305-6307.
7. P. G. Bruce, L. J. Hardwick and K. Abraham, *MRS Bull*, 2011, **36**, 506-512.
8. J. Xiao, D. Mei, X. Li, W. Xu, D. Wang, G. L. Graff, W. D. Bennett, Z. Nie, L. V. Saraf, I. A. Aksay, J. Liu and J.-G. Zhang, *Nano Letters*, 2011, **11**, 5071-5078.
9. Y. Chen, S. A. Freunberger, Z. Peng, O. Fontaine and P. G. Bruce, *Nature chemistry*, 2013, **5**, 489-494.
10. F. Cheng, J. Liang, Z. Tao and J. Chen, *Advanced Materials*, 2011, **23**, 1695-1715.
11. G. Girishkumar, B. McCloskey, A. C. Luntz, S. Swanson and W. Wilcke, *The Journal of Physical Chemistry Letters*, 2010, **1**, 2193-2203.
12. P. G. Bruce, S. A. Freunberger, L. J. Hardwick and J. M. Tarascon, *Nature materials*, 2011, **11**, 19-29.
13. A. Kraytsberg and Y. Ein-Eli, *Journal of Power Sources*, 2011, **196**, 886-893.
14. J. Read, *Journal of The Electrochemical Society*, 2002, **149**, A1190-A1195.
15. T. Zhang, N. Imanishi, Y. Takeda and O. Yamamoto, *Chemistry Letters*, 2011, **40**, 668-673.
16. E. N. S.J. Visco, B. Katz, L. Jonghe, M.Y. Chu, *12th International Meeting on Lithium Batteries, Nara, Japan, 27 June–2 July*, 2004.
17. E. N. S.J. Visco, B. Katz, L. Jonghe, M.Y. Chu, *Electrochem. Soc. Meeting, Cancun, Mexico, 29 October–3 November*, 2006.
18. S. J. Visco, Y. S. Nimon and B. D. Katz, Google Patents, 2007.
19. T. Zhang, N. Imanishi, S. Hasegawa, A. Hirano, J. Xie, Y. Takeda, O. Yamamoto and N. Sammes, *Journal of The Electrochemical Society*, 2008, **155**, A965-A969.
20. T. Zhang, N. Imanishi, S. Hasegawa, A. Hirano, J. Xie, Y. Takeda, O. Yamamoto and N. Sammes, *Electrochemical and Solid-State Letters*, 2009, **12**, A132-A135.
21. N. Imanishi, S. Hasegawa, T. Zhang, A. Hirano, Y. Takeda and O. Yamamoto, *Journal of Power Sources*, 2008, **185**, 1392-1397.
22. S. Hasegawa, N. Imanishi, T. Zhang, J. Xie, A. Hirano, Y. Takeda and O. Yamamoto, *Journal of Power Sources*, 2009, **189**, 371-377.
23. Y. Shimonishi, T. Zhang, P. Johnson, N. Imanishi, A. Hirano, Y. Takeda, O. Yamamoto and N. Sammes, *Journal of Power Sources*, 2010, **195**, 6187-6191.
24. T. Zhang, N. Imanishi, Y. Shimonishi, A. Hirano, J. Xie, Y. Takeda, O. Yamamoto and N. Sammes, *Journal of The Electrochemical Society*, 2010, **157**, A214-A218.
25. L. Li, X. Zhao and A. Manthiram, *Electrochemistry Communications*, 2012, **14**, 78-81.
26. E. Yoo and H. Zhou, *ACS Nano*, 2011, **5**, 3020-3026.
27. Y. Wang, P. He and H. Zhou, *Energy & Environmental Science*, 2011, **4**, 4994-4999.
28. P. He, Y. Wang and H. Zhou, *Electrochemistry Communications*, 2010, **12**, 1686-1689.
29. P. He, Y. Wang and H. Zhou, *Journal of Power Sources*, 2011, **196**, 5611-5616.
30. Y. Wang and H. Zhou, *Journal of Power Sources*, 2010, **195**, 358-361.
31. J. Zheng, R. Liang, M. Hendrickson and E. Plichta, *Journal of The Electrochemical Society*, 2008, **155**, A432-A437.
32. P. He, Y. Wang and H. Zhou, *Chemical Communications*, 2011, **47**, 10701-10703.

33. B. Kumar, J. Kumar, R. Leese, J. P. Fellner, S. J. Rodrigues and K. Abraham, *Journal of The Electrochemical Society*, 2010, **157**, A50-A54.
34. B. Kumar and J. Kumar, *Journal of The Electrochemical Society*, 2010, **157**, A611-A616.
35. J.-S. Lee, S. Tai Kim, R. Cao, N.-S. Choi, M. Liu, K. T. Lee and J. Cho, *Advanced Energy Materials*, 2011, **1**, 34-50.
36. J. Wang, Y. Li and X. Sun, *Nano Energy*, 2013, **2**, 443-467.
37. Q. Li, R. Cao, J. Cho and G. Wu, *Phys. Chem. Chem. Phys.*, 2014.
38. J. Nanda, H. Bilheux, S. Voisin, G. M. Veith, R. Archibald, L. Walker, S. Allu, N. J. Dudney and S. Pannala, *The Journal of Physical Chemistry C*, 2012, **116**, 8401-8408.
39. N. Tsiouvaras, S. Meini, K. U. Schwenke, M. Piana, H. Beyer, L. Lange and H. A. Gasteiger, *Physical Chemistry Chemical Physics*, 2013.
40. J.-J. Xu, Z.-L. Wang, D. Xu, L.-L. Zhang and X.-B. Zhang, *Nature communications*, 2013, **4**.
41. J. Yang, D. Zhai, H.-H. Wang, K. C. Lau, J. A. Schlueter, P. Du, D. J. Myers, Y.-K. Sun, L. A. Curtiss and K. Amine, *Physical Chemistry Chemical Physics*, 2013, **15**, 3764-3771.
42. P. Kichambare, J. Kumar, S. Rodrigues and B. Kumar, *Journal of Power Sources*, 2011, **196**, 3310-3316.
43. S. H. Oh, R. Black, E. Pomerantseva, J.-H. Lee and L. F. Nazar, *Nature chemistry*, 2012, **4**, 1004-1010.
44. Z. Guo, D. Zhou, X. Dong, Z. Qiu, Y. Wang and Y. Xia, *Advanced Materials*, 2013, n/a-n/a.
45. J. Li and Y. Zhang, *Nanoscale*, 2013.
46. R. Cao, J.-S. Lee, M. Liu and J. Cho, *Advanced Energy Materials*, 2012, **2**, 816-829.
47. F. Cheng and J. Chen, *Chemical Society Reviews*, 2012, **41**, 2172-2192.
48. F. Li, T. Zhang and H. Zhou, *Energy & Environmental Science*, 2013, **6**, 1125-1141.
49. Y. Shao, S. Park, J. Xiao, J.-G. Zhang, Y. Wang and J. Liu, *ACS Catalysis*, 2012, **2**, 844-857.
50. H. Kim, G. Jeong, Y.-U. Kim, J.-H. Kim, C.-M. Park and H.-J. Sohn, *Chemical Society Reviews*, 2013, **42**, 9011-9034.
51. M. Balaish, A. Kraytsberg and Y. Ein-Eli, *Physical Chemistry Chemical Physics*, 2013, **16**, 2801-2822.
52. L. A. Huff, J. L. Rapp, L. Zhu and A. A. Gewirth, *Journal of Power Sources*, 2013, **235**, 87-94.
53. N. K. Karan, M. Balasubramanian, T. T. Fister, A. K. Burrell and P. Du, *The Journal of Physical Chemistry C*, 2012, **116**, 18132-18138.
54. M. Leskes, N. E. Drewett, L. J. Hardwick, P. G. Bruce, G. R. Goward and C. P. Grey, *Angewandte Chemie International Edition*, 2012, **51**, 8560-8563.
55. Y.-C. Lu, H. A. Gasteiger, M. C. Parent, V. Chiloyan and Y. Shao-Horn, *Electrochemical and Solid-State Letters*, 2010, **13**, A69-A72.
56. Y.-C. Lu, D. G. Kwabi, K. P. C. Yao, J. R. Harding, J. Zhou, L. Zuin and Y. Shao-Horn, *Energy & Environmental Science*, 2011, **4**, 2999-3007.
57. S. R. Younesi, S. Urbonaite, F. Björefors and K. Edström, *Journal of Power Sources*, 2011, **196**, 9835-9838.
58. R. E. Williford and J.-G. Zhang, *Journal of Power Sources*, 2009, **194**, 1164-1170.
59. Y.-C. Lu, Z. Xu, H. A. Gasteiger, S. Chen, K. Hamad-Schifferli and Y. Shao-Horn, *Journal of the American Chemical Society*, 2010, **132**, 12170-12171.
60. J.-M. Tarascon and M. Armand, *Nature*, 2001, **414**, 359-367.
61. Z. Z. D.H. Wu, *Frontier of Physics*, 2011, **6**.
62. C. O. Laoire, S. Mukerjee, K. M. Abraham, E. J. Plichta and M. A. Hendrickson, *The Journal of Physical Chemistry C*, 2009, **113**, 20127-20134.
63. Y. Mo, S. P. Ong and G. Ceder, *Physical Review B*, 2011, **84**, 205446.
64. A. Kumar, F. Ciucci, A. N. Morozovska, S. V. Kalinin and S. Jesse, *Nature chemistry*, 2011, **3**, 707-713.
65. Z.-L. Wang, D. Xu, J.-J. Xu and X.-B. Zhang, *Chemical Society Reviews*, 2014.

66. J. Christensen, P. Albertus, R. S. Sanchez-Carrera, T. Lohmann, B. Kozinsky, R. Liedtke, J. Ahmed and A. Kojic, *Journal of The Electrochemical Society*, 2011, **159**, R1-R30.
67. E. L. Littauer and K. C. Tsai, *Journal of the Electrochemical Society*, 1976, **123**, 771-776.
68. K. Abraham and Z. Jiang, *Journal of The Electrochemical Society*, 1996, **143**, 1-5.
69. M. W. Chase, *J. Phys. Chem. Ref. Data Monograph*, 1998, 1506, 1510.
70. M. D. Radin, J. F. Rodriguez, F. Tian and D. J. Siegel, *Journal of the American Chemical Society*, 2011, **134**, 1093-1103.
71. T. Fujinaga and S. Sakura, *Bull. Chem. Soc. Jpn*, 1974, **47**, 2781-2786.
72. D. Aurbach, M. Daroux, P. Faguy and E. Yeager, *Journal of electroanalytical chemistry and interfacial electrochemistry*, 1991, **297**, 225-244.
73. D. T. Sawyer, G. Chiericato Jr, C. T. Angelis, E. J. Nanni Jr and T. Tsuchiya, *Analytical Chemistry*, 1982, **54**, 1720-1724.
74. Y.-C. Lu, H. A. Gasteiger, E. Crumlin, R. McGuire and Y. Shao-Horn, *Journal of The Electrochemical Society*, 2010, **157**, A1016-A1025.
75. C. O. Laoire, S. Mukerjee, K. M. Abraham, E. J. Plichta and M. A. Hendrickson, *The Journal of Physical Chemistry C*, 2010, **114**, 9178-9186.
76. S. A. Freunberger, Y. Chen, N. E. Drewett, L. J. Hardwick, F. Bardé and P. G. Bruce, *Angewandte Chemie International Edition*, 2011, **50**, 8609-8613.
77. A. A. Franco and K.-H. Xue, *ECS Journal of Solid State Science and Technology*, 2013, **2**, M3084-M3100.
78. M.-K. Song, S. Park, F. M. Alamgir, J. Cho and M. Liu, *Materials Science and Engineering: R: Reports*, 2011, **72**, 203-252.
79. L. J. Hardwick and P. G. Bruce, *Current Opinion in Solid State and Materials Science*, 2012.
80. Y. Shao, F. Ding, J. Xiao, J. Zhang, W. Xu, S. Park, J.-G. Zhang, Y. Wang and J. Liu, *Advanced Functional Materials*, 2012, n/a-n/a.
81. Y.-C. Lu, B. M. Gallant, D. G. Kwabi, J. R. Harding, R. R. Mitchell, M. S. Whittingham and Y. Shao-Horn, *Energy & Environmental Science*, 2013, **6**, 750-768.
82. J. Hou, M. Yang, M. W. Ellis, R. B. Moore and B. Yi, *Physical Chemistry Chemical Physics*, 2012, **14**, 13487-13501.
83. M. Mirzaeian and P. J. Hall, *Electrochimica Acta*, 2009, **54**, 7444-7451.
84. Y. Zhang, H. Zhang, J. Li, M. Wang, H. Nie and F. Zhang, *Journal of Power Sources*, 2013, **240**, 390-396.
85. M. M. Ottakam Thotiyl, S. A. Freunberger, Z. Peng and P. G. Bruce, *Journal of the American Chemical Society*, 2012.
86. J. R. Harding, Y.-C. Lu, Y. Tsukada and Y. Shao-Horn, *Physical Chemistry Chemical Physics*, 2012, **14**, 10540-10546.
87. A. Débart, J. Bao, G. Armstrong and P. G. Bruce, *Journal of Power Sources*, 2007, **174**, 1177-1182.
88. H.-G. Jung, H.-S. Kim, J.-B. Park, I.-H. Oh, J. Hassoun, C. S. Yoon, B. Scrosati and Y.-K. Sun, *Nano Letters*, 2012, **12**, 4333-4335.
89. Y.-C. Lu and Y. Shao-Horn, *The Journal of Physical Chemistry Letters*, 2012, 93-99.
90. R. Younesi, S. Urbonaite, K. Edström and M. Hahlin, *The Journal of Physical Chemistry C*, 2012, **116**, 20673-20680.
91. B. D. Adams, C. Radtke, R. Black, M. L. Trudeau, K. Zaghib and L. F. Nazar, *Energy & Environmental Science*, 2013, **6**, 1772-1778.
92. W. Fan, Z. Cui and X. Guo, *The Journal of Physical Chemistry C*, 2013.
93. B. M. Gallant, D. G. Kwabi, R. R. Mitchell, J. Zhou, C. Thompson and Y. Shao-Horn, *Energy & Environmental Science*, 2013.
94. B. Horstmann, B. Gallant, R. Mitchell, W. G. Bessler, Y. Shao-Horn and M. Z. Bazant, *The Journal of Physical Chemistry Letters*, 2013, 4217-4222.

95. B. D. McCloskey, A. Valery, A. C. Luntz, S. R. Gowda, G. M. Wallraff, J. M. Garcia, T. Mori and L. E. Krupp, *The Journal of Physical Chemistry Letters*, 2013, 2989-2993.
96. R. R. Mitchell, B. M. Gallant, Y. Shao-Horn and C. V. Thompson, *The Journal of Physical Chemistry Letters*, 2013, 1060-1064.
97. F. Mizuno, K. Takechi, S. Higashi, T. Shiga, T. Shiotsuki, N. Takazawa, Y. Sakurabayashi, S. Okazaki, I. Nitta, T. Kodama, H. Nakamoto, H. Nishikoori, S. Nakanishi, Y. Kotani and H. Iba, *Journal of Power Sources*, 2013, **228**, 47-56.
98. N. Tsiouvaras, S. Meini, I. Buchberger and H. Gasteiger, *Journal of The Electrochemical Society*, 2013, **160**, A471-A477.
99. L. Zhong, R. R. Mitchell, Y. Liu, B. M. Gallant, C. V. Thompson, J. Y. Huang, S. X. Mao and Y. Shao-Horn, *Nano Letters*, 2013.
100. E. Yilmaz, C. Yogi, K. Yamanaka, T. Ohta and H. R. Byon, *Nano Letters*, 2013, **13**, 4679-4684.
101. R. Black, J.-H. Lee, B. Adams, C. A. Mims and L. F. Nazar, *Angewandte Chemie International Edition*, 2012, n/a-n/a.
102. D. Xu, Z.-l. Wang, J.-j. Xu, L.-l. Zhang and X.-b. Zhang, *Chemical Communications*, 2012, **48**, 6948-6950.
103. J.-H. Lee, R. Black, G. Popov, E. Pomerantseva, F. Nan, G. A. Botton and L. F. Nazar, *Energy & Environmental Science*, 2012, **5**, 9558-9565.
104. D. Zhai, H.-H. Wang, J. Yang, K. C. Lau, K. Li, K. Amine and L. A. Curtiss, *Journal of the American Chemical Society*, 2013, **135**, 15364-15372.
105. R. R. Mitchell, B. M. Gallant, C. V. Thompson and Y. Shao-Horn, *Energy & Environmental Science*, 2011, **4**, 2952-2958.
106. D. Xu, Z.-l. Wang, J.-j. Xu, L.-l. Zhang, L.-m. Wang and X.-b. Zhang, *Chemical Communications*, 2012, **48**, 11674-11676.
107. H.-D. Lim, K.-Y. Park, H. Song, E. Y. Jang, H. Gwon, J. Kim, Y. H. Kim, M. D. Lima, R. O. Robles, X. Lepró, R. H. Baughman and K. Kang, *Advanced Materials*, 2013, **25**, 1348-1352.
108. Z. L. Wang, D. Xu, J. J. Xu, L. L. Zhang and X. B. Zhang, *Advanced Functional Materials*, 2012, **22**, 3699-3705.
109. R. Black, S. H. Oh, J.-H. Lee, T. Yim, B. Adams and L. F. Nazar, *Journal of the American Chemical Society*, 2012, **134**, 2902-2905.
110. Y. Cui, Z. Wen and Y. Liu, *Energy & Environmental Science*, 2011, **4**, 4727-4734.
111. Z.-W. Fu, W.-M. Liu, T.-T. Gao, Y. Yang and Q. Sun, *Physical Chemistry Chemical Physics*, 2013.
112. M. M. O. Thotiyl, S. A. Freunberger, Z. Peng, Y. Chen, Z. Liu and P. G. Bruce, *Nature materials*, 2013.
113. S. Ma, L. Sun, L. Cong, X. Gao, C. Yao, X. Guo, L. Tai, P. Mei, Y. Zeng, H. Xie and R. Wang, *The Journal of Physical Chemistry C*, 2013.
114. R. Choi, J. Jung, G.-B. Kim, K.-S. Song, Y. Kim, S. C. Jung, Y.-K. Han, H. Song and Y. Kang, *Energy & Environmental Science*, 2014.
115. K.-S. Song, J. Jung, Y. U. Heo, Y. C. Lee, K. Cho and Y. Kang, *Physical Chemistry Chemical Physics*, 2013.
116. Y. Hu, X. Han, F. Cheng, Q. Zhao, Z. Hu and J. Chen, *Nanoscale*, 2014, **6**, 177-180.
117. H. Beyer, S. Meini, N. Tsiouvaras, M. Piana and H. A. Gasteiger, *Physical Chemistry Chemical Physics*, 2013, **15**, 11025-11037.
118. J. Read, *Journal of The Electrochemical Society*, 2006, **153**, A96-A100.
119. G. A. Elia, J.-B. Park, B. Scrosati, Y.-K. Sun and J. Hassoun, *Electrochemistry Communications*, 2013, **34**, 250-253.
120. D. M. Itkis, D. A. Semenenko, E. Y. Kataev, A. I. Belova, V. S. Neudachina, A. P. Sirotina, M. Hävecker, D. Teschner, A. Knop-Gericke, P. Dudin, A. Barinov, E. A. Goodilin, Y. Shao-Horn and L. V. Yashina, *Nano Letters*, 2013, **13**, 4697-4701.

121. W. Xu, J. Hu, M. H. Engelhard, S. A. Towne, J. S. Hardy, J. Xiao, J. Feng, M. Y. Hu, J. Zhang, F. Ding, M. E. Gross and J.-G. Zhang, *Journal of Power Sources*, 2012, **215**, 240-247.
122. H.-D. Lim, K.-Y. Park, H. Gwon, J. Hong, H. Kim and K. Kang, *Chemical Communications*, 2012, **48**, 8374-8376.
123. P. Du, J. Lu, K. C. Lau, X. Luo, J. Bareno, X. Zhang, Y. Ren, Z. Zhang, L. A. Curtiss, Y.-K. Sun and K. Amine, *Physical Chemistry Chemical Physics*, 2013, **15**, 5572-5581.
124. J. Li, N. Wang, Y. Zhao, Y. Ding and L. Guan, *Electrochemistry Communications*, 2011, **13**, 698-700.
125. Y. Li, J. Wang, X. Li, J. Liu, D. Geng, J. Yang, R. Li and X. Sun, *Electrochemistry Communications*, 2011, **13**, 668-672.
126. G. Zhang, J. Zheng, R. Liang, C. Zhang, B. Wang, M. Au, M. Hendrickson and E. Plichta, *Journal of The Electrochemical Society*, 2011, **158**, A822-A827.
127. T. Zhang and H. Zhou, *Angewandte Chemie*, 2012, **124**, 11224-11229.
128. Y. Chen, F. Li, D.-M. Tang, Z. Jian, C. Liu, D. Golberg, A. Yamada and H. Zhou, *Journal of Materials Chemistry A*, 2013.
129. Z. H. Cui, W. G. Fan and X. X. Guo, *Journal of Power Sources*, 2013, **235**, 251-255.
130. Y. Li, Z. Huang, K. Huang, D. Carnahan and Y. Xing, *Energy & Environmental Science*, 2013, **6**, 3339-3345.
131. H. W. Park, D. U. Lee, L. F. Nazar and Z. Chen, *Journal of The Electrochemical Society*, 2013, **160**, A344-A350.
132. Y. Shen, D. Sun, L. Yu, W. Zhang, Y. Shang, H. Tang, J. Wu, A. Cao and Y. Huang, *Carbon*, 2013, **62**, 288-295.
133. S. Wang, S. Dong, J. Wang, L. Zhang, P. Han, C. Zhang, X. Wang, K. Zhang, Z. Lan and G. Cui, *Journal of Materials Chemistry*, 2012.
134. G. Zhang, J. Zheng, R. Liang, C. Zhang, B. Wang, M. Hendrickson and E. Plichta, *Journal of The Electrochemical Society*, 2010, **157**, A953-A956.
135. J. Shui, F. Du, C. Xue, Q. Li and L. Dai, *ACS Nano*, 2014.
136. X. Lin, L. Zhou, T. Huang and A. Yu, *Journal of Materials Chemistry A*, 2013, **1**, 1239-1245.
137. J.-B. Park, J. Lee, C. S. Yoon and Y.-K. Sun, *ACS Applied Materials & Interfaces*, 2013, **5**, 13426-13431.
138. P. Kichambare, S. Rodrigues and J. Kumar, *ACS Applied Materials & Interfaces*, 2011, **4**, 49-52.
139. V. Etacheri, D. Sharon, A. Garsuch, M. Afri, A. A. Frimer and D. Aurbach, *Journal of Materials Chemistry A*, 2013, **1**, 5021-5030.
140. J. Park, Y.-S. Jun, W.-r. Lee, J. A. Gerbec, K. A. See and G. D. Stucky, *Chemistry of Materials*, 2013.
141. W. Zhang, J. Zhu, H. Ang, Y. Zeng, N. Xiao, Y. Gao, W. Liu, H. H. Hng and Q. Yan, *Nanoscale*, 2013, **5**, 9651-9658.
142. B. Sun, B. Wang, D. Su, L. Xiao, H. Ahn and G. Wang, *Carbon*, 2012, **50**, 727-733.
143. Y. Li, J. Wang, X. Li, D. Geng, M. N. Banis, R. Li and X. Sun, *Electrochemistry Communications*, 2012, **18**, 12-15.
144. Y. Li, J. Wang, X. Li, D. Geng, R. Li and X. Sun, *Chemical Communications*, 2011, **47**, 9438-9440.
145. Y. Wang and H. Zhou, *Energy & Environmental Science*, 2011, **4**, 1704-1707.
146. G. Wu, N. H. Mack, W. Gao, S. Ma, R. Zhong, J. Han, J. K. Baldwin and P. Zelenay, *ACS Nano*, 2012, **6**, 9764-9776.
147. C. Selvaraj, S. Kumar, N. Munichandraiah and L. Scanlon, *Journal of The Electrochemical Society*, 2014, **161**, A554-A560.
148. Y. Yang, Q. Sun, Y.-S. Li, H. Li and Z.-W. Fu, *Journal of The Electrochemical Society*, 2011, **158**, B1211-B1216.

149. S. Liu, Z. Wang, C. Yu, Z. Zhao, X. Fan, Z. Ling and J. Qiu, *Journal of Materials Chemistry A*, 2013, **1**, 12033-12037.
150. B. M. Gallant, R. R. Mitchell, D. G. Kwabi, J. Zhou, L. Zuin, C. V. Thompson and Y. Shao-Horn, *The Journal of Physical Chemistry C*, 2012, **116**, 20800-20805.
151. G. O. Shitta-Bey, M. Mirzaeian and P. J. Hall, *Journal of The Electrochemical Society*, 2012, **159**, A315-A320.
152. A. Débart, A. J. Paterson, J. Bao and P. G. Bruce, *Angewandte Chemie*, 2008, **120**, 4597-4600.
153. A. K. Thapa, K. Saimen and T. Ishihara, *Electrochemical and Solid-State Letters*, 2010, **13**, A165-A167.
154. A. K. Thapa and T. Ishihara, *Journal of Power Sources*, 2011, **196**, 7016-7020.
155. Y. Cao, Z. Wei, J. He, J. Zang, Q. Zhang, M. Zheng and Q. Dong, *Energy & Environmental Science*, 2012, **5**, 9765-9768.
156. T. T. Truong, Y. Liu, Y. Ren, L. Trahey and Y. Sun, *ACS Nano*, 2012, **6**, 8067-8077.
157. Y. Qin, J. Lu, P. Du, Z. Chen, Y. Ren, T. Wu, J. T. Miller, J. Wen, D. J. Miller, Z. Zhang and K. Amine, *Energy & Environmental Science*, 2013, **6**, 519-531.
158. L. Trahey, N. K. Karan, M. K. Chan, J. Lu, Y. Ren, J. Greeley, M. Balasubramanian, A. K. Burrell, L. A. Curtiss and M. M. Thackeray, *Advanced Energy Materials*, 2013, **3**, 75-84.
159. J. Zeng, J. R. Nair, C. Francia, S. Bodoardo and N. Penazzi, *Int. J. Electrochem. Sci*, 2013, **8**, 3912-3927.
160. H. Cheng and K. Scott, *Journal of Power Sources*, 2010, **195**, 1370-1374.
161. E. M. Benbow, S. P. Kelly, L. Zhao, J. W. Reutenauer and S. L. Suib, *The Journal of Physical Chemistry C*, 2011, **115**, 22009-22017.
162. J.-S. Lee, G. S. Park, H. I. Lee, S. T. Kim, R. Cao, M. Liu and J. Cho, *Nano Letters*, 2011, **11**, 5362-5366.
163. R. S. Kalubarme, C.-H. Ahn and C.-J. Park, *Scripta Materialia*, 2013, **68**, 619-622.
164. J. Zhang, C. X. Guo, L. Zhang and C. M. Li, *Chemical Communications*, 2013.
165. V. M. B. Crisostomo, J. K. Ngala, S. Alia, A. Dobley, C. Morein, C.-H. Chen, X. Shen and S. L. Suib, *Chemistry of Materials*, 2007, **19**, 1832-1839.
166. L. Jin, L. Xu, C. Morein, C. h. Chen, M. Lai, S. Dharmarathna, A. Dobley and S. L. Suib, *Advanced Functional Materials*, 2010, **20**, 3373-3382.
167. S. Ida, A. K. Thapa, Y. Hidaka, Y. Okamoto, M. Matsuka, H. Hagiwara and T. Ishihara, *Journal of Power Sources*, 2012, **203**, 159-164.
168. Y. Yu, B. Zhang, Y.-B. He, Z.-D. Huang, S.-W. Oh and J.-K. Kim, *Journal of Materials Chemistry A*, 2013, **1**, 1163-1170.
169. X. Hu, X. Han, Y. Hu, F. Cheng and J. Chen, *Nanoscale*, 2014, **6**, 3522-3525.
170. C. S. Park, K. S. Kim and Y. J. Park, *Journal of Power Sources*, 2013, **244**, 72-79.
171. Z. Ren, Y. Guo, Z. Zhang, C. Liu and P.-X. Gao, *Journal of Materials Chemistry A*, 2013, **1**, 9897-9906.
172. A. Riaz, K.-N. Jung, W. Chang, S.-B. Lee, T.-H. Lim, S.-J. Park, R.-H. Song, S. Yoon, K.-H. Shin and J.-W. Lee, *Chemical Communications*, 2013, **49**, 5984-5986.
173. Q.-c. Liu, J.-j. Xu, Z.-w. Chang and X.-b. Zhang, *Journal of Materials Chemistry A*, 2014, **2**, 6081-6085.
174. Y. Cui, Z. Wen, S. Sun, Y. Lu and J. Jin, *Solid State Ionics*, 2012, **225**, 598-603.
175. W. Yang, J. Salim, C. Ma, Z. Ma, C. Sun, J. Li, L. Chen and Y. Kim, *Electrochemistry Communications*, 2012, **28**, 13-16.
176. F. Kong, *Electrochimica Acta*, 2012, **68**, 198-201.
177. J. Ming, Y. Wu, J.-B. Park, J. K. Lee, F. Zhao and Y.-K. Sun, *Nanoscale*, 2013, **5**, 10390-10396.
178. B. Sun, H. Liu, P. Munroe, H. Ahn and G. Wang, *Nano Research*, 2012, **5**, 460-469.
179. Y. Yang, Q. Sun, Y.-S. Li, H. Li and Z.-W. Fu, *Journal of Power Sources*, 2012, **223**, 312-318.
180. J. Lu, Y. Qin, P. Du, X. Luo, T. Wu, Y. Ren, J. Wen, D. J. Miller, J. T. Miller and K. Amine, *RSC Advances*, 2013, **3**, 8276-8285.

181. L. Wang, X. Zhao, Y. Lu, M. Xu, D. Zhang, R. S. Ruoff, K. J. Stevenson and J. B. Goodenough, *Journal of The Electrochemical Society*, 2011, **158**, A1379-A1382.
182. H. Wang, Y. Yang, Y. Liang, G. Zheng, Y. Li, Y. Cui and H. Dai, *Energy & Environmental Science*, 2012, **5**, 7931-7935.
183. Y. Zhao, L. Xu, L. Mai, C. Han, Q. An, X. Xu, X. Liu and Q. Zhang, *Proceedings of the National Academy of Sciences*, 2012, **109**, 19569-19574.
184. J. Chen, X. Han, Y. Hu, J. Yang and F. Cheng, *Chemical Communications*, 2013.
185. W. G. Hardin, D. A. Slanac, X. Wang, S. Dai, K. P. Johnston and K. J. Stevenson, *The Journal of Physical Chemistry Letters*, 2013, 1254-1259.
186. J.-J. Xu, D. Xu, Z.-L. Wang, H.-G. Wang, L.-L. Zhang and X.-B. Zhang, *Angewandte Chemie International Edition*, 2013, **52**, 3887-3890.
187. Z. Fu, X. Lin, T. Huang and A. Yu, *Journal of Solid State Electrochemistry*, 2012, **16**, 1447-1452.
188. W. Yang, J. Salim, S. Li, C. Sun, L. Chen, J. B. Goodenough and Y. Kim, *Journal of Materials Chemistry*, 2012, **22**, 18902-18907.
189. J.-J. Xu, Z.-L. Wang, D. Xu, F.-Z. Meng and X.-B. Zhang, *Energy & Environmental Science*, 2014.
190. B. D. McCloskey, R. Scheffler, A. Speidel, D. S. Bethune, R. M. Shelby and A. C. Luntz, *Journal of the American Chemical Society*, 2011, **133**, 18038-18041.
191. M. J. Armstrong, C. O'Dwyer, W. J. Macklin and J. D. Holmes, *Nano Research*, 2014, **7**, 1-62.
192. J. G. Lu, P. Chang and Z. Fan, *Materials Science and Engineering: R: Reports*, 2006, **52**, 49-91.
193. P. Poizot, S. Laruelle, S. Grugeon, L. Dupont and J. Tarascon, *Nature*, 2000, **407**, 496-499.
194. X. Wang and Y. D. Li, *Journal of the American Chemical Society*, 2002, **124**, 2880-2881.
195. F. S. Gittleson, R. C. Sekol, G. Doubek, M. Linardi and A. Taylor, *Physical Chemistry Chemical Physics*, 2013, **16**, 3230-3237.
196. Z. Peng, S. A. Freunberger, L. J. Hardwick, Y. Chen, V. Giordani, F. Bardé, P. Novák, D. Graham, J.-M. Tarascon and P. G. Bruce, *Angewandte Chemie International Edition*, 2011, **50**, 6351-6355.
197. Z. Peng, S. A. Freunberger, Y. Chen and P. G. Bruce, *Science*, 2012, **337**, 563-566.
198. D. Zhu, L. Zhang, M. Song, X. Wang and Y. Chen, *Chemical Communications*, 2013.
199. J. Lu, Y. Lei, K. C. Lau, X. Luo, P. Du, J. Wen, R. S. Assary, U. Das, D. J. Miller and J. W. Elam, *Nature communications*, 2013, **4**, 2383.
200. Y.-C. Lu, H. A. Gasteiger and Y. Shao-Horn, *Journal of the American Chemical Society*, 2011, **133**, 19048-19051.
201. Y. Yang, M. Shi, Q.-F. Zhou, Y.-S. Li and Z.-W. Fu, *Electrochemistry Communications*, 2012, **20**, 11-14.
202. H.-D. Lim, H. Song, H. Gwon, K.-Y. Park, J. Kim, Y. Bae, H. Kim, S.-K. Jung, T. Kim, Y. H. Kim, X. Lepro, R. Ovalle-Robles, R. H. Baughman and K. Kang, *Energy & Environmental Science*, 2013, **6**, 3570-3575.
203. L. Wang, M. Ara, K. Wadumesthrige, S. Salley and K. Y. S. Ng, *Journal of Power Sources*, 2013, **234**, 8-15.
204. Y. Lu, Z. Wen, J. Jin, Y. Cui, M. Wu and S. Sun, *Journal of Solid State Electrochemistry*, 2012, **16**, 1863-1868.
205. S. Lee, S. Zhu, C. C. Milleville, C.-Y. Lee, P. Chen, K. J. Takeuchi, E. S. Takeuchi and A. C. Marschilok, *Electrochemical and Solid-State Letters*, 2010, **13**, A162-A164.
206. A. C. Marschilok, S. Zhu, C. C. Milleville, S. H. Lee, E. S. Takeuchi and K. J. Takeuchi, *Journal of The Electrochemical Society*, 2011, **158**, A223-A226.
207. C. Wang, N. M. Markovic and V. R. Stamenkovic, *ACS Catalysis*, 2012, **2**, 891-898.
208. J. Zhang, G. Chen, M. An and P. Wang, *Int. J. Electrochem. Sci*, 2012, **7**, 11957-11965.
209. G. Collins, M. Blömker, M. Osiak, J. D. Holmes, M. Bredol and C. O'Dwyer, *Chemistry of Materials*, 2013, **25**, 4312-4320.
210. T. K. Sau, A. L. Rogach, F. Jäckel, T. A. Klar and J. Feldmann, *Advanced Materials*, 2010, **22**, 1805-1825.

211. T. K. Sau and A. L. Rogach, *Advanced Materials*, 2010, **22**, 1781-1804.
212. F. Li, D.-M. Tang, Y. Chen, D. Golberg, H. Kitaura, T. Zhang, A. Yamada and H. Zhou, *Nano Letters*, 2013, **13**, 4702-4707.
213. C. Sun, F. Li, C. Ma, Y. Wang, Y. Ren, W. Yang, Z. Ma, J. Li, Y. Chen, Y. Kim and L. Chen, *Journal of Materials Chemistry A*, 2014, **2**, 7188-7196.
214. F. Li, D.-M. Tang, Y. Chen, D. Golberg, H. Kitaura, T. Zhang, A. Yamada and H. Zhou, *Nano Letters*, 2013.
215. T. Zhang and H. Zhou, *Nature communications*, 2013, **4**, 1817.
216. J. G. Zhang, D. Wang, W. Xu, J. Xiao and R. E. Williford, *Journal of Power Sources*, 2010, **195**, 4332-4337.
217. W. Xu, J. Xiao, J. Zhang, D. Wang and J.-G. Zhang, *Journal of The Electrochemical Society*, 2009, **156**, A773-A779.
218. D. Wang, J. Xiao, W. Xu and J.-G. Zhang, *Journal of The Electrochemical Society*, 2010, **157**, A760-A764.
219. S. R. Gowda, A. Brunet, G. M. Wallraff and B. D. McCloskey, *The Journal of Physical Chemistry Letters*, 2012, 276-279.
220. H.-K. Lim, H.-D. Lim, K.-Y. Park, D.-H. Seo, H. Gwon, J. Hong, W. A. Goddard III, H. Kim and K. Kang, *Journal of the American Chemical Society*, 2013, **135**, 9733-9742.
221. X.-h. Yang and Y.-y. Xia, *Journal of Solid State Electrochemistry*, 2010, **14**, 109-114.
222. E. J. Nemanick and R. P. Hickey, *Journal of Power Sources*, 2014, **252**, 248-251.
223. M. Song, D. Zhu, L. Zhang, X. Wang, L. Huang, Q. Shi, R. Mi, H. Liu, J. Mei and L. W. Lau, *Journal of Solid State Electrochemistry*, 2013, 1-9.
224. M. Song, D. Zhu, L. Zhang, X. Wang, R. Mi, H. Liu, J. Mei, L. W. Lau and Y. Chen, *Journal of Solid State Electrochemistry*, 2013, 1-7.
225. J.-B. Park, J. Hassoun, H.-G. Jung, H.-S. Kim, C. S. Yoon, I. Oh, B. Scrosati and Y.-K. Sun, *Nano Letters*, 2013.
226. G. M. Veith and N. J. Dudney, *Journal of The Electrochemical Society*, 2011, **158**, A658-A663.
227. Z.-K. Luo, C.-S. Liang, F. Wang, Y.-H. Xu, J. Chen, D. Liu, H.-Y. Sun, H. Yang and X.-P. Fan, *Advanced Functional Materials*, 2013, n/a-n/a.
228. C. Tran, J. Kafle, X.-Q. Yang and D. Qu, *Carbon*, 2011, **49**, 1266-1271.
229. C. Tran, X.-Q. Yang and D. Qu, *Journal of Power Sources*, 2010, **195**, 2057-2063.
230. T. Zhang, N. Imanishi, Y. Shimonishi, A. Hirano, Y. Takeda, O. Yamamoto and N. Sammes, *Chemical Communications*, 2010, **46**, 1661-1663.
231. W. Xu, J. Xiao, D. Wang, J. Zhang and J.-G. Zhang, *Journal of The Electrochemical Society*, 2010, **157**, A219-A224.
232. J. Wang, H.-x. Zhong, Y.-l. Qin and X.-b. Zhang, *Angewandte Chemie International Edition*, 2013, n/a-n/a.
233. W. Walker, V. Giordani, J. Uddin, V. S. Bryantsev, G. V. Chase and D. Addison, *Journal of the American Chemical Society*, 2013.
234. H.-G. Jung, Y. S. Jeong, J.-B. Park, Y.-K. Sun, B. Scrosati and Y. J. Lee, *ACS Nano*, 2013, **7**, 3532-3539.
235. Z. Jian, P. Liu, F. Li, P. He, X. Guo, M. Chen and H. Zhou, *Angewandte Chemie International Edition*, 2014, **53**, 442-446.
236. K. Guo, Y. Li, J. Yang, Z. Zou, X. Xue, X. Li and H. Yang, *Journal of Materials Chemistry A*, 2014, **2**, 1509-1514.
237. B. Sun, P. Munroe and G. Wang, *Scientific reports*, 2013, **3**.
238. F. Li, Y. Chen, D.-M. Tang, L. Z. Jian, C. Liu, D. Golberg, A. Yamada and H. Zhou, *Energy & Environmental Science*, 2014.
239. S. Dong, X. Chen, K. Zhang, L. Gu, L. Zhang, X. Zhou, L. Li, Z. Liu, P. Han, H. Xu, J. Yao, C. Zhang, X. Zhang, C. Shang, G. Cui and L. Chen, *Chemical Communications*, 2011, **47**, 11291-11293.

240. K. Zhang, L. Zhang, X. Chen, X. He, X. Wang, S. Dong, L. Gu, Z. Liu, C. Huang and G. Cui, *ACS Applied Materials & Interfaces*, 2013.
241. K. Zhang, L. Zhang, X. Chen, X. He, X. Wang, S. Dong, P. Han, C. Zhang, S. Wang, L. Gu and G. Cui, *The Journal of Physical Chemistry C*, 2012.
242. S. Dong, S. Wang, J. Guan, S. Li, Z. Lan, C. Chen, C. Shang, L. Zhang, X. Wang, L. Gu, G. Cui and L. Chen, *The Journal of Physical Chemistry Letters*, 2014, 615-621.
243. M. J. Trahan, Q. Jia, S. Mukerjee, E. J. Plichta, M. A. Hendrickson and K. Abraham, *Journal of The Electrochemical Society*, 2013, **160**, A1577-A1586.
244. X. Ren, S. S. Zhang, D. T. Tran and J. Read, *Journal of Materials Chemistry*, 2011, **21**, 10118-10125.
245. S. H. Oh and L. F. Nazar, *Advanced Energy Materials*, 2012, **2**, 903-910.
246. L. Zhang, S. Zhang, K. Zhang, G. Xu, X. He, S. Dong, Z. Liu, C. Huang, L. Gu and G. Cui, *Chemical Communications*, 2013.
247. D. Wu, Z. Guo, X. Yin, Q. Pang, B. Tu, L. Zhang, Y.-G. Wang and Q. Li, *Advanced Materials*, 2014, n/a-n/a.
248. G. M. Veith, N. J. Dudney, J. Howe and J. Nanda, *The Journal of Physical Chemistry C*, 2011, **115**, 14325-14333.
249. B. D. McCloskey, D. S. Bethune, R. M. Shelby, G. Girishkumar and A. C. Luntz, *The Journal of Physical Chemistry Letters*, 2011, **2**, 1161-1166.
250. B. D. McCloskey, R. Scheffler, A. Speidel, G. Girishkumar and A. C. Luntz, *The Journal of Physical Chemistry C*, 2012, **116**, 23897-23905.
251. B. D. McCloskey, D. S. Bethune, R. M. Shelby, T. Mori, R. Scheffler, A. Speidel, M. Sherwood and A. C. Luntz, *The Journal of Physical Chemistry Letters*, 2012, **3**, 3043-3047.
252. R. Younesi, M. Hahlin and K. Edström, *ACS Applied Materials & Interfaces*, 2013.
253. R. Younesi, M. Hahlin, F. Björefors, P. Johansson and K. Edström, *Chemistry of Materials*, 2012.
254. G. M. Veith, J. Nanda, L. H. Delmau and N. J. Dudney, *The Journal of Physical Chemistry Letters*, 2012, **3**, 1242-1247.
255. B. D. McCloskey, A. Speidel, R. Scheffler, D. C. Miller, V. Viswanathan, J. S. Hummelshøj, J. K. Nørskov and A. C. Luntz, *The Journal of Physical Chemistry Letters*, 2012, **3**, 997-1001.
256. Y.-C. Lu, E. J. Crumlin, G. M. Veith, J. R. Harding, E. Mutoro, L. Baggetto, N. J. Dudney, Z. Liu and Y. Shao-Horn, *Scientific reports*, 2012, **2**.
257. H. Lim, E. Yilmaz and H. R. Byon, *The Journal of Physical Chemistry Letters*, 2012, **3**, 3210-3215.
258. V. S. Bryantsev, J. Uddin, V. Giordani, W. Walker, D. Addison and G. V. Chase, *Journal of The Electrochemical Society*, 2013, **160**, A160-A171.
259. V. S. Bryantsev and F. Faglioni, *The Journal of Physical Chemistry A*, 2012, **116**, 7128-7138.
260. Y. Chen, S. A. Freunberger, Z. Peng, F. Bardé and P. G. Bruce, *Journal of the American Chemical Society*, 2012, **134**, 7952-7957.
261. Z. Zhang, J. Lu, R. S. Assary, P. Du, H.-H. Wang, Y.-K. Sun, Y. Qin, K. C. Lau, J. Greeley, P. C. Redfern, H. Iddir, L. A. Curtiss and K. Amine, *The Journal of Physical Chemistry C*, 2011, **115**, 25535-25542.
262. C. K. Chan, H. Peng, G. Liu, K. McIlwrath, X. F. Zhang, R. A. Huggins and Y. Cui, *Nature nanotechnology*, 2007, **3**, 31-35.
263. A. Magasinski, P. Dixon, B. Hertzberg, A. Kvit, J. Ayala and G. Yushin, *Nature materials*, 2010, **9**, 353-358.
264. M.-H. Park, M. G. Kim, J. Joo, K. Kim, J. Kim, S. Ahn, Y. Cui and J. Cho, *Nano Letters*, 2009, **9**, 3844-3847.
265. I. Kowalczk, J. Read and M. Salomon, *Pure and applied chemistry*, 2007, **79**, 851-860.
266. J. Read, K. Mutolo, M. Ervin, W. Behl, J. Wolfenstine, A. Driedger and D. Foster, *Journal of The Electrochemical Society*, 2003, **150**, A1351-A1356.

267. M. Eswaran, N. Munichandraiah and L. Scanlon, *Electrochemical and Solid-State Letters*, 2010, **13**, A121-A124.
268. P. Albertus, G. Girishkumar, B. McCloskey, R. S. Sánchez-Carrera, B. Kozinsky, J. Christensen and A. Luntz, *Journal of The Electrochemical Society*, 2011, **158**, A343-A351.
269. W. Xu, K. Xu, V. V. Viswanathan, S. A. Towne, J. S. Hardy, J. Xiao, Z. Nie, D. Hu, D. Wang and J.-G. Zhang, *Journal of Power Sources*, 2011, **196**, 9631-9639.
270. S. S. Zhang, D. Foster and J. Read, *Journal of Power Sources*, 2010, **195**, 1235-1240.
271. S. A. Freunberger, Y. Chen, Z. Peng, J. M. Griffin, L. J. Hardwick, F. Bardé, P. Novák and P. G. Bruce, *Journal of the American Chemical Society*, 2011, **133**, 8040-8047.
272. F. Mizuno, S. Nakanishi, Y. Kotani, S. Yokoishi and H. Iba, *Electrochemistry*, 2010, **78**, 403-405.
273. V. S. Bryantsev, V. Giordani, W. Walker, M. Blanco, S. Zecevic, K. Sasaki, J. Uddin, D. Addison and G. V. Chase, *The Journal of Physical Chemistry A*, 2011, **115**, 12399-12409.
274. W. Xu, K. Xu, V. V. Viswanathan, S. A. Towne, J. S. Hardy, J. Xiao, Z. Nie, D. Hu, D. Wang and J.-G. Zhang, *Journal of Power Sources*, 2011, **196**, 9631-9639.
275. H. Wang and K. Xie, *Electrochimica Acta*, 2012, **64**, 29-34.
276. K. R. Ryan, L. Trahey, B. J. Ingram and A. K. Burrell, *The Journal of Physical Chemistry C*, 2012, **116**, 19724-19728.
277. D. Sharon, V. Etacheri, A. Garsuch, M. Afri, A. A. Frimer and D. Aurbach, *The Journal of Physical Chemistry Letters*, 2012, 127-131.
278. H.-G. Jung, J. Hassoun, J.-B. Park, Y.-K. Sun and B. Scrosati, *Nature chemistry*, 2012, **4**, 579-585.
279. D. Zhu, L. Zhang, M. Song, X. Wang, J. Mei, L. W. Lau and Y. Chen, *Journal of Solid State Electrochemistry*, 2013, **17**, 2865-2870.
280. R. S. Assary, K. C. Lau, K. Amine, Y.-K. Sun and L. A. Curtiss, *The Journal of Physical Chemistry C*, 2013, **117**, 8041-8049.
281. Y. Cui, Z. Wen, X. Liang, Y. Lu, J. Jin, M. Wu and X. Wu, *Energy Environ. Sci.*, 2012, **5**, 7893-7897.
282. C. Laoire, S. Mukerjee, E. J. Plichta, M. A. Hendrickson and K. Abraham, *Journal of The Electrochemical Society*, 2011, **158**, A302-A308.
283. K. U. Schwenke, S. Meini, X. Wu, H. A. Gasteiger and M. Piana, *Physical Chemistry Chemical Physics*, 2013.
284. M. Marinaro, S. Theil, L. Jörissen and M. Wohlfahrt-Mehrens, *Electrochimica Acta*, 2013, **108**, 795-800.
285. C. Liang, *New Journal of Chemistry*, 2013.
286. Y. Wang, L. Xing, W. Li and D. Bedrov, *The Journal of Physical Chemistry Letters*, 2013, **4**, 3992-3999.
287. B. Sun, X. Huang, J. Zhang, S. Chen and G. Wang, *RSC Advances*, 2014.
288. M. J. Trahan, S. Mukerjee, E. J. Plichta, M. A. Hendrickson and K. Abraham, *Journal of The Electrochemical Society*, 2013, **160**, A259-A267.
289. D. Sharon, M. Afri, M. Noked, A. Garsuch, A. A. Frimer and D. Aurbach, *The Journal of Physical Chemistry Letters*, 2013, **4**, 3115-3119.
290. S. Meini, M. Piana, N. Tsiouvaras, A. Garsuch and H. A. Gasteiger, *Electrochemical and Solid-State Letters*, 2012, **15**, A45-A48.
291. T. Kuboki, T. Okuyama, T. Ohsaki and N. Takami, *Journal of Power Sources*, 2005, **146**, 766-769.
292. C. J. Allen, S. Mukerjee, E. J. Plichta, M. A. Hendrickson and K. M. Abraham, *The Journal of Physical Chemistry Letters*, 2011, **2**, 2420-2424.
293. C. J. Allen, J. Hwang, R. Kautz, S. Mukerjee, E. J. Plichta, M. A. Hendrickson and K. M. Abraham, *The Journal of Physical Chemistry C*, 2012, **116**, 20755-20764.
294. F. Soavi, S. Monaco and M. Mastragostino, *Journal of Power Sources*, 2013, **224**, 115-119.

295. F. MIZUNO, S. NAKANISHI, A. SHIRASAWA, K. TAKECHI, T. SHIGA, H. NISHIKOORI and H. IBA, *Electrochemistry*, 2011, **79**, 876-881.
296. H. Wang, X.-Z. Liao, L. Li, H. Chen, Q.-Z. Jiang, Y.-S. He and Z.-F. Ma, *Journal of The Electrochemical Society*, 2012, **159**, A1874-A1879.
297. L. Cecchetto, M. Salomon, B. Scrosati and F. Croce, *Journal of Power Sources*, 2012, **213**, 233-238.
298. J. Herranz, A. Garsuch and H. A. Gasteiger, *The Journal of Physical Chemistry C*, 2012, **116**, 19084-19094.
299. S. Higashi, Y. Kato, K. Takechi, H. Nakamoto, F. Mizuno, H. Nishikoori, H. Iba and T. Asaoka, *Journal of Power Sources*, 2013, **240**, 14-17.
300. E. Nasybulin, W. Xu, M. H. Engelhard, Z. Nie, S. D. Burton, L. Cosimbescu, M. E. Gross and J.-G. Zhang, *The Journal of Physical Chemistry C*, 2013.
301. G. A. Elia, J.-B. Park, Y.-K. Sun, B. Scrosati and J. Hassoun, *ChemElectroChem*, 2014, **1**, 47-50.
302. F. Li, T. Zhang, Y. Yamada, A. Yamada and H. Zhou, *Advanced Energy Materials*, 2013, **3**, 532-538.
303. D. Chalasani and B. L. Lucht, *ECS Electrochemistry Letters*, 2012, **1**, A38-A42.
304. R. A. Huggins, *Journal of Power Sources*, 1999, **81**, 13-19.
305. R. Bhattacharyya, B. Key, H. Chen, A. S. Best, A. F. Hollenkamp and C. P. Grey, *Nature materials*, 2010, **9**, 504-510.
306. G. Yu Aleshin, D. A. Semenenko, A. I. Belova, T. K. Zakharchenko, D. M. Itkis, E. A. Goodilin and Y. D. Tretyakov, *Solid State Ionics*, 2011, **184**, 62-64.
307. J. Hassoun, F. Croce, M. Armand and B. Scrosati, *Angewandte Chemie International Edition*, 2011, **50**, 2999-3002.
308. Y. Inaguma and M. Nakashima, *Journal of Power Sources*, 2013, **228**, 250-255.
309. T. Katoh, Y. Inda, K. Nakajima, R. Ye and M. Baba, *Journal of Power Sources*, 2011, **196**, 6877-6880.
310. F. Ding, W. Xu, Y. Shao, X. Chen, J. Xiao, L. Xingjiang and J.-G. Zhang, Meeting Abstracts, 2011.
311. C. R. Mariappan, M. Gellert, C. Yada, F. Rosciano and B. Roling, *Electrochemistry Communications*, 2012, **14**, 25-28.
312. Y. Sun, *Nano Energy*, 2013, **2**, 801-816.
313. F. Li, H. Kitaura and H. Zhou, *Energy & Environmental Science*, 2013.
314. J.-L. Shui, J. S. Okasinski, P. Kenesei, H. A. Dobbs, D. Zhao, J. D. Almer and D.-J. Liu, *Nature communications*, 2013, **4**.
315. V. S. Bryantsev, V. Giordani, W. Walker, J. Uddin, I. Lee, A. C. T. van Duin, G. V. Chase and D. Addison, *The Journal of Physical Chemistry C*, 2013, **117**, 11977-11988.
316. R. Younesi, M. Hahlin, M. Roberts and K. Edström, *Journal of Power Sources*, 2013, **225**, 40-45.
317. C. K. Chan, R. N. Patel, M. J. O'Connell, B. A. Korgel and Y. Cui, *ACS Nano*, 2010, **4**, 1443-1450.
318. A. M. Chockla, J. T. Harris, V. A. Akhavan, T. D. Bogart, V. C. Holmberg, C. Steinhagen, C. B. Mullins, K. J. Stevenson and B. A. Korgel, *Journal of the American Chemical Society*, 2011, **133**, 20914-20921.
319. E. Mullane, T. Kennedy, H. Geaney, C. Dickinson and K. M. Ryan, *Chemistry of Materials*, 2013, **25**, 1816-1822.
320. C. K. Chan, X. F. Zhang and Y. Cui, *Nano Letters*, 2007, **8**, 307-309.
321. T. Kennedy, E. Mullane, H. Geaney, M. Osiak, C. O'Dwyer and K. M. Ryan, *Nano Letters*, 2014, **14**, 716-723.
322. F.-W. Yuan, H.-J. Yang and H.-Y. Tuan, *ACS Nano*, 2012, **6**, 9932-9942.
323. Y. Idota, T. Kubota, A. Matsufuji, Y. Maekawa and T. Miyasaka, *Science*, 1997, **276**, 1395-1397.

324. H. S. Im, Y. J. Cho, Y. R. Lim, C. S. Jung, D. M. Jang, J. Park, F. Shojaei and H. S. Kang, *ACS Nano*, 2013, **7**, 11103-11111.
325. M. J. Osiak, E. Armstrong, T. Kennedy, C. M. Sotomayor Torres, K. M. Ryan and C. O'Dwyer, *ACS Applied Materials & Interfaces*, 2013, **5**, 8195-8202.
326. C. Park, S. Park, S. Lee, H. Lee, H. Jang and W. Cho, *Bulletin of the Korean Chemical Society*, 2010, **31**, 3221-3224.
327. A. K. Thapa, Y. Hidaka, H. Hagiwara, S. Ida and T. Ishihara, *Journal of The Electrochemical Society*, 2011, **158**, A1483-A1489.
328. D. Zhang, Z. Fu, Z. Wei, T. Huang and A. Yu, *Journal of The Electrochemical Society*, 2010, **157**, A362-A365.
329. M. D. Radin, F. Tian and D. J. Siegel, *Journal of Materials Science*, 2012, **47**, 7564-7570.
330. M. D. Radin, J. F. Rodriguez and D. J. Siegel, Proceedings of the Battery Congress, 2011.
331. N. Seriani, *Nanotechnology*, 2009, **20**, 445703.
332. S. Kang, Y. Mo, S. P. Ong and G. Ceder, *Chemistry of Materials*, 2013, **25**, 3328-3336.
333. W. Xu, V. V. Viswanathan, D. Wang, S. A. Towne, J. Xiao, Z. Nie, D. Hu and J.-G. Zhang, *Journal of Power Sources*, 2011, **196**, 3894-3899.
334. J. Chen, J. S. Hummelshøj, K. S. Thygesen, J. S. Myrdal, J. K. Nørskov and T. Vegge, *Catalysis Today*, 2011, **165**, 2-9.
335. J. S. Hummelshøj, J. Blomqvist, S. Datta, T. Vegge, J. Rossmeisl, K. S. Thygesen, A. Luntz, K. W. Jacobsen and J. K. Nørskov, *The Journal of chemical physics*, 2010, **132**, 071101-071101-071104.
336. S. P. Ong, Y. Mo and G. Ceder, *Physical Review B*, 2012, **85**, 081105.
337. V. Viswanathan, K. S. Thygesen, J. Hummelshøj, J. K. Nørskov, G. Girishkumar, B. McCloskey and A. Luntz, *The Journal of chemical physics*, 2011, **135**, 214704-214704-214710.
338. Y. Zhao, C. Ban, J. Kang, S. Santhanagopalan, G.-H. Kim, S.-H. Wei and A. C. Dillon, *Applied Physics Letters*, 2012, **101**, 023903.
339. V. S. Bryantsev, *Theoretical Chemistry Accounts*, 2012, **131**, 1-11.
340. J. Kang, Y. S. Jung, S.-H. Wei and A. C. Dillon, *Physical Review B*, 2012, **85**, 035210.
341. V. Timoshevskii, Z. Feng, K. H. Bevan, J. Goodenough and K. Zaghib, *Applied Physics Letters*, 2013, **103**, 073901.
342. M. D. Radin and D. J. Siegel, *Energy & Environmental Science*, 2013, **6**, 2370-2379.
343. D. Capsoni, M. Bini, S. Ferrari, E. Quartarone and P. Mustarelli, *Journal of Power Sources*, 2012, **220**, 253-263.
344. Y. Xu and W. A. Shelton, *The Journal of chemical physics*, 2010, **133**, 024703.
345. A. Christensen and E. A. Carter, *Physical Review B*, 1998, **58**, 8050.
346. D. Kramer and G. Ceder, *Chemistry of Materials*, 2009, **21**, 3799-3809.
347. M. Ramamoorthy, D. Vanderbilt and R. King-Smith, *Physical Review B*, 1994, **49**, 16721.
348. K. Reuter and M. Scheffler, *Physical Review B*, 2001, **65**, 035406.
349. K. Reuter and M. Scheffler, *Physical review letters*, 2003, **90**, 046103.
350. L. Wang, F. Zhou and G. Ceder, *Electrochemical and Solid-State Letters*, 2008, **11**, A94-A96.
351. L. Wang, F. Zhou, Y. Meng and G. Ceder, *Physical Review B*, 2007, **76**, 165435.
352. X.-G. Wang, A. Chaka and M. Scheffler, *Physical Review Letters*, 2000, **84**, 3650.
353. J. Sangster and A. Pelton, *Journal of phase equilibria*, 1992, **13**, 296-299.
354. K. C. Lau, L. A. Curtiss and J. Greeley, *The Journal of Physical Chemistry C*, 2011, **115**, 23625-23633.
355. B. McEnaney, *Carbon*, 1988, **26**, 267-274.
356. O. Crowther, B. Meyer, M. Morgan and M. Salomon, *Journal of Power Sources*, 2011, **196**, 1498-1502.
357. J. Dai, T. Kogut, L. Jin and D. Reisner, *ECS Transactions*, 2008, **6**, 381-387.
358. X.-h. Yang, P. He and Y.-y. Xia, *Electrochemistry Communications*, 2009, **11**, 1127-1130.
359. M. Mirzaeian and P. J. Hall, *Journal of Power Sources*, 2010, **195**, 6817-6824.

360. P. J. H. M. Mirazaeian, *Polymer System Technology (Beijing)*, 2007, **31**.
361. C. Punckt, M. A. Pope, J. Liu, Y. Lin and I. A. Aksay, *Electroanalysis*, 2010, **22**, 2834-2841.
362. C. Liu, Z. Yu, D. Neff, A. Zhamu and B. Z. Jang, *Nano Letters*, 2010, **10**, 4863-4868.
363. D. Wang, D. Choi, J. Li, Z. Yang, Z. Nie, R. Kou, D. Hu, C. Wang, L. V. Saraf, J. Zhang, I. A. Aksay and J. Liu, *ACS Nano*, 2009, **3**, 907-914.
364. R. Kou, Y. Shao, D. Mei, Z. Nie, D. Wang, C. Wang, V. V. Viswanathan, S. Park, I. A. Aksay and Y. Lin, *Journal of the American Chemical Society*, 2011, **133**, 2541-2547.
365. F. Renner, H. Kageyama, Z. Siroma, M. Shikano, S. Schöder, Y. Gründer and O. Sakata, *Electrochimica Acta*, 2008, **53**, 6064-6069.
366. P. G. Bruce, B. Scrosati and J.-M. Tarascon, *Angewandte Chemie International Edition*, 2008, **47**, 2930-2946.
367. A. Debart, J. Bao, G. Armstrong and P. G. Bruce, *ECS Transactions*, 2007, **3**, 225-232.
368. M. Brandbyge, J.-L. Mozos, P. Ordejón, J. Taylor and K. Stokbro, *Physical Review B*, 2002, **65**, 165401.
369. C. Johnson and M. Thackeray, *Journal of power sources*, 2001, **97**, 437-442.
370. M. Thackeray, M. Rossouw, A. De Kock, A. De la Harpe, R. Gummow, K. Pearce and D. Liles, *Journal of power sources*, 1993, **43**, 289-300.
371. M. Thackeray, M. Rossouw, R. Gummow, D. Liles, K. Pearce, A. De Kock, W. David and S. Hull, *Electrochimica acta*, 1993, **38**, 1259-1267.
372. N. S. P. M.W. Raphel, L.B. Khalil, *J. Power Sources*, 1988, **22**.
373. T. A. Mellan, K. P. Maenetja, P. E. Ngoepe, S. M. Woodley, C. R. A. Catlow and R. Grau-Crespo, *Journal of Materials Chemistry A*, 2013, **1**, 14879-14887.
374. R. S. Assary, J. Lu, P. Du, X. Luo , X. Zhang, Y. Ren, L. A. Curtiss and K. Amine, *ChemSusChem*, 2013, **6**, 51-55.
375. A. K. Padhi, K. Nanjundaswamy and J. B. d. Goodenough, *Journal of The Electrochemical Society*, 1997, **144**, 1188-1194.
376. T. T. Truong, Y. Qin, Y. Ren, Z. Chen, M. K. Chan, J. P. Greeley, K. Amine and Y. Sun, *Advanced Materials*, 2011, **23**, 4947-4952.
377. V. S. Bryantsev and M. Blanco, *The Journal of Physical Chemistry Letters*, 2011, **2**, 379-383.
378. C. Nanjundiah, S. McDevitt and V. Koch, *Journal of The Electrochemical Society*, 1997, **144**, 3392-3397.
379. J. S. Wilkes and M. J. Zaworotko, *J. Chem. Soc., Chem. Commun.*, 1992, 965-967.
380. J. Fuller, R. T. Carlin and R. A. Osteryoung, *Journal of the Electrochemical Society*, 1997, **144**, 3881-3886.
381. D. Zhang, R. Li, T. Huang and A. Yu, *Journal of Power Sources*, 2010, **195**, 1202-1206.
382. R. S. Assary, L. A. Curtiss, P. C. Redfern, Z. Zhang and K. Amine, *The Journal of Physical Chemistry C*, 2011, **115**, 12216-12223.